2-1-2013

A study of the ionic diffusion under the effect of electric field (computer simulation with reference to biological membrane)

Hagar Mohamed Fawzy

The American University in Cairo
School of Sciences and Engineering

A STUDY OF THE IONIC DIFFUSION UNDER THE EFFECT OF ELECTRIC FIELD (COMPUTER SIMULATION WITH REFERENCE TO BIOLOGICAL MEMBRANE)

A Thesis Submitted to

The Physics Graduate Program

In partial fulfillment of the requirements for
the degree of Master of Science

by Hagar Mohamed Fawzy

Under the supervision of: Prof.Dr. Salah El-Sheikh
Physics department, American University in Cairo, Egypt

Prof.Dr. Medhat A. El-Messiery
Engineering, Mathematics and Physics department
Faculty of Engineering, Cairo University, Egypt

Dr. Noha Salem
Ass.Prof. Engineering, Mathematics and Physics department
Faculty of Engineering, Cairo University, Egypt

January 2013

DEDICATION

This thesis is dedicated to my family. I would like to express my deep love and appreciation to all my family members who are always by my side. I thank my husband who constantly encourages me to find and realize my potential in my life. I thank my mother who always gave me complete support and truly believes in me. I thank my father who gave me unconditional love and support. I would like to thank my sister and brother who took care of my little baby during the endless hours of sitting in front of the computer. Then I thank all my family members and friends who are always around and believe that I will succeed.

I dedicate this work to my daughter Sara who made my thesis voyage an amazing and memorable one by her joyful presence.

This thesis was made possible because of them, and I hope to make them proud in this journey and future ones.

ACKNOWLEDGEMENTS

I want to express my deep appreciation to my advisors for accepting me as a M.Sc. student for this thesis, their advices were crucial for my research and learning experience. I express my deep thanks to Prof.Dr.Salah El-Sheikh who provided me with all the support to complete this thesis. In addition, he found the fund at the American University in Cairo for me to present the research work in the 7th International Workshop on Biological effects of Electromagnetic fields in Malta. I consider Dr.Salah not only my advisor, but a kind father who always supported me and helped me setting the priorities in my life.

I sincerely thank Prof. Dr. Medhat El-Messiery who was a true inspiration since I entered the Masters program. He was the first who introduced me and others to the promising area of computer modeling and gave me an essence to its application in physics. He taught me how the physical phenomenon of diffusion could be analyzed and modeled. His expert experience helped me in interpreting the results of the model outcomes. The valuable discussion and continuous assistance which were so willingly given by Dr.Medhat during the course of this work will never be forgotten. I will always remember his professional advices in the conference in Malta. His experience improved my research skills and prepared me for future challenges. Dr.Medhat is a true mentor for all his students.

I also want to thank Dr.Noha Salem who encouraged me to complete the Masters degree. Her inputs in building the theoretical model were certainly helpful.

I owe my deepest gratitude to Dr.Ahmed Shawky from the faculty of Computer Science at Cairo University and his students, Sara Salem and Doha Ehab. The interdisciplinary collaboration was made true with them. They gave us all the time and effort to transform our code from Matlab language to the C language. This transformation gave the chance for a broader application of the model and extremely saved time. It was a fruitful time which promises for more future team work.

I sincerely express my deepest gratitude to the Chair of the physics department and colleagues at the Physics department for their faithful help and their beneficial support during the research program.

It is an honor to have worked with my advisors. I learnt a lot, not only as a student, but also as a person, and I truly owe them for that.

Thank you for making this thesis happens.

ABSTRACT

The biophysical studies of the biological system are far from being conclusive. Not only because this science is relatively recent, but also because of the lack of physical data. Also there are a lot of contradicting views among researchers as well as the poor theoretical interpretation of the reported experimental data. However, the advent of computer science with the considerable storage capability and highly vast calculations gives modeling techniques a great advantage and opens a real door to better understanding of the complicated biological phenomena.

The present thesis addressed the problem of ionic penetration through biological tissue under the effect of external electric field (DC and AC). This was done by studying the diffusion coefficient D as an indicating parameter for such effects.

The work was based on stochastic computer simulation of the problem such that the tissue was considered as a matrix that contains the elements under study. The size of the matrix was up to 30,000 x 30,000. Two dimensional honey comb cellular pattern was simulated such that it allowed six maximum possible element-to-element communications.

The diffusants were let to diffuse under different electric field strengths in DC forward and opposite directions, and AC field with different frequencies.

The effect of vacancies concentration and annealing time were tested in the absence of electric field. Two different vacancies concentrations were studied under the effect of electric field. Fist, 90% of the tissue was vacant and subjected to DC and AC fields as well as zero field. Second, 50% of the tissue was vacant and investigated under similar conditions.

The results showed that for the 90% case, the penetration increased with increasing of electric field strength. While in the 50% case, the penetration increases with increasing the current until a point at which the diffusion is hindered.

The DC results of forward current were compared to that of backward direct current and the results showed that the backward direction hindered diffusion.

The effect of alternating current shows that penetration was inversely proportional with the frequency which agrees with literature. Comparisons of the effects of sinusoidal and square waves were illustrated. The square waves showed to have more ionic penetration and diffusion coefficient values than the sinusoidal ones.

As the frequency of alternating current is decreased, its effect on diffusion became close to that of direct current.

Despite the fact that the results obtained by simulation are in essence virtual and based on arbitrary units, yet the effects were clear and indicative.

TABLE OF CONTENTS

LIST OF FIGURES

LIST OF TABLES

LIST OF APPENDIXES

LIST OF ABBREVIATIONS

D	Diffusion coefficient
R	Gas constant
T	Absolute temperature
N_a	Avogadro's number ($6x10^{23}$ molecule/mole)
V	Viscosity of the solvent
r	Radius of particle or molecule
MD	Molecular dynamics
INDO	Neglect of differential overlap
D_{seff}	Effective diffusion coefficient
PEF	Pulsed electric fields
BBB	Blood-brain barrier
ECS	Extracellular space
ELF	Extremely low frequency
v_{rms}	Root-mean-square velocity
D_o	Diffusion coefficient at 0^ok
Q	Activation energy.
T_m	Melting point
RBCs	Red blood cells
J	Flux
C	Concentration
ΔG_v	Free energy of vacancies formation
ω_o	Frequency of vibration

N_V	Number of vacancies
ΔH*	Enthalpy of formation per mole of vacancies
ΔS*	Entropy of motion per mole of activated complexes
ΔSv	Entropy of formation per mole of vacancies
Δv_V	Change in the volume of the solid due to the vacancy creation at non zero pressure
Δv^*	Change in the volume due to atomic migration
M	Mobility of the charge carriers
E	Electric field strength
DC	Direct current
EM	Electromagnetic
σ	Conductivity
δ	Skin depth
ε	Permittivity
PDF	Probability density function
randn	Random normal distribution
randint	Random integer generator
randperm	Random permutation of numbers

Chapter 1: Introduction

1.1. The diffusion process

Diffusion is one of the fundamental processes by which material moves. It is important in biology, chemistry, geology, engineering and physics. It is the movement of molecules from a region of higher concentration to one of lower concentration. This movement occurs because the molecules are constantly colliding with one another. The net movement of the molecules is away from the region of high concentration to the region of low concentration.

Most changes in structure occur by diffusion, any real understanding of phase changes must be based on knowledge of diffusion. Also diffusion process plays an important role in many surface phenomena including thin film growth, surface chemical reactions.

The dependence of life processes on diffusion mechanisms could not be more prevalent. All living things have certain requirements they must satisfy in order to remain alive. These include exchanging gases (usually CO_2 and O_2), taking in water, minerals, and eliminating wastes. These tasks ultimately occur at the cellular level, and require that molecules move through the membrane that surrounds the cell. This membrane is a complex structure that is responsible for separating the contents of the cell from its surroundings, for controlling the movement of materials into and out of the cell, and for interacting with the environment surrounding the cell. Diffusion is a passive process that requires no energy from the cell.

Osmosis is a special example of diffusion. It is the diffusion of water through a semi- permeable membrane from a more dilute solution to a more concentrated solution – down the water potential gradient). A semi-permeable membrane lets only certain molecules pass through while keeping other molecules out.

Examples of diffusion in biology are:

• Absorption of water by plant roots.

• Re-absorption of water by the proximal and distal convoluted tubules of the nephron.

• Re-absorption of tissue fluid into the venule ends of the blood capillaries.

• Absorption of water by the alimentary canal: stomach, small intestine and the colon.

• Gas exchange at the alveoli: oxygen from air to blood, carbon dioxide from blood to air.

• Gas exchange for photosynthesis: carbon dioxide from air to leaf, oxygen from leaf to air.

• Gas exchange for respiration: oxygen from blood to tissue cells, carbon dioxide in opposite direction.

• Transfer of transmitter substance: acetylcholine from presynaptic to postsynaptic membrane at a synapse.

1.2. Literature review:

In 1827, Brown noticed that when pollen is dispersed in water, the individual particles did not obey Newtonian dynamics and move down in straight lines until they settle down. They kept moving around in a lively unpredictable manner.

Various explanations of the phenomenon were put forward, it was thought to be caused by irregular heating for incident light, or electrical forces, or temperature differences in the liquid. ln 1877, Delsaux first expressed the theory that the motion was caused by collision of the molecules of the liquid on the immersed particles. When a heavy particle is immersed in a fluid which consists of light molecules in a constant motion due to the heat, the velocity of this particle will vary constantly due to a large number of very small collisions each time the particle runs in to a molecule [1].

In 1905 the, breakthrough occurred when Albert Einstein published a series of papers on diffusion and viscosity. His papers on diffusion came from his PhD thesis, namely, Diffusion. Einstein's contribution can be reviewed as following:

1. Brownian motion of individual jumps of the particle observed at desired time intervals show that the particle has undergone many variation in velocity and what we observe is the net displacement.

2. Brownian motion of particles was basically the same process as diffusion. Thus we can use the same equations for Brownian motion and diffusion.

3. The average distance moved in a given time during Brownian motion is given by

$$\langle x^2 \rangle = 2Dt \qquad (1.1)$$

$\langle x^2 \rangle$ is the average value of the square of the distance, D is the diffusion constant and t is the time of diffusion

4. The equation for the diffusion coefficient of a substance in terms of the radius of the diffusing particles or molecules and other known parameters is given by:

$$D = RT/6\,\pi\, N_a v\, r \qquad (1.2)$$

Where R is a gas constant

T is the absolute temperature

N_a is Avogadro's number ($6x10^{23}$ molecule/mole)

V is the viscosity of the solvent

r is the radius of particle or molecule.

The importance of explanation of Brownian motion was not only a verification of molecular theory which at the turn of century wasn't universally accepted but also a confirmation of what is called now a diffusion process.

There have been several studies on the field of diffusion modeling. Some of them has followed a pure mathematical modeling approach, while others used computer modeling techniques to avoid the apparent mathematical complications.

F. Buda and M. Parrinello studied the diffusion of Hydrogen in crystalline Silicon using the ab initio molecular dynamics (MD) simulations [2].

ln this method, they compute numerically the atomic trajectories resulting from the interatomic forces. Trajectories appropriate to different temperatures can be generated by changing the initial conditions for particle motion. They performed several MD runs at different temperatures higher than 1000 °K. The Hydrogen diffusion coefficient was obtained by measuring the mean square displacement.

A very interesting study was performed by Eric Weeks [3] in the field of diffusion in fluids. He distinguished between two types of random walks, the normal random walks such as those taken by dye molecules diffusing by Brownian motion and a super-diffusion random walk such as that in the stirred fluid systems.

Moshfegh [4] developed a 2D computer simulation model to monitor the diffusion process for Cu/Si and C/Fe with the use of numerical method called a Finite Element Method (FEM). ln the finite element method (FEM), the system under consideration is divided into smaller elements, this discretization process based on concentration gradient and the physical properties of each element. By applying the equations governing the system and imposing boundary conditions (if exist) on each element, a series of linear equation can be obtained. Then, they are assembled based on topology and situation of element, yielding a system of equations. The system equations are adjusted for boundary conditions then solved. This gives the value of c(x,y) at the nodes.

Moshfegh [4] proposed two different thin film system namely Cu/ Si if and C/Fe. In both systems, the variation of Cu concentration was monitored for different temperature, time and space.

Many theoretical efforts have been devoted to calculating diffusion correlation factors. One of them is proposed by Sholl [5] who used the concept of an atom vacancy encounter.

An atom-vacancy encounter is the sequence of exchanges between a particular atom and a particular vacancy. At low vacancy concentrations a vacancy will undergo a

random walk which will result in return visits to a particular atom. The diffusion of an atom in three dimensions is due to sequence of distinct encounters with different vacancies. The successive steps of the atom within an encounter are correlated but the successive encounters are uncorrelated. However, Sholl applied the random walk theory of the atom-vacancy encounters to calculate the solute and solvent diffusivity.

J. A Szpuner developed a two dimensional computer model based on random walk theory and applied it in crystalline and polycrystalline solids [6]. The model is based on the equation:

$$D = 1/4\Gamma r^2 \qquad (1.3)$$

ln this model, the polycrystalline solid is represented by a number of grains and each grain is digitized into number of cells. The cell is small area of the solid and has a square shape. Each cell has three parameters. The first one is the label of the cell which is used to specify the different regions through the sample such that each region has a specific diffusivity. The second set of parameters of the cell is a pair (x,y) to specify the coordinates of the cell in two dimensions. The third parameter of the cell is an integer used to count the number of diffusing atoms in the cell. This model is capable of simulating the effects of texture and microstructure defects.

Kuklja and Popov [7] used the modified semi-empirical simulation method of the Intermediate Neglect Of Differential Overlap (INDO) for studying the various diffusion mechanisms in ionic crystals and calculating the activation energy for diffusion of cation and anion vacancies in KCl as an example of these types of crystals. The relevant activation energies of 1.19 ev and 1.44 ev respectively agree well with the experimental data.

Liu and Shi [8] developed two-dimensional and three-dimensional FEM models to study the transport of ionic species in an externally applied electric field in cementitious samples. Electromigration tests were conducted for different mix designs, the results of which were utilized for inverse parameterization of diffusion coefficients necessary for model predictions. Under the investigated situations, more chlorides are driven out of concrete with increasing current density and treatment time. With increasing initial chloride content, the residual chloride percentage decreases slightly.

Bagno et al. [9] present a computer simulation study of the translational diffusion of the room-temperature ionic liquid [bmim][BF4]. Molecular dynamics simulations have been used, employing a recently developed classical, non-polarizable force field. They compare the results of the simulation with experimental data obtained by NMR spectroscopy and discuss some shortcomings of the simulations. The strong underestimation of calculated diffusion coefficients is traced to artefacts in the simulation and deficiencies in non-polarizable force fields.

The effect of electric field on diffusion of charge carriers in disordered materials is studied by Monte Carlo computer simulations and analytical calculations. It is shown how an electric field enhances the diffusion coefficient in the hopping transport mode. The enhancement essentially depends on the temperature and on the energy scale of the

disorder potential. It is shown that in one-dimensional hopping the diffusion coefficient depends linearly on the electric field, while for hopping in three dimensions the dependence is quadratic. [10]

Kusnadi, and Sudhir studied the effect of moderate electric fields on salt diffusion into vegetable tissue [11]. They determined the effective diffusion coefficients, D_{seff}, of salt into vegetable (celery, mushroom, and water chestnut) tissue under electric field at three temperatures (25, 50, and 80 ° C) and four electric field strengths (0, 658, 1316, and 1842 V/m). Although in an alternating field the electrophoretic driving force either aligns with or opposes diffusion during each half cycle, the net result is an increase in ion transport over time. This is consistent with the rectification theory as expressed by the Nernst‑Planck equation.

Mass transfer in potato slices and strips after Pulsed Electric Fields (PEF) treatment was examined by Janositz et al. to evaluate potential application of PEF in potato processing [12]. PEF treatment on cell material leads to pore formation in cell membrane and thus modifies diffusion of intra- and extracellular media. Results showed enhanced release of intracellular molecules from permeabilized tissue as well as improved uptake of low molecular substances into the sample. This effect increased with the treatment intensity. Furthermore, it was revealed that PEF application leads to a distinct reduction of fat content after deep fat frying and thus provides a potential for the production of low-fat French fries.

Krogh [13] stated that the diffusion of gases through animal tissues must take place in the same way as their diffusion through fluids or colloidal membranes. The gases are dissolved in the tissue fluids and diffuse in a liquid state. The laws governing the diffusion of gases through water and watery solutions have been worked out by Exner [14], who found that the rates of diffusion for different gases in the same fluid are proportional to the absorption coefficients of the gases in the fluid and inversely proportional to the square roots of their molecular weights.

Tachiya studied the relation between the fractal geometry of reactant trajectories and the rate of diffusion-controlled reactions [15]. He proposed a possible mechanism for the effect of an external electric field on the rate of reactions on the basis of this consideration. The proposed mechanism predicts an increase in the rate constant with increasing electric field strength.

Salford [16] studied the effect of electromagnetic fields on the blood-brain barrier. He concluded that the man made EMFs, such as those utilized in mobile communication, even at extremely low SAR values, causes the users' own albumin to leak out through the BBB which is meant to protect the brain. Also other unwanted and toxic molecules in the blood may leak into the brain tissue. There they concentrate in, and damage, the neurones and glial cells of the brain according to their studies.

Smith and Sansom [17] studied the effective diffusion coefficients of K+ and Cl− ions in ion channel models. They found that the diffusion coefficients of both ions are

appreciably reduced in the narrower channels, the extent of the reduction being similar for both the anionic and cationic species.

Diffusion in the extracellular space (ECS) of the brain was studied by Sykova and Nicholson [18]. They found that diffusion in ECS is constrained by the volume fraction and the tortuosity and a modified diffusion equation represents the transport behavior of many molecules in the brain. Deviations from the equation reveal loss of molecules across the blood-brain barrier, through cellular uptake, binding, or other mechanisms. They used the real-time iontophoresis (RTI) method to study diffusion of small ions.

1.3. The aim of the present work:

In response to the increasing global concern about the biological effects of electromagnetic fields (EMF) around us, the present work is to prove some insight on such effects. The aim of the present work is to study the diffusion process in biological material and the possible effects of electric field on diffusion. A computer model is built to simulate the diffusion process.

The free random walk pattern is simulated. The algorithm follows the free movement of a number of particles that start from an origin. After considerable time the pattern is predicted and effect of time on mean square displacement is tested.

The model employs simulation to study the effect of annealing time and vacancies concentration on diffusion in thin film method. The penetration distance is tested and the diffusion coefficient is calculated.

The effect of direct current (both forward and negative directions) and extremely low frequency (ELF) on ionic diffusion is tested. The effect is compared by calculating the diffusion coefficient in each case.

The effect of alternating current is investigated. The present model compares the effects of sinusoidal and square waves on penetration of positive ions through biological tissues.

The effect of tissue structure on diffusion is investigated under the electric field.

CHAPTER 2: DIFFUSION IN BIOLOGICAL MEDIA

2.1. Diffusion in matter:

The elements and their chemical compounds generally exist in three states namely the solid, liquid and gaseous states. In solids and liquids the distance between neighboring atoms is of order of a few Angstroms, they contain 10^{22}-10^{23} atoms per cm^3 [19].

This may be compared with a density of about $2.7*10^{19}$ molecules in a gas at room temperature under atmospheric pressure, corresponding to an average distance of approximately 30°A between molecules.

There are many models and theories to understand the nature of a gas. In the hard sphere model each molecule is considered to be a hard sphere that collides elastically with other molecules and with the container wall. The model assumes that the molecules do not interact with each other except during collisions and that they are not deformed by collisions [20].

Liquid state is the region in which matter is stable at densities and temperatures intermediate between the regions of stability of the solid and gaseous states. Brownian motion is well observed in liquid state. If a drop of solution such as ink is placed in water, it will tend to spread out and the mixture will ultimately become homogeneous. In this latter experiment a concentration gradient is present and the flux of the ink molecules exists, a diffusion coefficient could be measured. There are many theories about the diffusion in liquids [21]. The hole model is accepted by several investigators [22,23]. Eyring suggested that atoms which possess enough energy to surmount the potential energy barrier, will jump from one hole to another. After making their jumps they should stay at the new configuration long enough to dissipate their excess energy.

The model suggests the applicability of Arrhenius equation to the diffusion coefficient in liquids which is given by

$$D=D_o e^{(-Q/KT)} \qquad (2.1)$$

Where D is the diffusion coefficient, D_o: is the diffusion coefficient at 0^oK and Q: is the activation energy.

The Cell model assumes that, firstly, each particle in the liquid is assigned to a certain cage made by its nearest neighbors. The central particle spends most of its time within this cage. Secondly, the potential energy is constant inside the cage and is infinitely at the boundary. Thirdly, the total potential energy of the system is the sum of the potential energy of the individual particles. Finally, the model suggests that the particles inside their cages move with a gas velocity.

The temperature dependence of the diffusion coefficient D has been a potent source of controversy and a number of relations have been proposed such as, $D\alpha T^2$ [24],

$D\alpha T_m$ [25] and $D = a + b \times T$ [26]. Where a, b are characteristic constants which differ from one liquid to and T_m is the melting point.

The gas model treats the dense liquids and fluids as a continuation of the gaseous state; hence the diffusion coefficient of liquid D should be related to that of a perfect gas D_g. The mean free path of a liquid is in the same order of magnitude of the atomic dimension [27].

Generally, the basic laws which govern the diffusion in liquid are Fick's laws as in the solids. In most solids and particularly in crystalline ones, the atoms are more tightly bound to their equilibrium positions. However, there still remains an element of uncertainty caused by thermal vibration occurring in a solid which permits some atoms to move through the lattice at random. A large number of such movements results in a significant transport of material. This phenomenon is called solid state diffusion. Even in a pure substance a particular atom doesn't remain at one equilibrium site indefinite, rather, it moves from place to place in the material.

2.2. Examples of diffusion in biology

2.2.1. Blood filtering in the kidney (glomerular filtration barrier)

One of the fundamental requirements for life is the ability to eliminate toxic metabolic byproducts. This process takes place in the renal corpuscle of the kidney. The glomerular filter through which the ultrafiltrate has to pass consists of three layers: the fenestrated endothelium, the intervening glomerular basement membrane, and the epithelial podocyte foot processes. This filtration barrier behaves as a size-selective sieve restricting the passage of macromolecules on the basis of their size, shape, and charge [28,29,30]. Podocytes are the visceral epithelial cells of the kidney glomerulus [31,32,33]. They elaborate long, regularly spaced, interdigitated foot processes that completely enwrap the glomerular capillaries. Interdigitating podocyte foot processes form an ~40-nm-wide filtration slit and are connected by a continuous membrane-like structure called the slit diaphragm.

Glomerular Filtration Process

An almost protein-free ultrafiltrate passes into Bowman's capsule from the glomerular capillaries. Molecular size is the main determinant of whether a substance will be filtered or will be retained in the capillaries. However, molecular shape and charge also influence the filtration process, although these factors are of significance only for large molecules. For example, the rate of filtration of albumin (molecular weight 68,000), which has a negative charge, is only about 1/20 that of uncharged dextran molecules of the same molecular weight. This finding suggests that the glomerular filtration barrier has fixed anions, which repel anionic macromolecules and thereby hinder or prevent the filtration of such molecules.

In the glomerulus, the molecular weight cut-off for the filter is about 70,000. Plasma albumin, with a molecular weight of 68,000, passes through the filter in minute

quantities (retarded also by its charge, as mentioned above). Smaller molecules pass through the filter more easily, but the filter is freely permeable only to those molecules with a molecular weight less than about 7,000.

Since the glomerular filter permits the free passage of molecules of molecular weight less than 7,000, the initial glomerular filtrate will contain small molecules and ions (e.g. glucose, amino acids, urea, sodium, potassium) in almost exactly the same concentrations as the afferent arteriolar concentrations, and similarly the efferent arteriolar concentrations of such substances will not have been significantly altered by the filtration process.

The permeability of glomerular capillaries is about 100 times greater than the permeability of capillaries elsewhere in the body.

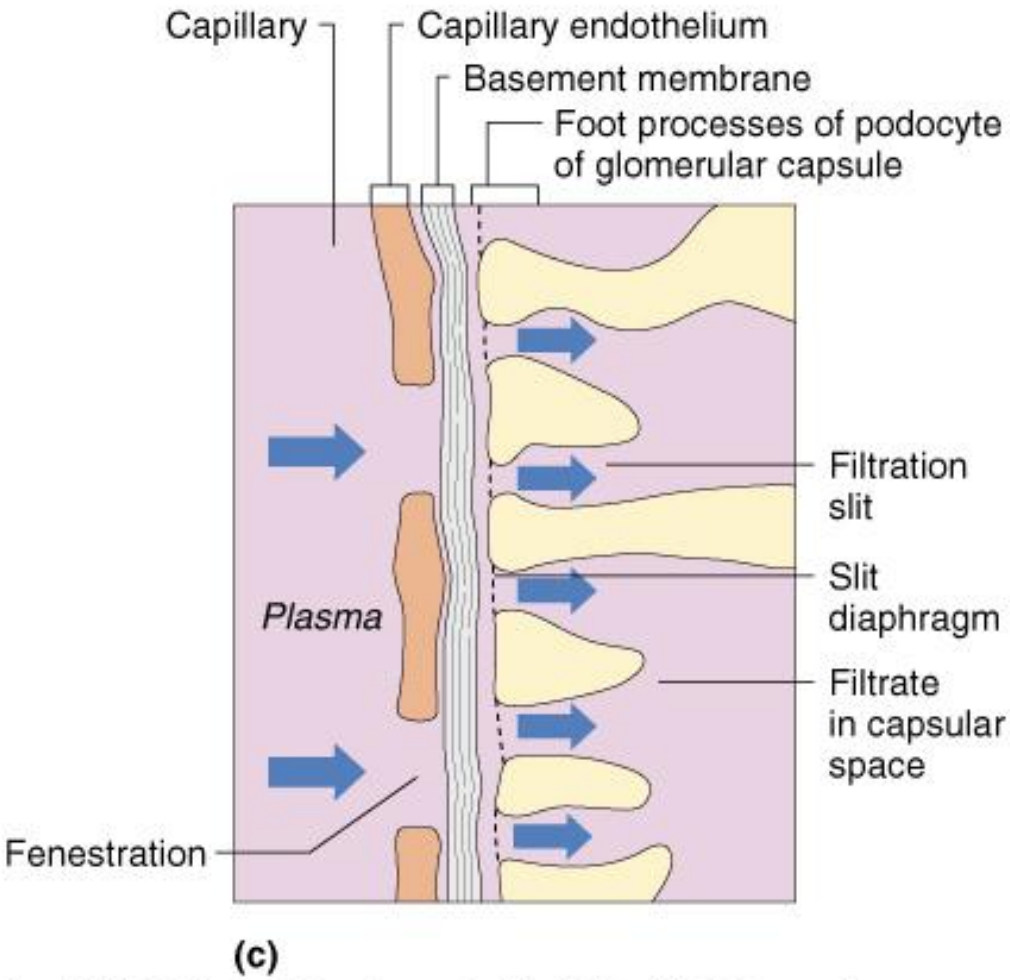

Figure (2.1) Blood filtering in the glomerulus

2.2.2. Blood-air barrier

The alveolar–capillary barrier or blood–air barrier exists in the gas exchanging region of the lungs. It exists to prevent air bubbles from forming in the blood, and from blood entering the alveoli. It is formed by the type 1 pneumocytes of the alveolar wall, the endothelial cells of the capillaries and the basement membrane between the two cells. The barrier is permeable to molecular oxygen, carbon dioxide, carbon monoxide and many other gases [34].

This blood gas barrier is extremely thin (varying in thickness from 0.4 to 2μm) (600–800 nm; in some places merely 200 nm) to allow sufficient oxygen diffusion, yet it is extremely strong.

The diffusion of gases through animal tissues must take place in the same way as their diffusion through fluids or colloidal membranes [13]. The gases are dissolved in the tissue fluids and diffuse in a liquid state. The laws governing the diffusion of gases through water and watery solutions have been worked out by Exner [14] who found that the rates of diffusion for different gases in the same fluid are proportional to the absorption coefficients of the gases in the fluid and inversely proportional to the square roots of their molecular weights.

Effective pulmonary gas exchange relies on the free diffusion of gases across the thin tissue barrier separating airspace from the capillary red blood cells (RBCs). Pulmonary pathologies, such as inflammation, fibrosis, and edema, which cause an increased blood–gas barrier thickness, impair the efficiency of this exchange.

The value of D for oxygen diffusing through connective tissue was found by Krogh [13] to be 1.5×10^{-5} cm^2/sec and that for hydrogen will be approximately four fold greater, or 6×10^{-5} cm^2/sec.

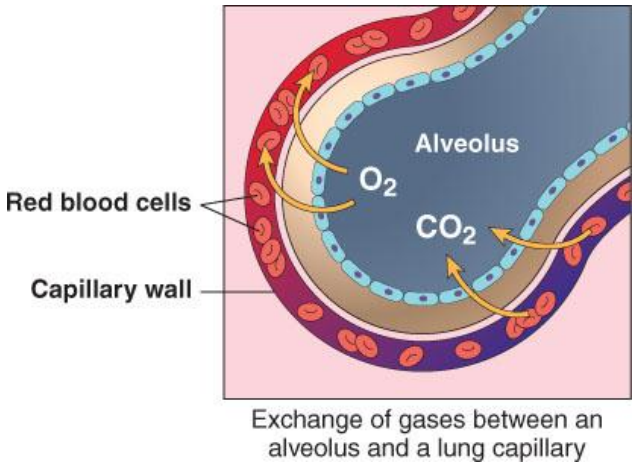

Figure (2.2) Blood-air barrier

2.2.3. Blood brain barrier

The mammalian brain is protected from exposure to potentially harmful compounds in the blood by the blood-brain barrier. Being formed by the vascular endothelial cells of the capillaries in the brain, this hydrophobic barrier maintains and regulates the very sensitively tuned environment within the mammalian brain [16].

The blood-brain barrier is a highly complex system, in which several kinds of cells exert a wide range of functions. Some of the main characteristics are described below [16]:

- The cell-to-cell contacts between the capillary endothelial cells are sealed with tight junctions, forming a permeability barrier, which is much more selective as compared to the fenestrated sealing of other capillaries.

- The outer surface of the endothelial cells is surrounded by protrusions (end feet) from astrocytes. Thereby, the endothelial cells and the neurons are connected and also, a second hydrophilic barrier is formed. Also, the astrocytes are implicated in the maintenance, functional regulation and repair of the blood-brain barrier.

- A bilayer basal membrane supports the ablumenal surface of the endothelial cells. This membrane might also further restrict the passage of macromolecules into the brain parenchyma.

- Pericytes are other periendothelial accessory structures of the blood-brain barrier. These have capacity for phagocytosis as well as antigen presentation and in fact, they seem to contribute significantly to the immune mechanisms of the central nervous system. All these characteristics of the blood-brain barrier guarantee that only those molecules, which are either hydrophobic (such as oxygen, nitric oxygen and steroid hormones), or bind to specific receptors (such as certain amino acids and sugars), can pass freely from the blood circulation out into the brain parenchyma.

Additionally, there is also a weight-selectivity, where particles of a larger molecular weight are more electively excluded from passage over the blood-brain barrier.

In a number of pathological conditions, such as epileptic seizures, sepsis and severe hypertension, the integrity of the blood-brain barrier is disturbed. The sensitively tuned balance within the brain parenchyma is thereby disrupted. This might lead to cerebral oedema, increased intracranial pressure and in the worst case, irreversible brain damage. In conclusion, an intact and fully functioning blood-brain barrier is essential for the proper function of the mammalian brain.

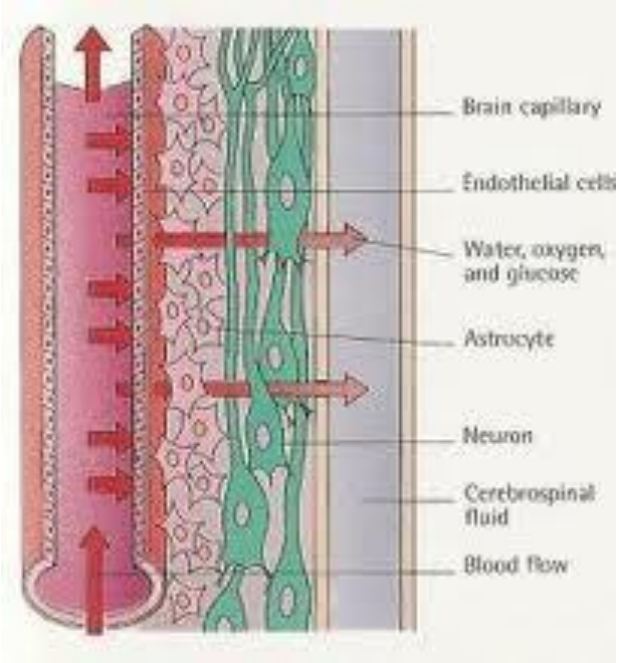

Figure (2.3) Blood-brain barrier

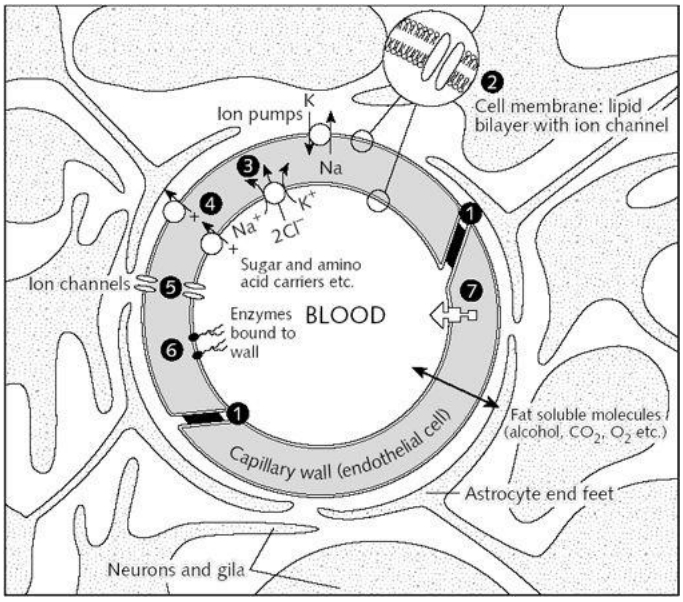

2.3. Mathematical description of diffusion:

2.3.1. The diffusion coefficient and random walk

There are two equivalent ways in which to think of the average value of any intensive property of a statistically large collection of particles in thermal equilibrium. One Method consists of performing the desired calculations by assuming the appropriate distribution function. Secondly, a more convenient method's to perform the calculation using a single particle which is postulated to have the mean value of the property of interest.

Consider a single particle executing random walk in two dimensions of individual steps r_n, all jump directions have equal priori probability and are uncorrelated with the preceding jumps.

After executing n elementary jumps, as shown in figure (2.4) the particle has moved an absolute distance $|R_n|$ from its origin. Hence, we can write the following vector equation

$$\overrightarrow{R_n} = \sum_{i=1}^{n} \vec{r_i} \qquad (2.2)$$

and squaring both sides gives

$$R_n^2 = \overrightarrow{R_n}.\overrightarrow{R_n}$$

$$= r_1.r_1 + r_1.r_2 + \cdots\cdots\cdots + r_1.r_n$$

$$+r_2.r_1 + r_2.r_2 + \cdots\cdots\cdots + r_2.r_n$$

$$+r_n.r_1 + r_n.r_2 + \cdots\cdots\cdots + r_n.r_n$$

$$=\sum_{i=1}^{n} r_i.r_i + 2\sum_{i=1}^{n-1} r_i.r_{i+1} + 2\sum_{i=1}^{n-2} r_i.r_{i+2} + \cdots$$

$$=\sum_{i=1}^{n} r_i^2 + 2\sum_{j=1}^{n-1}\sum_{i=1}^{n-j} r_i.r_{i+j} \qquad (2.3)$$

The average value of R_n^2 is given by (Shewmon, 1989):

$$\overline{R_n^2} = nr^2\left[1 + \frac{2}{n}\overline{\sum_{J=1}^{n-1}\sum_{\iota=1}^{n-J} cos\Theta_{\iota,\iota+J}}\right] \qquad (2.4)$$

Where $\Theta_{i,i+j}$ is the angle between i^{th} and $(i+j)^{th}$ jump. As all jump directions are equally probable, the term containing the double sum vanishes as the values of - $\Theta_{i,i+j}$ and $\Theta_{i,i+j}$ occur with the same probability. Hence:

$$\overline{R_n^2} = nr^2 \tag{2.5}$$

ln order to relate the results of (2.5) to the diffusion coefficient, We begin by selecting a specific solution (2.20) which is appropriate for diffusion from an thin planer source into a semi-infinite solid. We notice that (2.20) is a solution to Fick's second law by differentiation

$$c(x) = \alpha t^{-1/2} e^{-x^2/4Dt} \tag{2.6}$$

Where $\alpha = bc_o/2(\pi D)^{1/2}$, bc_o is the total amount of diffused material and t is the time over which diffusion occurred. The probability p(x) of finding an atom between x and x+Δx is given by the fraction of atoms between these two points:

$$p(x)dx = \frac{c(x)dx}{\int_{-\infty}^{+\infty} c(x)dx} = \frac{\alpha}{\sqrt{t}} e^{-x^2/4Dt} \tag{2.7}$$

The integral in (2.7) is equal to unity and the numerator is the distribution function p(x). The average value of x^2 is calculated in the usual manner using (2.8)

$$< x^2 >= \int_{-\infty}^{+\infty} x^2 p(x)dx = \frac{\alpha}{\sqrt{t}} \int_{-\infty}^{+\infty} x^2 e^{-x^2/4Dt}\, dx \tag{2.8}$$

Let $\zeta = x^2/4Dt$ we get:

$$< x^2 >= \frac{\alpha}{\sqrt{t}} \int_{-\infty}^{+\infty} (Dt)^{3/2} \zeta^2 e^{-\zeta^2}\, d\zeta \tag{2.9}$$

$$< x^2 \geq \frac{4Dt}{\pi^{1/2}} \int_{-\infty}^{+\infty} \zeta^2 e^{-\zeta^2}\, d\zeta = \frac{4Dt}{\pi^{1/2}} \frac{\pi^{1/2}}{2} = 2Dt \tag{2.10}$$

we can identify $< x^2 >$ with $< R_n^2 >$ in one dimension and write it as:

$$< R^2 >= 2Dt = nr^2 \tag{2.11}$$

$$D = nr^2/2t \tag{2.12}$$

The similar treatment is for random walk and diffusion in two dimensions and three dimensions except that the factor 2 in the denominator is four in the case of the two dimensions and six in the case of three dimensions as follows:

$$D_{2D} = < R_n^2 > /4t \tag{2.13}$$

$$D_{3D} = < R_n^2 > /6t \tag{2.14}$$

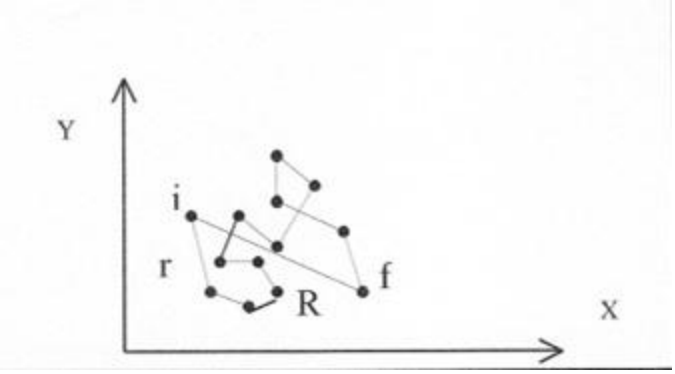

Figure (2.4) a particle executing a random walk of equal length jumps. The particle starts walk at (i) and ends at (f) with total net displacement R

2.3.2. Fick's laws:

In 1855, Fick proposed his first law of diffusion namely,

$$J = -D_i \nabla c_i \tag{2.15}$$

Where J, the flux , is the number of particles passing through a plane of unit area per unit time, c is the concentration and D is the diffusion coefficient along one of the principle axis x or y or z. For an isotropic medium, such as a gas or liquid or for a solid with cubic symmetry $D_x=D_y=D_z$

For crystals that have two perpendicular axes of symmetry, e. g, tetragonal, hexagonal, (2.15) becomes

$$J = -D_x \frac{\partial c}{\partial x} - D_y \frac{\partial c}{\partial y} \tag{2.16}$$

Also, the Fick's law can be extended to describe the diffusion in three dimensions as follows:

$$J = -D_x \frac{\partial c}{\partial x} - D_y \frac{\partial c}{\partial y} - D_z \frac{\partial c}{\partial z} \tag{2.17a}$$

Or

$$J = -D \nabla c \tag{2.17b}$$

Combination of Fick's first law together with the law of conservation of mass gives

$$\frac{\partial c}{\partial t} = \nabla D \nabla c \tag{2.18}$$

The above equation is known as Fick's second law. lf, D, is independent of concentration , c, the latter equation can be written as

$$\frac{\partial c}{\partial t} = D\nabla^2 c \qquad (2.19)$$

The experimenter allows the diffusion to proceed for a fixed period of time, then halts it abruptly usually by rapidly lowering the temperature and the concentration gradient is directly determined. The detection of the concentration c of the diffusant species is carried out by using chemical techniques. The discovery of radioactivity helps the measurements. The radioactive tracer could be very small still could be measured accurately [36]. This permits calculation of D by solving (2.19) in which the flux at any given point is time dependent.

2.3.3. Solution of diffusion equation:

Thin film solution

A thin planer source of the solute of concentration c_o is plated on the flat surface of long rod of the solvent bar then another solvent bar is welded to the plated end, sandwiching the solute between the two rods. The rod is then annealed for a time t so that diffusion can occur.

The concentration of solute along the bar will be given by the equation [35]:

$$c(x,t) = \frac{bc_o}{2\sqrt{\pi Dt}} \exp\left[\frac{-x^2}{4Dt}\right] \qquad (2.20)$$

where b is the thickness of the film , x is the penetration measured from the boundary surface between the diffusant and solvent and t is the time of annealing or the time of diffusion . D is the diffusion constant and b is the thickness of the film.

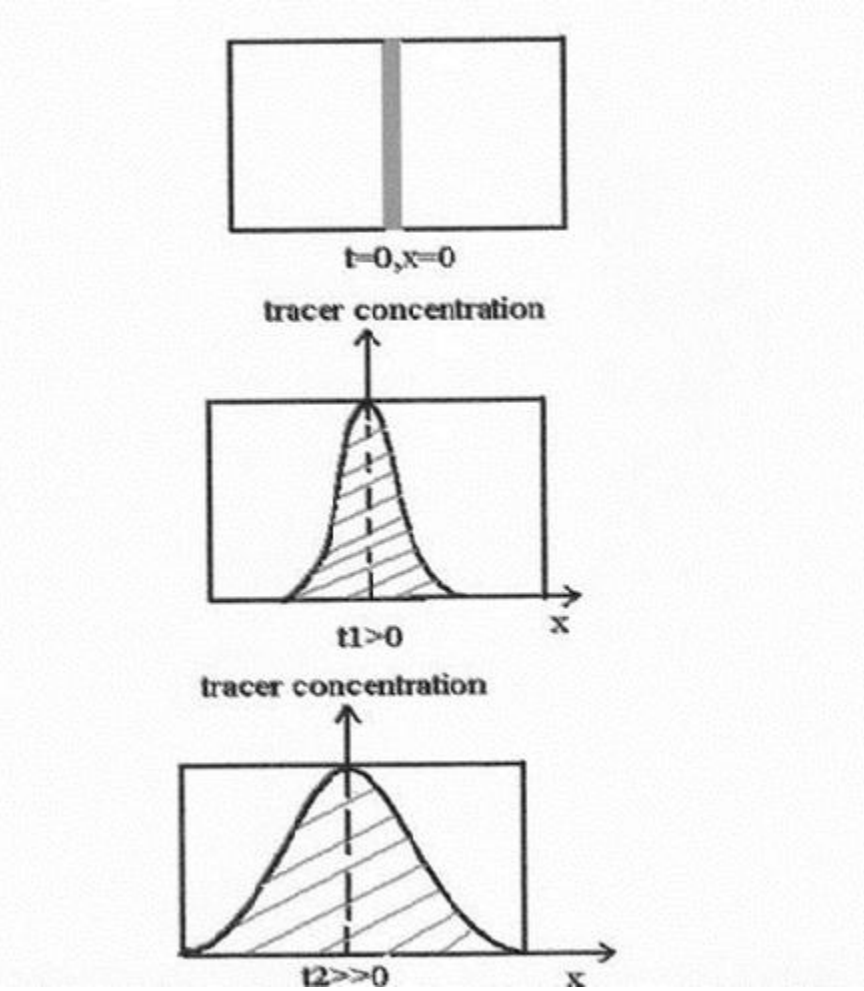

Figure (2.5) The time sequence of diffusion profiles displaying the tracer concentration against penetration distance

2.4. Diffusion Mechanisms:

2.4.1. Vacancy mechanism

In the material structures some of the sites are unoccupied. These unoccupied sites are called vacancies. If one of the atoms on an adjacent site jumps into the vacancy, the atom is said to be diffused via vacancy mechanism as shown in figure (2.6).

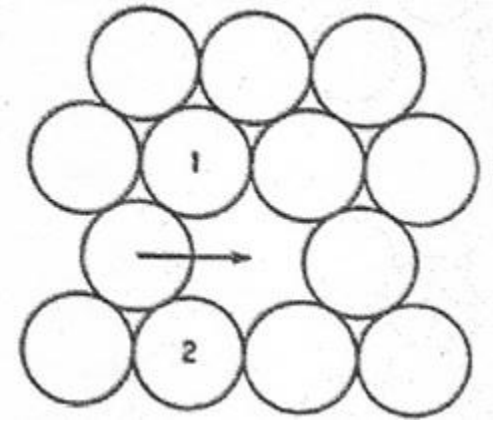

Figure (2.6) Vacancy mechanism

2.4.2. Interstitial mechanism

An atom is said to diffuse by an interstitial mechanism when it passes from one interstitial site to one of its nearest-neighbor interstitial sites without permanently displacing any of the matrix atoms. Figure (2.7) shows an interstitial atom in a group of packed spheres. Before the atom labeled l can jump to the nearest neighbor site 2 the matrix atoms labeled 3 and 4 must move apart enough to let it through. Accordingly, local dilation of the structure must occur before the jump can happen. This dilation constitutes the barrier to an interstitial atom changing sites. The jump frequency is determined by how often this barrier can be surmounted.

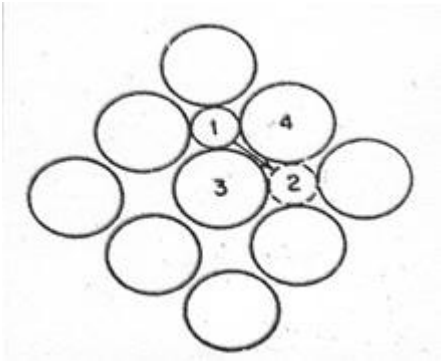

Figure (2.7) interstitial mechanism

2.5. Temperature dependence of diffusion:

2.5.1. Arrhenius equation

A simple exponential dependence of specific rate theory upon temperature implies the existence of an energy barrier situated between the initial and final configuration which can be surmounted by a thermal activation. In fact, diffusion in general is a thermally activated process. Thus, the diffusive jump mechanism is characterized by an initial configuration which passes through the continuous changes in the coordinates to a final equilibrium configuration as shown in figure (2.8).

There is an intermediate configuration which is decisive to the process so that if the system gets this configuration, it has a high probability that the jump will occur. This critical configuration is called the saddle point and the particles at the saddle point are called activated complex.

The above configuration is called continuous Boltzmann distribution of energy among the individual atoms of the system [35].

Consider particle moving in a fixed potential energy curve as shown in figure (2.5). Let the potential minimum (I) correspond to the position in which the particle finds itself and let (F) correspond to a neighboring vacant position. Assuming the potential to be a parabolic, the particle will vibrate as a harmonic oscillator. The frequency of vibration ω_o may be considered as the number of attempts per second made by the particle to cross the barrier [36]. However, any attempt can succeed only if the energy of the particle larger than or equal to ΔG^*.

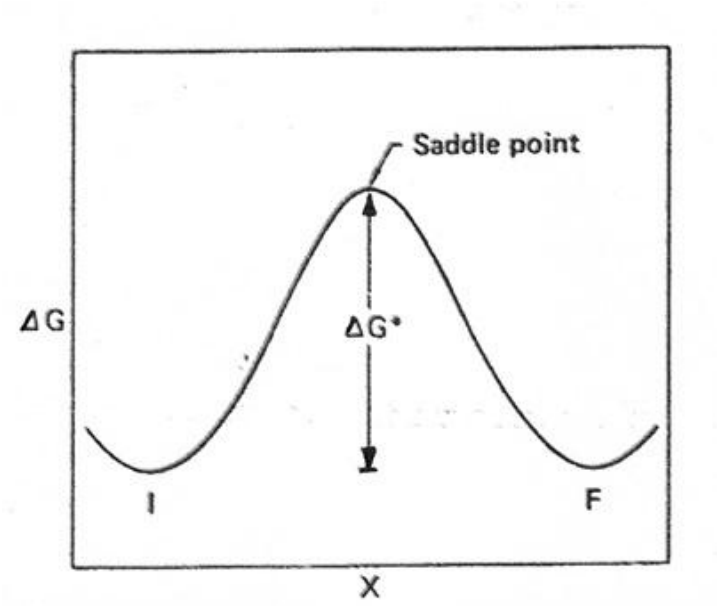

Figure (2.8) The potential energy curve according to the rate theory [36]

The Arrhenius relationship is a valid description of the temperature dependence of the diffusion coefficient. The empirical equation is written according to:

$$D = D_o e^{-Q/RT} \tag{2.21}$$

Where Q is the activation energy.

The fraction of time spent by the particle in energy state larger than or equal to ΔG^* is simply given by exp(-ΔG^*/Rt). Hence, for probability of a jump from (a) to (b) per second is given by:

$$\gamma = \omega_o e^{-\Delta G^*/RT} \tag{2.22}$$

Remembering that D in one dimension is given by:

$$D = \frac{1}{2}\gamma a^2 \tag{2.23}$$

Where a is the elementary jump distance, substituting for γ in the above relation, we obtain:

$$D = \frac{a^2}{2}\omega_o e^{-\Delta G^*/RT}$$
$$= \frac{a^2}{2}\omega_o e^{-(\Delta S^*/RT - \Delta H^*/RT)} \tag{2.24}$$

We note that the same derivation for diffusion in three dimensions for an isotropic or isometric medium merely replaces 1/2 by l/6 in the right hand side of equation (2.24).

ln order for an atom to diffuse via vacancy mechanism, a vacancy must first exist as a nearest neighbor to diffusing atom, hence the diffusion coefficient must be multiplied by the probability of formation of an adjacent vacancy governed by Boltzmann factor which is given by

$$X_V = \frac{N_V}{N} = e^{-\Delta G_V/RT} \tag{2.25}$$

where N_V is the number of vacancies through N total lattice sites and ΔG_v is the free energy of formation of one mole of vacancy . Hence, the diffusion coefficient becomes:

$$D = \frac{a^2}{2}\omega_o e^{-\Delta G^*/RT} p_o e^{-\Delta G_V/RT}$$

$$D = \frac{a^2}{2}\omega_o p_o e^{-(\Delta G_V + \Delta G^*)/RT} \tag{2.26}$$

Decomposing the free energy terms into its thermodynamical equivalent, we obtain [19]:

$$D = \frac{a^2}{2}\omega_o p_o e^{-(\Delta S_V + \Delta S^*)/RT} e^{-(\Delta H_V + \Delta H^*)/RT} \tag{2.27}$$

Where ΔH^*: the enthalpy of motion per mole of activated complexes

ΔH_v : enthalpy of formation per mole of vacancies

ΔS^*: entropy of motion per mole of activated complexes

ΔS_v: entropy of formation per mole of vacancies.

Comparing equation (2.29) with equation (2.23), we find the value of D_o which is given by:

$$D_o = \frac{a^2}{2}\omega_o p_o e^{-(\Delta S_V + \Delta S^*)/RT} \tag{2.28}$$

2.6. Correlation factor

The correlation factor is a numerical correlation which accounts for the fact that an atom which diffuses via vacancies doesn't execute a strictly random walk. It was pointed out by Bardeen and Herring that even though the vacancies each jump at random, successive jumps of any particular atom are not at random [37]. In other words, after exchanging sites with a vacancy, the two entities namely particle and vacancy remain nearest neighbors. Hence, the next jump of the atom has a greater probability of returning to its previous position because the atom has just deposited the vacancy behind it, so the directions of successive atomic jumps are correlated. Accordingly, in travelling a given distance R_n from the origin, more jumps are required by the atom to achieve R_n than would be expected when successive jumps were not correlated, as in interstitial diffusion.

This means that the expression of the diffusion coefficient D should contain a factor less or equal to unity for any correlation

The correlation factor can be written as [35];

$$f = lim \frac{\overline{R_n^2}(correlated)}{\overline{R_n^2}(random)} \tag{2.29a}$$

Or

$$f = lim \frac{\overline{R_n^2}(particle)}{\overline{R_n^2}(vacancy)} \tag{2.29b}$$

$$f = 1 + 2\overline{cos\theta_1} + 2\overline{cos\theta_2} + 2\overline{cos\theta_3} + \cdots\cdots\cdots + 2\overline{cos\theta_{n-1}} \tag{2.30}$$

Where $\cos\theta_i$, is the average value of cosine the angle between the first jump and the ith following jump.

Accordingly, the diffusion coefficient has the form

$$D_o = \frac{a^2}{2} f \omega_o e^{-(\Delta G_V + \Delta G^*)/RT} \tag{2.31}$$

For self diffusion, f is a geometrical factor that depends only on the diffusion mechanism and the crystal structure. Thus, values of f for self diffusion in different lattice structures by vacancy mechanisms, were obtained experimentally [35].

In the case of impurity diffusion, the correlation factor f is a function of the relative jump frequencies, thus f can be written as:

$$f = \frac{\omega_1}{\omega_1 + \omega_2} \tag{2.32}$$

Where ω_1, ω_2 are the atomic jump frequencies for the host atom and tracer atom respectively.

2.7. Pressure dependence of diffusion

The response of D to the application of relatively large pressure is small compared to thermal effects. Additionally, almost all diffusive processes of interest to material scientists occur near the ambient value of atmospheric pressure. Nevertheless, significant information can be derived from the weak pressure dependence of D. Also, diffusion under high pressure takes place for raw materials as we do deep below the surface of the earth. These materials are subjected to influential effects resulting from enormous pressure.

When a vacancy is formed in a solid, the volume of the crystal increases by the volume of one atom. If the hydrostatic pressure is applied to a solid at equilibrium one might expect that the equilibrium concentration of vacancies would decrease, allowing the external pressure to do work on the system. Thus if the self diffusion occurs by vacancy mechanism, one would expect the diffusion coefficient to decrease appreciably with increasing pressure.

The relation between the diffusion coefficient D and the applied pressure is derived by taking the logarithm of (2.28) and differentiating with respect to pressure, P, at constant temperature. Finally, the pressure dependence of diffusion is given by equation [36]:

$$\left[\frac{\partial \ln(D/a^2\omega_o}{\partial P}\right] = -\frac{1}{RT}[\Delta v^* + \Delta v_V] \tag{2.33}$$

Where Δv_V and Δv^* are the change in the volume of the solid due to the vacancy creation at non zero pressure and the change in the volume due to atomic migration respectively

2.8. Electric field dependence of diffusion:

Charge carrier transport in disordered materials - inorganic, organic and biological systems has been in the focus of intensive experimental and theoretical study for several decades due to various current and potential applications of such materials in modern electronic devices [38]. An essential part of the research is dedicated to the study of the mobility of the charge carriers, μ, and their diffusion coefficient, D, as the decisive transport coefficients responsible for performance of most devices. Among other features, the relation between these two transport coefficients is the subject of intensive research, since this relation (called the "Einstein relation") often provides significant information on the underlying transport mechanism. The conventional form:

$$\mu = \frac{e}{KT} D \tag{2.34}$$

Where e is the elementary charge, T is the temperature and k is the Boltzmann constant. According to Einstein, such a relation between μ and D is valid in the case of thermal equilibrium for a non-degenerate system of charge carriers.

The movement of ions under an electric field occurs because of two driving forces [39,40]: the concentration gradient and the electric field.

$$J_i = \frac{-D_{s0} \nabla C_i}{l} + \mu_i C_i E \tag{2.35}$$

Where J_i is the current due to species i, D_{s0} is the effective diffusivity at zero electric field strength,C_i concentration of species i, μ_i ionic mobility of species i, E is electric field strength. This expression is principally applicable for direct current (D.C.). Under the alternating conditions, the movement of anions and cations would alternately coincide with, or oppose the concentration gradient each half cycle. Thus, the approach has limitations, but it can be used to gain understanding of field strength effects.

2.8.1. Penetration in biological tissues:

When a conductive material is exposed to an EM field, it is submitted to current density caused by moving charges. In solids, the current is limited by the collision of electrons moving in a network of positive ions. Good conductors such as gold, silver, and copper are those in which the density of free charges is negligible, the conduction current is proportional to the electric field through the conductivity, and the displacement current is negligible with respect to the conduction current. The propagation of an EM wave inside such a material is governed by the diffusion equation, to which Maxwell's equations reduce in this case. Biological materials are not good conductors. They do conduct a current, however, because the losses can be significant: They cannot be considered as lossless. [41]

Solving the diffusion equation, which is valid mainly for good conductors, where the conduction current is large with respect to the displacement current, shows that the

amplitude of the fields decays exponentially inside of the material, with the decay parameter

$$\delta = \frac{1}{(\omega\mu\sigma/2)^{1/2}} \tag{2.36}$$

Where ω is the frequency, μ is the permeability of the material, σ is the conductivity. The parameter δ is called the skin depth, It is equal to the distance within the material at which the fields reduce to 1/2.7 (approximately 37%) of the value they have at the interface. One main remark is that the skin depth decreases when the frequency increases, being inversely proportional to the square root of frequency. It also decreases when the conductivity increases: The skin depth is smaller in a good conductor that in another material. Furthermore, it can be shown that the fields have a phase lag equal to z/δ at depth z. For most biological materials the displacement current is of the order of the conduction current over a wide frequency range. When this is the case, a more general expression should then be used instead of (2.36) [42]

	$\delta = \left(\frac{1}{\omega}\right)\left\{\left(\frac{\mu\varepsilon}{2}\right)\left[(1+p^2)^{1/2}-1\right]\right\}^{1/2}$	(2.37)

Where $p = \sigma/\omega\varepsilon$ is the ratio of the amplitudes of the conduction current to the displacement current. ε is the permittivity of the material.

It is easily verified that Eqn. (2.37) reduces to Eqn. (2.36) when *p* is large.

The following important observations can be deduced from Eqn. (2.36):

1. The fields exist in every point of the material.

2. The field amplitude decays exponentially when the depth increases.

3. The skin depth decreases when the frequency, the permeability, and the conductivity of the material increase. For instance, the skin depth of copper is about 10mm at 50Hz, 3mm at 1kHz, and 3μm at 1GHz. It is equal to 1.5 cm at 900 MHz and of the order of 1 mm at 100 GHz in living tissues.

These results are strictly valid for solids limited by plane boundaries. They are applicable to materials limited by curved boundaries when the curvature radius is more than five times larger than the skin depth. In the other cases, a correction has to be applied. The phenomenon just described is the *skin effect*: Fields, currents, and charges concentrate near the surface of a conducting material. This is a shielding effect: At a depth of 3δ, the field amplitude is only 5% of its amplitude at the interface, and the corresponding power is only 0.25%; at a depth of 5 δ, the field amplitude reduces to 1% and the corresponding power to 10^{-4}, which is an isolation of 40dB. This shows that, at extremely low frequency, for instance at 50Hz, it is illusory to try to shield a transformer with a copper plate: A plate 5 cm thick would be necessary to reduce the field to 1%! This is the reason why materials which are simultaneously magnetic and conducting,

such as metals, are used for low-frequency shielding. In practice, the skin effect becomes significant for humans and larger vertebrates at frequencies above 10MHz. [41]

Shielding is much easier to achieve at higher frequencies. The skin effect implies that, when using microwaves for a medical application, the higher the frequency, the smaller the penetration, which may lower the efficiency of the application. Hence, the choice of frequency is important. It also implies that if a human being, for instance, is submitted to a microwave field, the internal organs are more protected at higher than at lower frequencies. As an example, the skin depth is three times smaller at 900MHz, a mobile telephony frequency, than at 100MHz, an FM radio frequency, which means that the fields are three times more concentrated near the surface of the body at 900MHz than at 100MHz. It also means that internal organs of the body are submitted to higher fields at lower than at higher frequency.

Table (2.1) summarizes some skin depth values for human tissues at some frequencies. The EM properties of the tissues as well as their variation as a function of frequency have been taken into account.

Parameter	Radio FM	TV Transmitter	Telephony Mobile	Telephony Mobile
Frequency (MHz)	100	450	900	1800
Skin depth (cm)	3	1.5	1	0.7
Depth at which power reduces to 1% (cm)	9	4.5	3	2

Table (2.1) Typical skin depths in human tissue

Figure (2.9) shows the variation of the power absorbed inside a human body as a function of the penetration depth at several microwave frequencies: We are less and less transparent to nonionizing EM radiation when the frequency increases. In the optical range, skin depth is extremely small: We are not transparent anymore. Variation of the dielectric constant as a function of frequency was taken into account in this figure. There is a tendency to believe that RFs and microwaves exert more significant biological effects at low and extremely low frequencies. This is not necessarily true: The dielectric constant of living materials is about 10,000 times larger at ELF than at microwaves. The dielectric constant is important because it is the link between the source field and the electric flux density (also called the displacement field). A dielectric constant 10,000 larger implies the possibility of an electric flux density of a given value with a source field 10,000 times smaller. Figure (2.10) shows the dielectric constant of living material (muscle) as a function of frequency [43]. There is a level of about 1,000,000 at ELF up to 100Hz, then a second level of about 100,000 from 100 Hz to 10kHz, and, after some slow decrease, a third level of about 70–80 from 100 MHz to some gigahertz. This last value is that of the dielectric constant of water at microwaves. One of the main constituents of human tissues is water. Hence, we have about the same microwave properties as water.

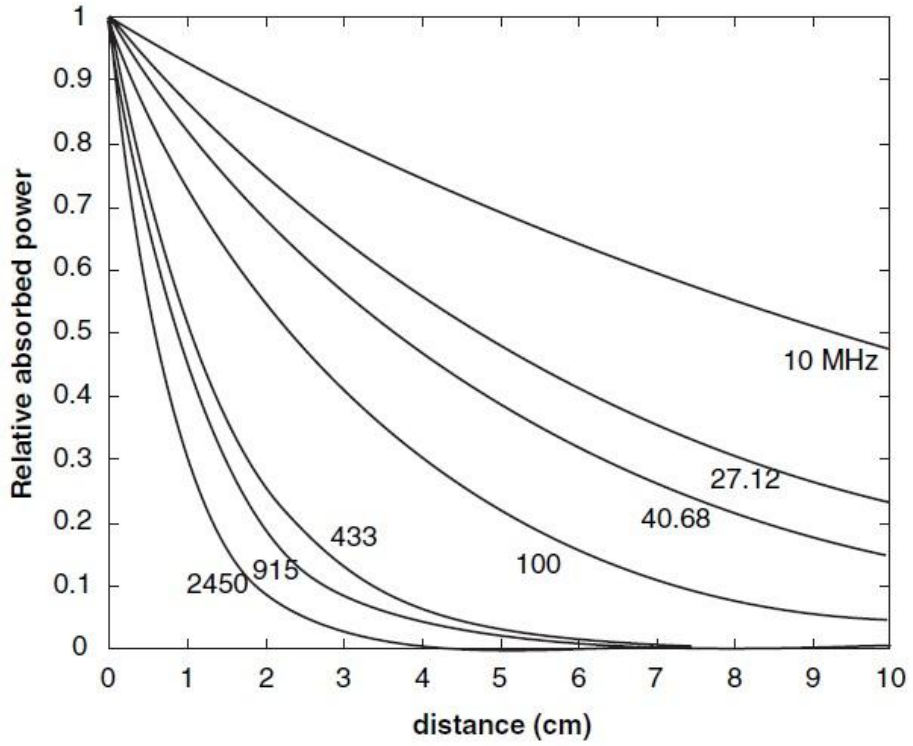

Figure (2.9) Power absorbed in muscles as a function of the skin depth at various frequencies

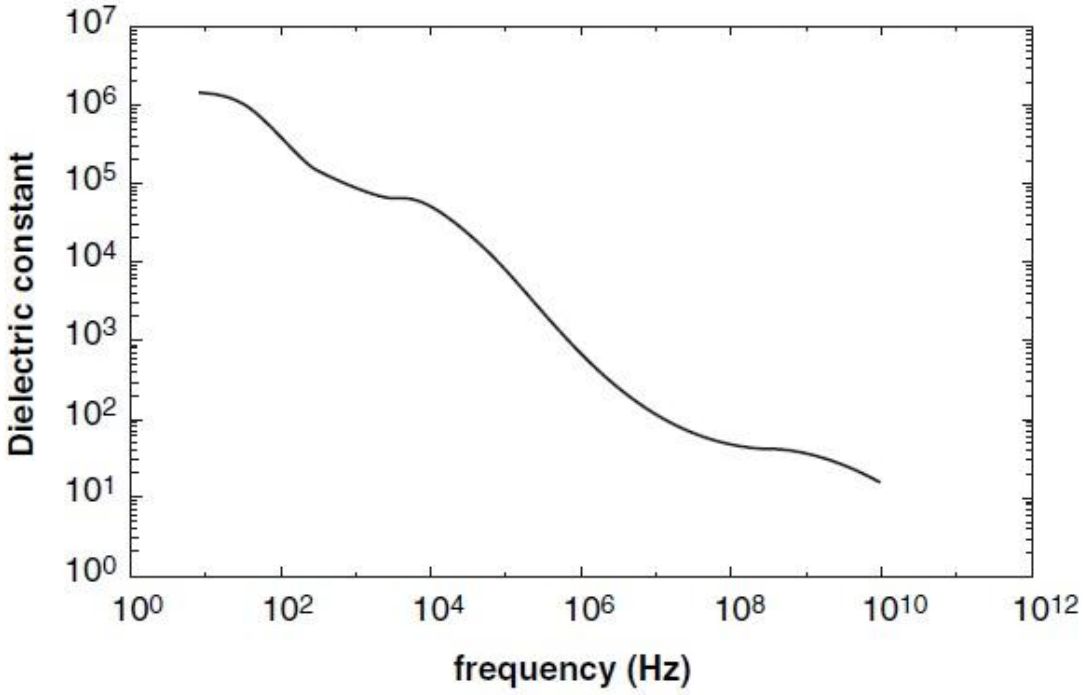

Figure (2.10) Dielectric constant of living material as a function of frequency

2.8.2. Conductivity of Biological Tissues

At low frequencies, below 100kHz, a cell is poorly conducting compared to the surrounding electrolyte, and only the extracellular fluid is available to current flow. A typical conductivity of soft, high-water-content tissues at low frequencies is 0.1 or 0.2 Sm^{-1}. It varies strongly on the volume fraction of extracellular fluid, which can be expected to vary with physiological changes in the cells. At RFs, from 1 to 100MHz, the cell membranes are largely shorted out and do not offer significant barrier to current flow. The tissues can be considered to be electrically equivalent to suspensions of nonconductive protein (and other solids) in electrolyte. The conductivity of most tissues approaches a plateau between 10 and 100MHz.

CHAPTER 3: SIMULATION AND MODELING

3.1. Introduction

Simulation is the use of a model to develop conclusions that provide insight on the behavior of any real world system. Computer simulation uses the same concept but require that the model be created through programming on a computer. The process of describing many complex real world systems using only analytical or mathematical models can be difficult or even impossible in some cases. This necessitates the employment of more sophisticated tool such as computer simulation. Simulation of real world requires that a set as assumptions taking the form of logical or mathematical relationships be developed and shaped into a model.

Computer simulation is a complicated solving technique. It should be used under certain circumstances;-
l- The real system doesn't exist and it is too costly, time consuming, hazardous, or simply impossible to build a prototype. Some examples might be an airplane or a nuclear reactor.

2- The real system exists but experimentation is expensive or hazardous. Some examples might be a material handling system. A military unit or a transportation system.

3- A forecasting model is required that would analyze long periods of time in a compressed format. An example is population growth.

4- Mathematical modeling of the system has no practical analytical or numeric solutions. This might occur in stochastic problems or in nonlinear differential equations or time varying of systems elements.

The main advantage in using simulation is the reduction of risk involved with implementing a new system or modifying an existing one. Several alternatives can be tested, and one that gives the best results can be chosen. Proposed solutions can be analyzed in less time. ln addition, the best control over experimentation condition can be maintained in a simulation. Also it is less expensive and faster than the physically constructing the real system. The knowledge gained during the simulation phase will be of great value throughout the entire lifetime of a simulation project. Also, computer simulation gives control over time that may be compressed or expanded. Simulation may gather data on many months of operations in minutes on computers.

A model is an approximation of the system being studied, it is not always best to develop a full scale representation. If the system were modeled down to finest details, excessive amounts of time and energy would be required with minimal gain useful information. The necessary level of details is a determination of how closely the model needs to emulate the real world system to still provide the required information. The model scope is defined as that portion of the system that is represented by the model. The best approach to model development is to incorporate the least amount of details while still maintaining veracity of the simulation.

3.2. Modeling

The simulation procedure can be considered as follows:-

l) Definition of the problem
2) Formation of the hypothesis
3) Testing of the hypothesis by Experimentation
4) Tabulation of results
5) Drawing conclusions from results

The scientific method can be used as a guideline formation setting up simulation experiments. The correspondence between simulation method and the scientific method can be seen in the following table:

Scientific method	Corresponding simulation
1. Problem definition	1. Setting simulation objectives
2. Hypothesis formulation	2. Defining model scope and selection of programming language
3. Experimentation	3. Running model
4. Results	4. Obtain data from model
5. Conclusion	5. Using statistics and judgment to evaluate results

Table (3.1) simulation vs. scientific method

3.3. Model inputs

Input data can take many forms. It can be quantitative or qualitative. Quantitative input data takes the form of numeric values. Qualitative input data represents the logarithms used to perform certain logical operations. [44].

Input data can be obtained in many ways: -

1-direct observations

2-estimation

3-interpolation

4-expert opinions

5-projections

After input data has been collected, two approaches can be taken to use the information in the simulation. The first approach is to use data as it is. This is called trace simulation .The second approach is to fit a standard statistical distribution to empirical

data .The key to this procedure is to find the probability distribution with random samples that will be indistinguishable from the collected input data.

3.3.1. Statistical methods and input data:

In order to carry out a simulation of a system having inputs (such as interarrival times) which are random variables, we have to specify the probability distributions of these inputs. There are two general approaches to specify a distribution: -

l. standard techniques of statistical inference are used to fit a theoretical distribution form, e. g., exponential, normal, or Poisson to the data and to perform hypothesis tests to determine how good the fit is. The distributions are then used to generate the corresponding random variables during the simulation.

2. The values of the data themselves are used directly to define an empirical distribution without relying on one of the common theoretical distribution forms. This empirical distribution is then directly used in simulation.

3.4. Validation

Validation is the process of determining that the real world system being studied is accurately represented by the simulation model [45]. The validation process should begin during the initial stages of a simulation and continue until the end.

3.4.1. Validation of simulation inputs:

Qualitative inputs are the rules and underlying assumption and nonnumeric data. This information should be validated through one or several of the following methods:

1- Observation. If a model of an existing system is being developed, the analyst can observe different situations and assure that the assumptions to be used in the model are valid.

2- Expert opinions. If the rules and assumptions are evaluated by experts, the modeler should interact with both system experts and model users throughout the life of a simulation.

3- Intuition and experience. If a simulation analyst frequently models systems that share many common characteristics, an intuitive feeling develop that will help give the model added validity. In addition, quantitative or numeric inputs can be validated in the following ways:

i) Statistical Testing:

If a theoretical input data distribution is being used to model empirical data, Chi-square or Kolmogorov goodness-of-fit tests should be used to assess the theoretical data. If the fit is close, the theoretical data can be considered a valid representation.

ii) Sensitivity Analysis:

This involves altering the model's input by a small amount and checking the corresponding effect on the model's output. If the output varies widely with a small change in an input parameter, the input parameter may need to be reevaluated.

3.4.2. Validation of simulation output:

If the model's output data closely represents the expected values for the system's real world data, it is considered to be valid. When a model is developed from an existing system, a validity test becomes a statistical comparison. Several methods can be used to increase the confidence level

l- Comparison with data from a similar system. If a system exists that is similar in nature to the one that is being modeled, an interpolation of system output can be considered and compared to the simulation.

2- Expert opinions. An Expert on the type of the system being modeled can be consulted and shown the output data. An expert's opinion will help lend more confidence that model is valid.

3- Calculated expectations. Expected output can be calculated and the model output compared to the result. If the model is too complex, it may be possible to analyze individual subsystems and perform calculations on each part to help establish validity.

3.5. Classifications of simulation models:

3.5.1. Deterministic or stochastic models:

In deterministic models neither the exogenous variables nor the endogenous variables are permitted to be random variables, and the operating characteristics are assumed to be exact relationships rather than probability density functions. Deterministic models are less demanding computationally than stochastic models and can frequently be solved analytically by such techniques as the calculus.

Stochastic models are those models in which at least one of the operating characteristics is given by a probability function. Because stochastic models are considerably more complex than deterministic models, the adequacy of analytical technique for obtaining solutions to the models is quite limited. For this reason simulation is much more attractive as a method of analyzing and solving stochastic models than deterministic models. Stochastic models are also of interest from the standpoint of generating random numbers samples of data to be used in either the "observation" or "testing" stages of scientific inquiry.

3.5.2. Static or dynamic models:

Static models are those models, which don't explicitly take the variable time into account. In operation research, with rare exceptions, most of the work in the area of linear programming, non-linear programming, and game theory has been concerned with static models. Most static models are completely deterministic, and solutions can usually be obtained by straight forward analytical techniques such as optimally calculus and mathematical programming [44].

Mathematical models that deal with time-varying interactions are said to be dynamic models.

3.5.3. Continuous or discrete

Discrete event simulation concerns about modeling of a system as it evolves over time. The state variables change only at certain number of points in time. These points are ones at which an event occurs. Continuous simulation represents the system experiencing smooth changes in characteristics over time. The objective of the model is to plot the simultaneous variations of the different state variables with time.

Continuous simulation involves differential equations which gives relationships for the rates of changes of the state variables with times. These equations may be solved analytically or by numerical techniques.

3.6. Monte Carlo simulation Method

Monte Carlo methods can be loosely described as statistical simulation methods, where statistical simulation is defined in quite general terms to be any method that utilizes sequences of random numbers to perform the simulation [46].

Statistical simulation methods may be contrasted to conventional numerical discretization methods, which typically start with the evaluation of mathematical model of the physical system, discretizing the differential equations that describe the system and solving a set of algebraic equations for the unknown state of the system. In many applications of Monte Carlo, the physical process is simulated directly and there is no need to even write down the differential equations that describe the behavior of the system. The only requirement is that the physical (or mathematical) system be described by probability density function (PDF). Once the (PDF) is known, the Monte Carlo simulation can proceed by random sampling from the (PDF). Many trails are then performed and the desired result is taken as an average over the number of observations. In many practical application, one can predict the statistical error in the average result, and hence an estimate of the number of Monte Carlo trials that are needed to achieve a given error. The most prevalent application of Monte Carlo is for the solution of complex problems that are encountered in particle transport applications. For example, the analysis of electron transport in a cloudy atmosphere, or the attenuation of neutrons in a biological shield and diffusion of atoms in solids.

3.7. Pseudo-Random generators:

Random numbers are stochastic variables which are uniformly distributed on the interval (0,1) and show stochastic independence.
Pseudo-random numbers are generated by applying a deterministic algebraic formula which results in producing numbers that for practical purposes are considered to behave as random numbers, i.e., they are uniformly distributed and mutually independent. The cycle length is the number of pseudo-random numbers that are generated before the same sequence of numbers are obtained again. The independence of the generated numbers implies that the cycle length is relatively long. A much used formula is the so called linear congruential generators methods.

CHAPTER 4: COMPUTER MODEL

4.1. General features of the present model

The basic modeling aspects can be summarized as following:

1-The biological tissue is represented as a 2D matrix of N*N elements, such that each element of the matrix is represented by a byte. Different types of elements can be found in system (biological tissue). Each type of elements is represented in the matrix by a specific byte. These are the host particles, vacancies and diffusants.

2-Each position is specified by two integers i and j. Each position is assumed to represent a particle, a vacancy or a diffusant. For any given position, there are six neighbors which are occupied by either a host particle, a diffusant or a vacancy. The system structure may take several forms. The model that closely represents the biological system is the close packed hexagonal shape.

3-The diffusion process generally expresses a random walk of particles either in space or in a constraint medium. A random generator is applied to study the diffusion process. A sequence of random numbers is generated to represent the movement of elements that are involved in diffusion throughout the matrix.

4- Matlab and C language use generators that are offered as algorithms in the program libraries. In the present work “RAND” and “RANDN” algorithms were proposed to be reliable for randomness.

“rand” function generates pseudorandom numbers drawn from a uniform distribution on the unit interval. “randn” algorithm generates pseudorandom numbers drawn from a normal distribution with mean 0 and standard deviation 1.

“randperm” does random permutation and calls “rand” function.

“randint” generates a matrix of uniformly distributed random integers

Randomization has been utilized in the model in three occasions. Firstly, it was used to create the initial uniform distribution of vacancies throughout the host. In order to create vacancy of concentration n% overall the whole matrix, a vector with the host positions is created, then “randperm” function is used to choose the places of vacancies at random among the host. The percentage of vacancies could be changed for each run of the model.

Secondly**,** the “rarndint” function is used to determine the element of the matrix to start with the jump. Thirdly, “randperm” function is used to determine the direction of the jump of the element among the possible six neighbors.

5-Naturally, the diffusion process takes a very long annealing time. The advance of time is expressed as the number of iteration steps in which the model executes the main

algorithm. Therefore, an increasing number of time steps is taken, so that the diffusion pattern is realized.

6-Naturally, the jumping process of the diffusing particle occurs simultaneously and in a stochastic manner through the host. Unfortunately, this can't be achieved by computer simulation which goes through ordered sequential method. To overcome this obstacle, the time is frozen each time step and all the possible diffusants are let to jump before going to next time step .

Programming of diffusion mechanisms

The aim of the present model is to simulate the diffusion phenomena in three cases:

1-Free random walk

2-Diffusion in host in the presence of vacancies

3-Diffusion under the effect of electric field

4.2. Free random walk:

In this model, a single particle executes the random walk in two dimensions. All jump directions have equal priori probability and are uncorrelated with the preceding jumps. The particle starts its motion from the origin, and then it jumps to a direction at random with an angle that takes a value from 0 to 360.

The choice of the direction is determined by "rand". Once the particle migrates to the new site, the new coordinates are determined according to the equations:

$$x_{i+1} = x_i + r\cos\theta_{i,i+1}$$

$$y_{i+1} = y_i + r\sin\theta_{i,i+1}$$

Where $\theta_{i,i+1}$is the angle that the vector connecting I,i+1 making with the x-axis and r is the average radial displacement and taken as an arbitrary constant value.

The new coordinates of the particle and the distance from the origin at the end of each iteration step is recorded.

The total x and y displacement along x and y axis can be calculated according to:

$$x_t = \sum_{k=1}^{n} r\cos\theta_k$$

$$y_t = \sum_{k=1}^{n} r\sin\theta_k$$

This type of diffusion resembles the diffusion in gases under the following conditions:

1-Perfect gas where there is no chemical reaction

2-The number of molecules is large and the average separation between them is large compared with their dimensions

3-No potential energy. In other words, the forces between molecules are negligible.

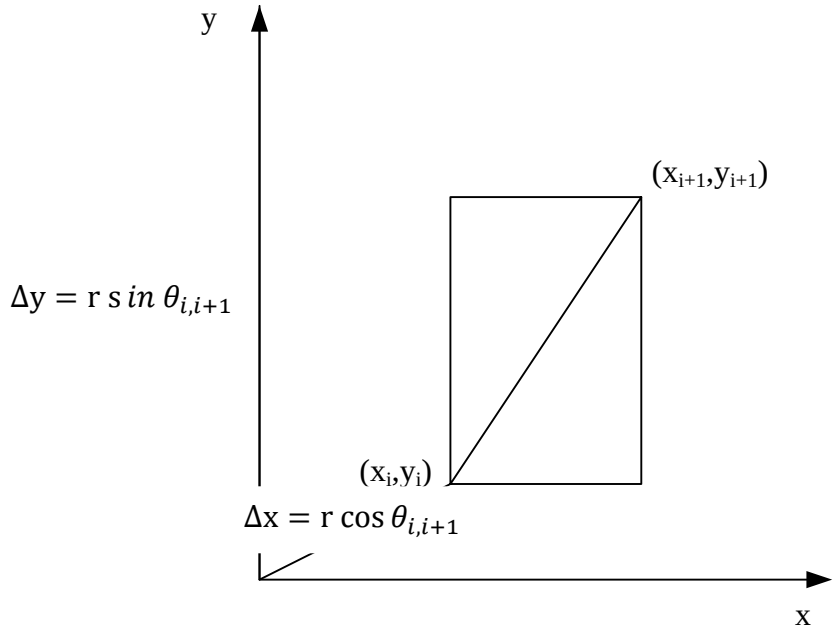

Figure (4.1) The x and y displacements

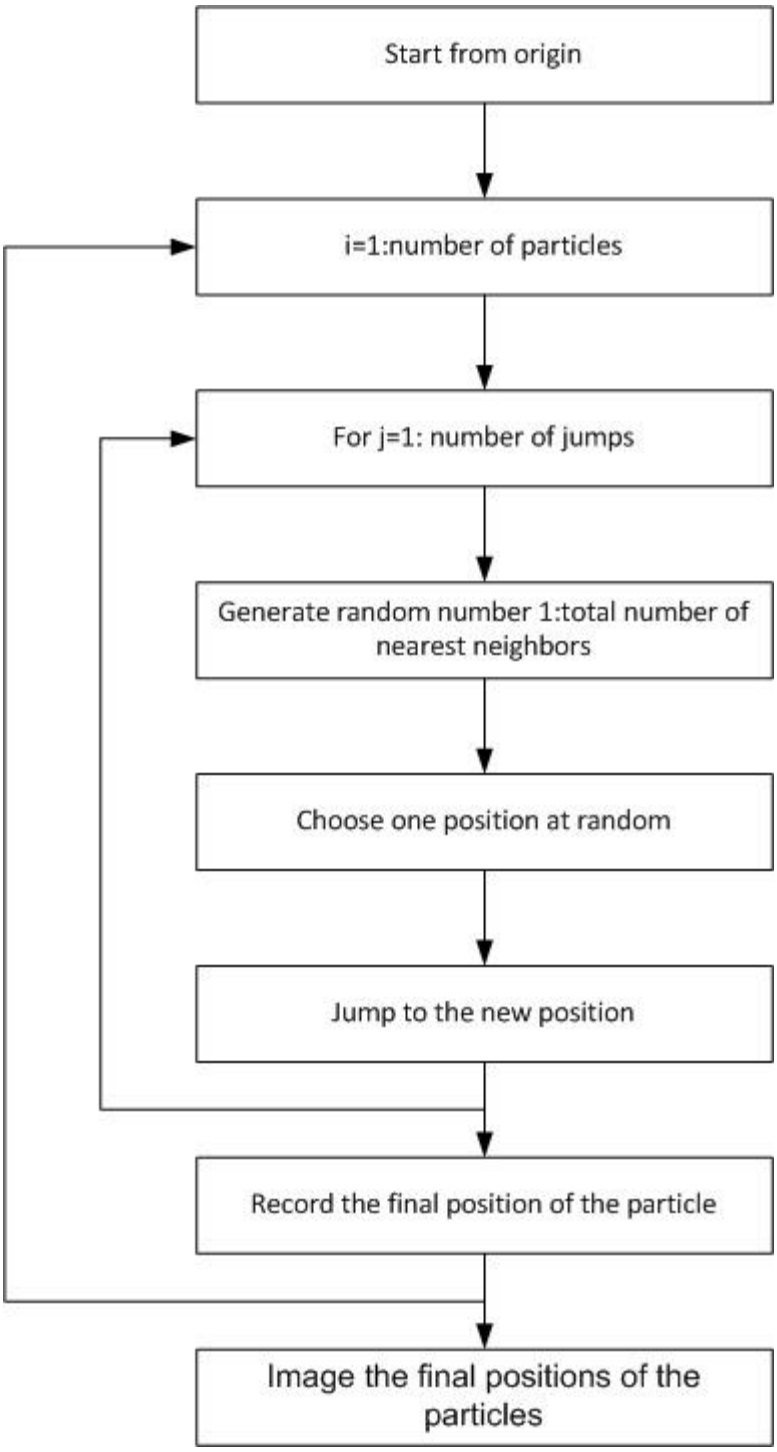

Figure (4.2) Random walk in an empty lattice diagram

4.2.1. Free diffusion in an empty host:

Free diffusion occurs in infinite space, which means that diffusion doesn't reach the boundaries in the given time. The details of the algorithm constructed to perform the free random walk in an empty lattice is shown in figure (4.2)

4.3. Diffusion in biological tissue via diffusant mechanism:

The biological tissue was constructed as a two-dimensional matrix. The matrix has a certain percentage of vacancies which present in nature throughout the tissue. The spatial distribution of vacancies among the matrix is simulated by using "rand".

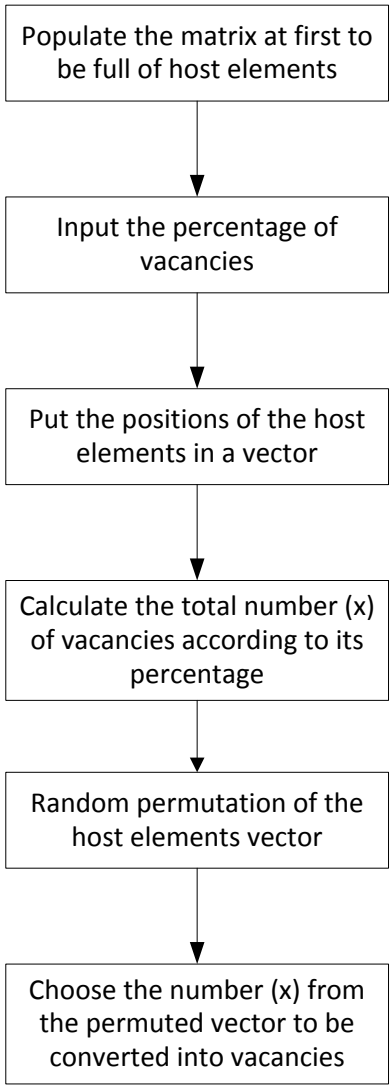

Figure (4.3) Flow chart of the algorithm for creating a matrix of initial distribution of vacancies

4.3.1. Biological tissue modeling

The biological tissue could be simply modeled as close-packed spherical array of cells.

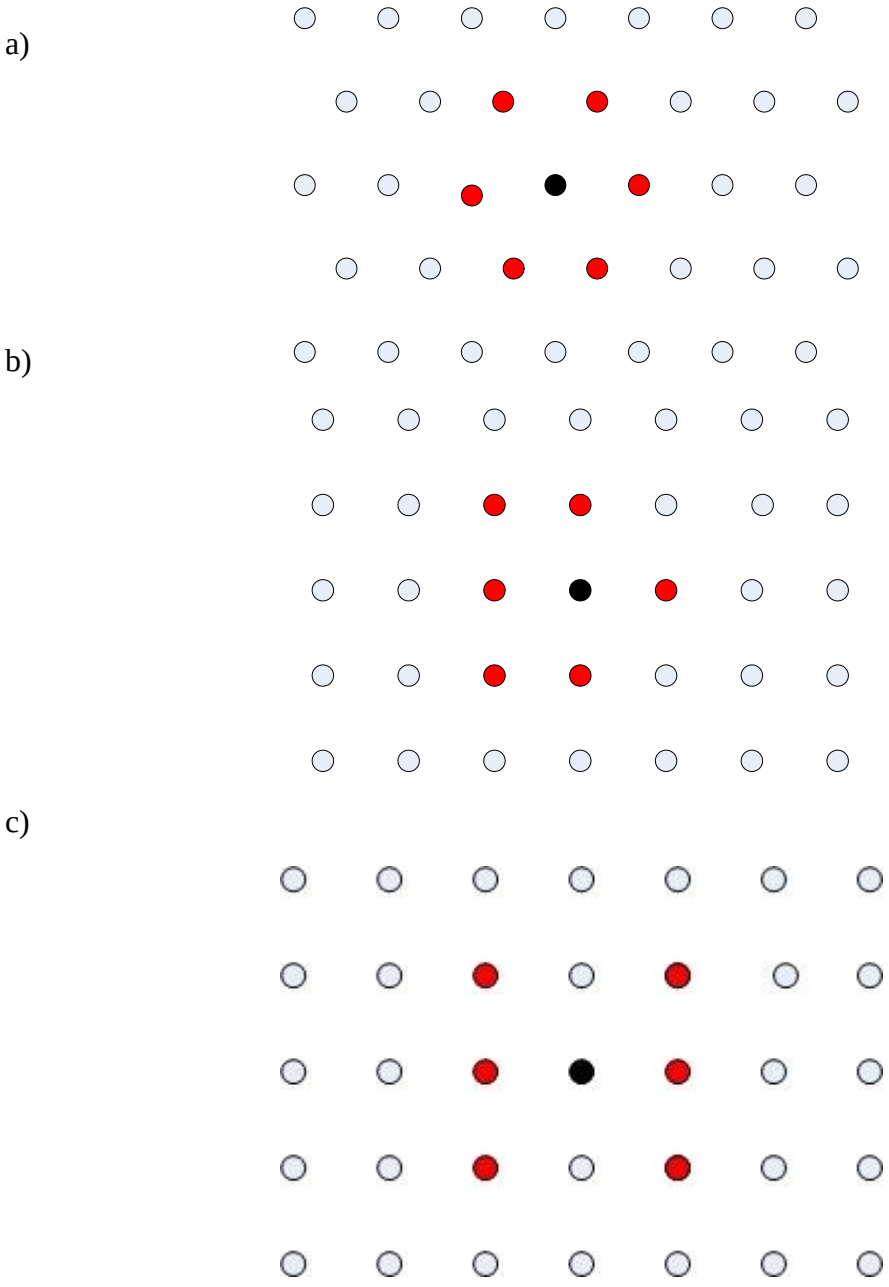

Figure (4.4) the six neighbors' structure in a hexagonal matrix. a) shift of rows to create hexagonal matrix. b) 1st model to represent the six neighbors in the real matrix. c) 2nd model to represent the six neighbors in the real matrix

There are maximum six chances around each element inside the two-dimensional matrix. The elements at the boundaries have different conditions; they are not allowed to leave the matrix. Accordingly, there are maximum four inward directions for boundary matrix sides and maximum two inward directions for matrix sites at the corners.

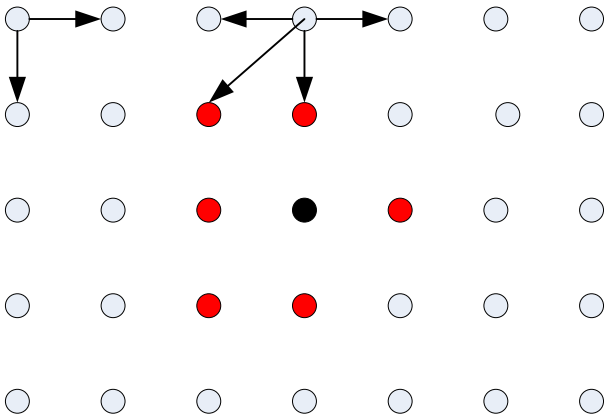

Figure (4.5) The boundaries' jumps

4.3.2. Dummy boundaries:

In order to avoid setting boundary conditions for each jump, the matrix is surrounded by dummy elements so that it wouldn't be selected in the 6-choices. For instance, if the matrix elements are (0,2,3) the dummy boundary is set to be (4). If the diffusant in the corner is to jump, it will look for the possible jumps around it in the six assigned places. The vector of selected elements will have only the neighboring vacancies excluding the boundaries.

4.3.3. Random scanning method:

In order to preserve the stochastic nature of the diffusion the random scanning technique was employed. The technique depends on choosing the diffusant elements at random for N times at each time step, where N is the number of diffusants. This will allow most of the diffusants to jump at the same time step. The probability of choosing an element in the matrix at random is $\frac{1}{N}$.

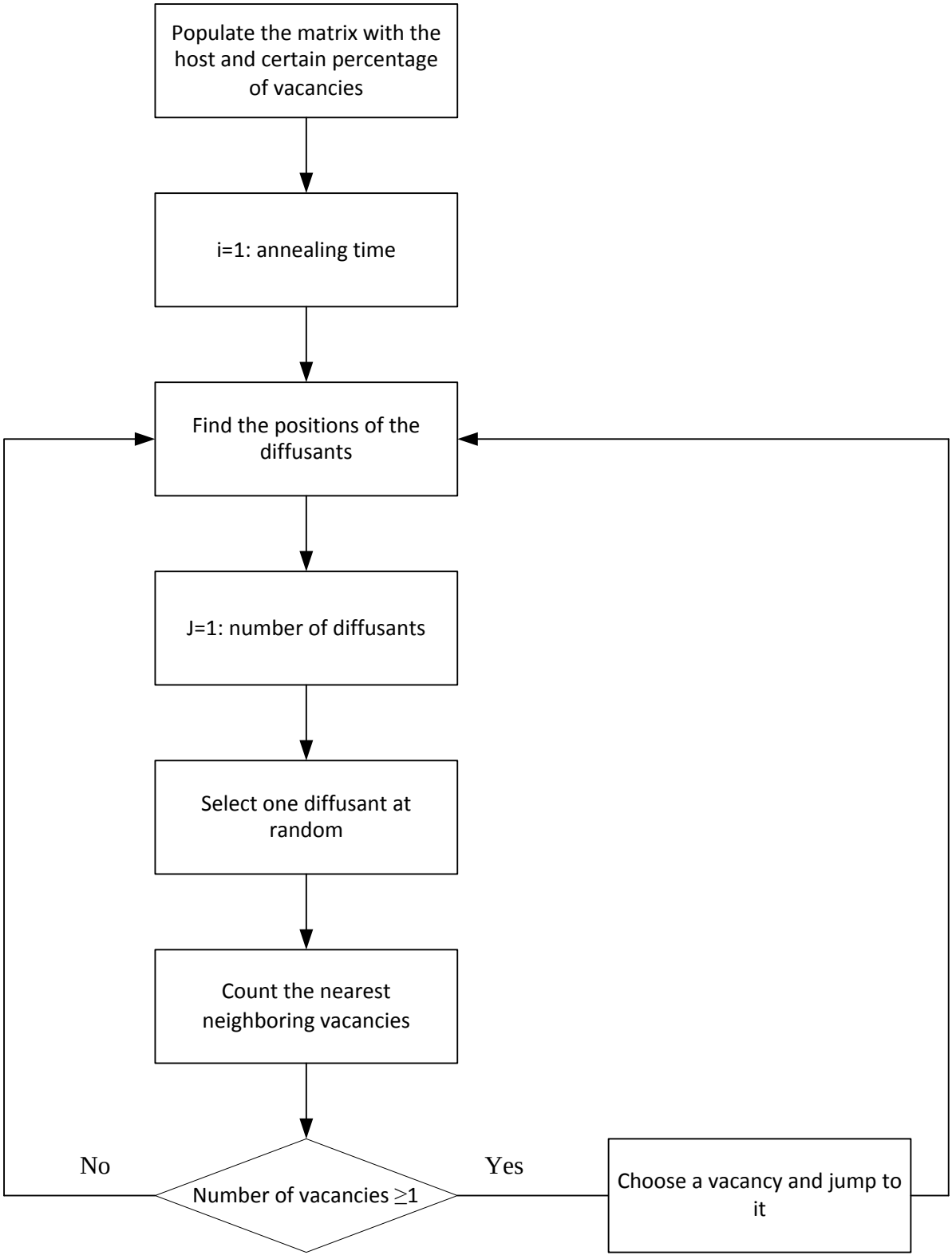

Figure (4.6) Flow chart of algorithm "Random selection of diffusants"

4.4. Simulation of diffusion of constant surface concentration of ions through infinite matrix of biological tissue:

The matrix consists of two types of elements; the biological elements and the diffusing ions. The biological elements could be cells or tissue or components inside or outside the cell according to the application of the model. The diffusant ions are represented as a row of elements placed above the matrix. They have different label than the host elements. The layer of diffusants is regenerated to represent continuous flow; when a diffusant jumps inside the matrix it is replaced by a new diffusant . The rest of the matrix consists of the host with a certain distribution of vacancies.

The diffusion pattern is followed over different long time steps. The initial concentration of the tracer could be varied and also the thickness of the host.

After the diffusion is run for a certain annealing time, the diffusion coefficient is calculated by using the "sectioning" algorithm. The whole matrix is sectioned to several layers such that each section has a small thickness compared to the sample size. The thickness of each layer is represented by the number of layers it includes. The concentration in each layer is the count of the diffusants it comprises. As the thickness of the layers becomes smaller, the accuracy of the penetration profile which describes the diffusion increases.

The flow chart that simulates the diffusion process in the presence of vacancies and calculation of the diffusion coefficient is illustrated in figure (4.8)

In biological systems, the events occur simultaneously. To overcome the disadvantage of sequential simulation, the time is frozen each step and all the diffusants are allowed to jump in the same time step. Then the program goes for the next step.

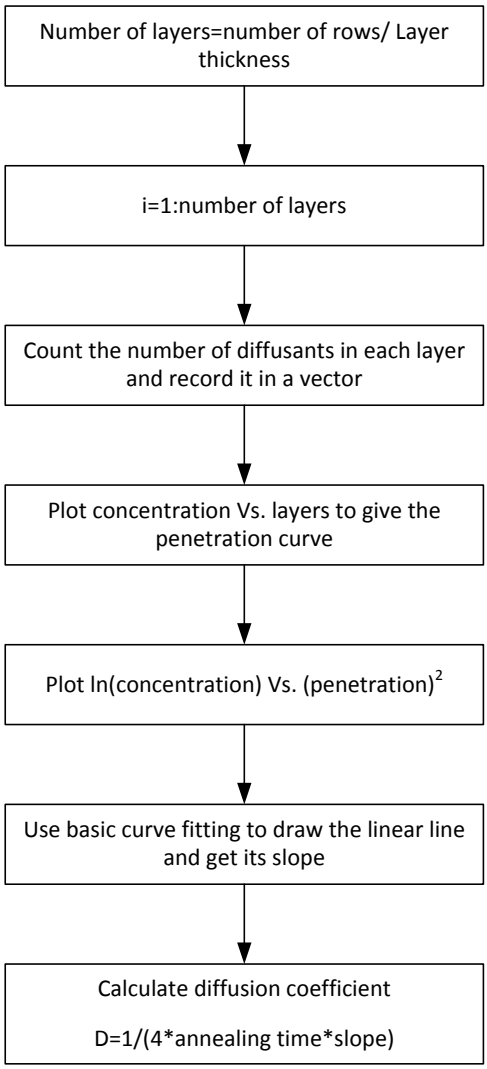

Figure (4.7) Sectioning the matrix and calculating the diffusion coefficient

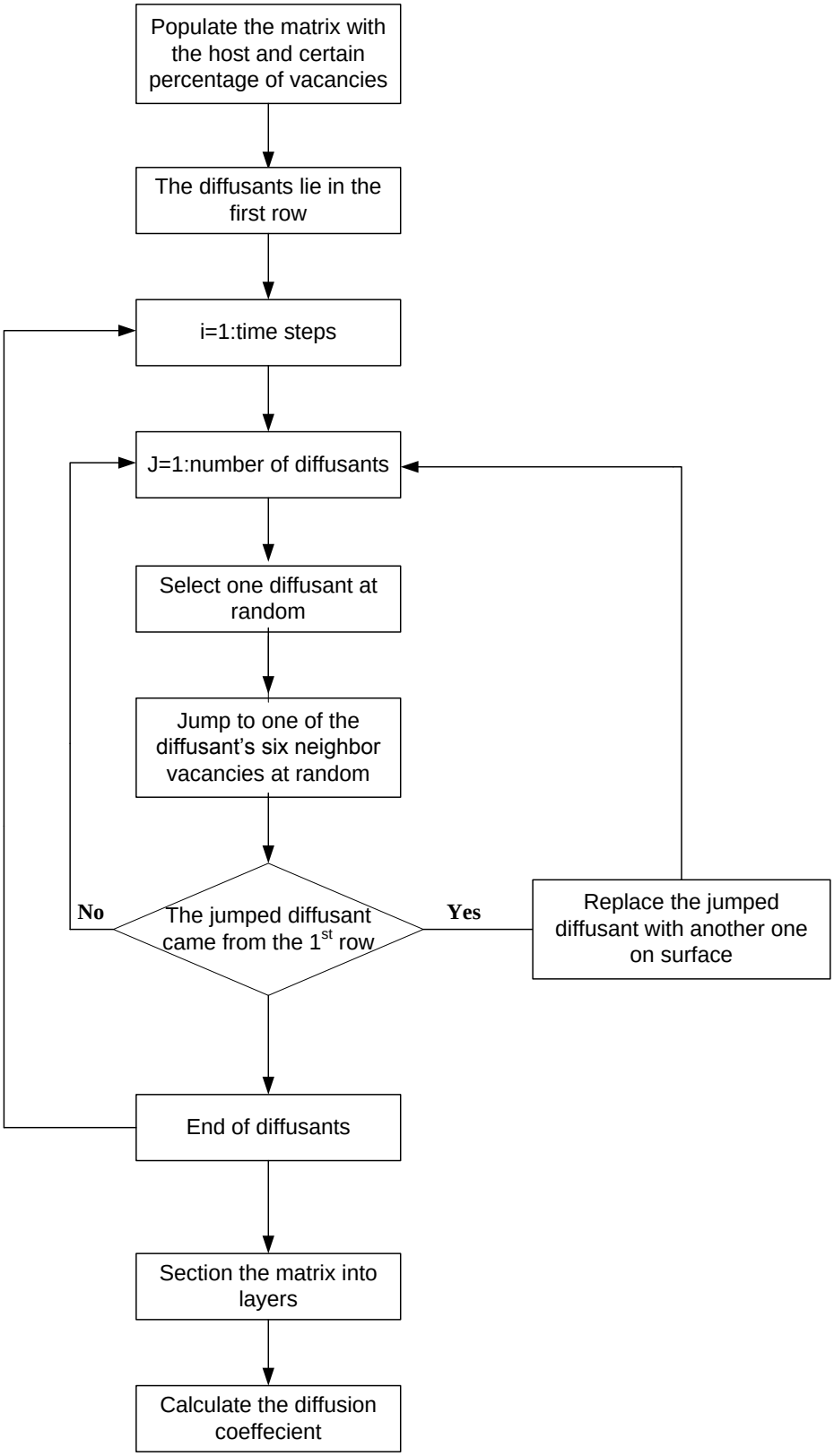

Figure (4.8) Flow chart of the diffusion in infinite system and constant surface concentration

4.5. Simulation of effect of electric field on diffusion in infinite biological system with constant surface concentration:

Most biological membranes are negatively charged, which makes them attract and adsorb positive ions. However, these ions are not stuck permanently to the membrane but are in dynamic equilibrium with the free ions in the environment. The relative amounts of each kind of ion attached at any one time depends mainly on its availability in the surroundings, the number of positive charges it carries and its chemical affinity for the membrane. Calcium normally predominates since it has a double positive charge that binds it firmly to the negative membrane. Potassium is also important since, despite having only one charge, its sheer abundance ensures it a good representation (potassium is by far the most abundant positive ion in virtually all living cells and outnumbers calcium by about ten thousand to one in the cytosol) [49].

4.5.1. Direct current:

The positively charged ions tend to be attracted to move with the direction of a negatively charged field. This effect increases with increasing the field's strength.

The effect of electric field is represented as bias in the jump to the six nearest neighbors. The six neighbors' choices are not equally probable now. If the field is applied on the surface of the matrix, the ions move forward. The 3rd row is the most preferable place to go to, then the second. The least preference will be for the 1st row; which means movement against the field. The two vacancies on the same row are assumed to have equal probability, as they are present at an equal position from the field.

To introduce the preference in choices after the application of EF, a random generator based on uniform distribution was used to create random numbers on the interval (0,1). 1 is the maximum strength for the electric field, and the threshold value is an input by the user depending on the application.

Before each jump a number is picked at random from a uniform random distribution. The probability of the most probable choice is related linearly to the EF strength according to the following equation: Given that:

When EF=0 P=0.333 (the choice will be equal for the three rows)
When EF=max P=1 (total propability) all the choices will be always given for the row in the direction of the field (3rd row in forward direction and 1st row in backward direction).

$$P=(0.667/Emax)*E+(1/3)$$

P: probability of choosing the most probable row (3rd in forward and 1st in backward)
Emax: maximum value of the electric field. It represents the maximum of effect of EF
E: electric field strength

When the electric field strength is increased, the probability of choosing a vacancy from the 3rd row is increased. And the rest of the total probability (1) is divided between the second and 1st rows according to (3:2).

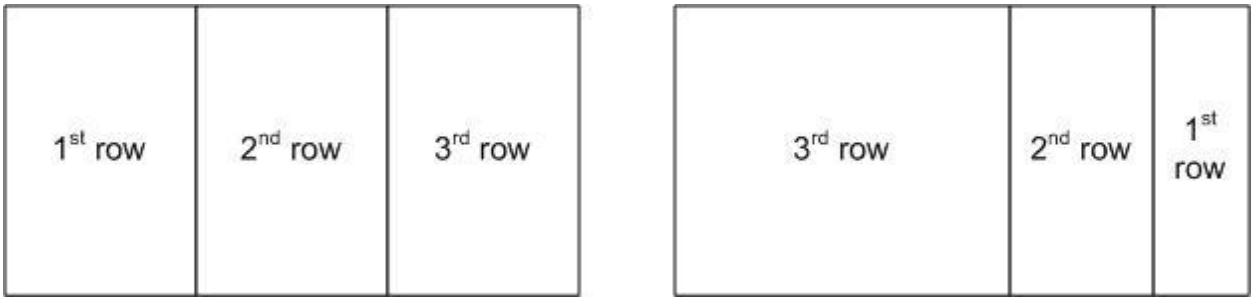

Figure (4.9) Effect of electric field on changing the probabilities of selection of each row

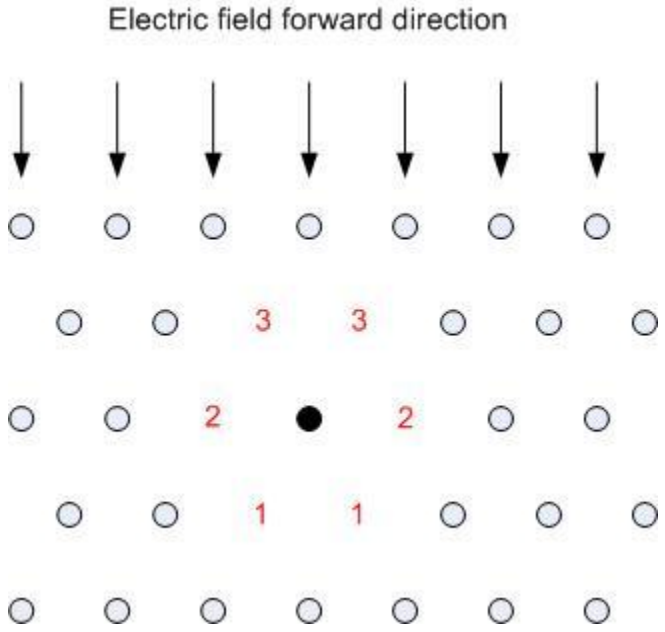

Figure (4.10) Effect of the direction of electric field on selecting neighbor vacancies

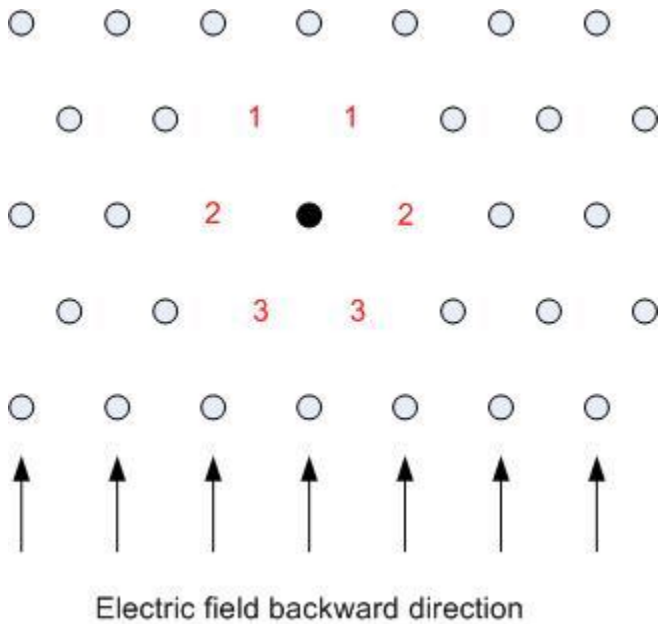

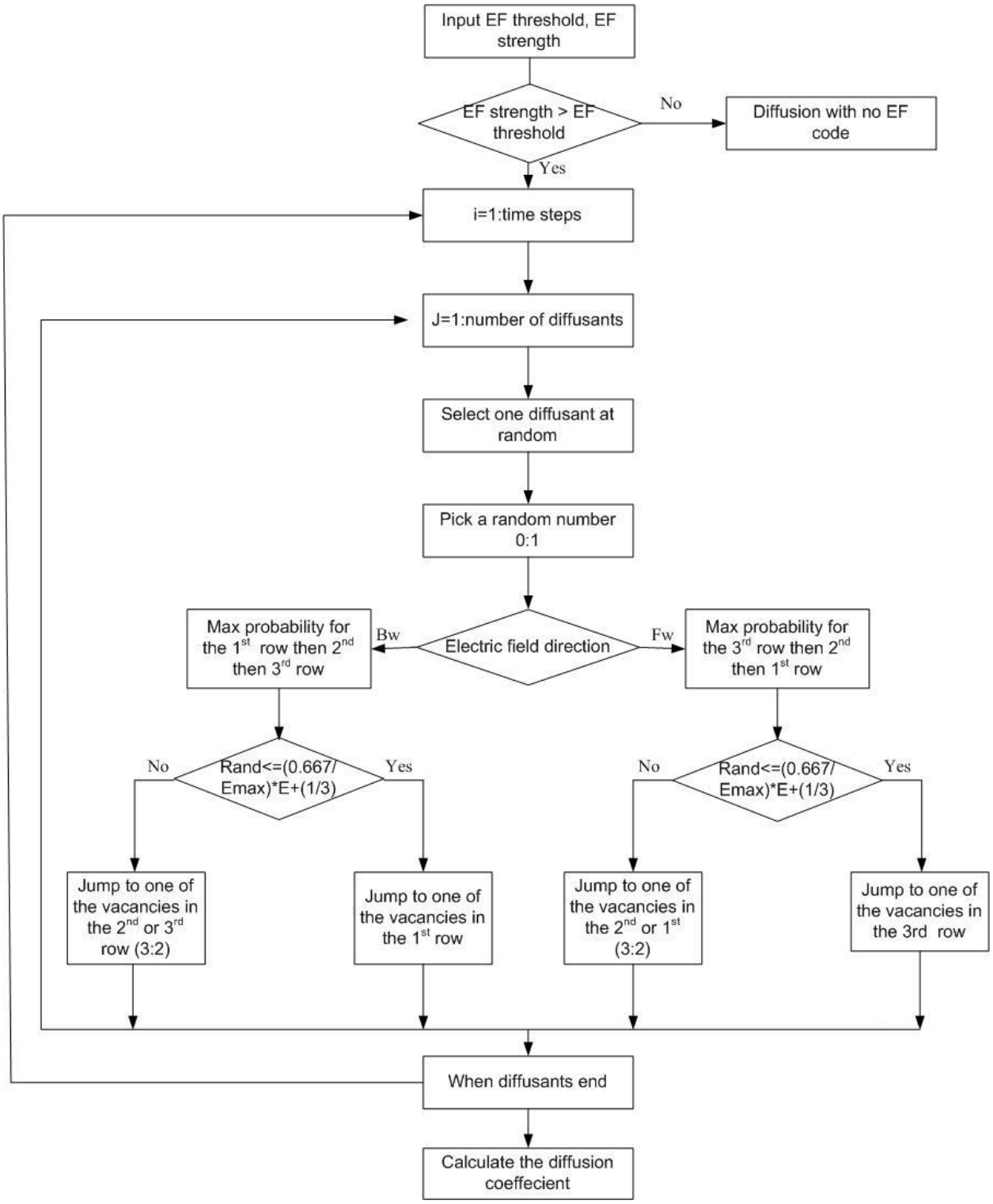

Figure (4.11) Flow chart for the direct current effect on diffusion in infinite host with constant concentration

4.5.2. Alternating current:

Before they can give biological effects, the electromagnetic fields must generate electrical 'eddy currents' flowing in and around the cells or tissues. Both the electrical and magnetic components of the fields can induce them and they tend to follow low impedance pathways. These can be quite extensive; for example in the human body, the blood system forms an excellent low resistance pathway for DC and low frequency AC. It is an all-pervading system of tubes filled with a highly conductive salty fluid. Even ordinary tissues carry signals well at high frequencies since they cross membranes easily via their capacitance. In effect, the whole body can act as an efficient antenna to pick up electromagnetic radiation [49].

When an alternating electrical field from an eddy current hits a membrane, it will tug the bound positive ions away during the negative half-cycle and drive them back in the positive half-cycle. If the field is weak, strongly charged ions (such as calcium with its double charge) will be preferentially dislodged. Potassium (which has only one charge) will be less attracted by the field and mostly stay in position. Also, the less affected free potassium will tend to replace the lost calcium. In this way, weak fields increase the proportion of potassium ions bound to the membrane, and release the surplus calcium into the surroundings. [49]

In the model, the periodic time is input by the user. The frequency is 1/T, number of cycles=t/T

The code switches direction of the field each half cycle (T/2). The minimum T is 2 steps (one up and one down).

Each cycle is cut into half forward, half backward. The EF strength is increased step wise (0:1:0). The EF strength in each step is calculated as:

$$\text{EF strength} = \sin\left(\frac{step\ number}{steps\ per\ half\ cycle}\right) * 180$$

In each step, the EF is assigned with a specific strength. The selection of the surrounding vacancies is according to the direction of the half cycle (positive or negative parts). The strength per step is applied similar to direct current.

The effect of square wave can be tested by making the EF strength always maximum (1) in the positive and negative parts of the wave.

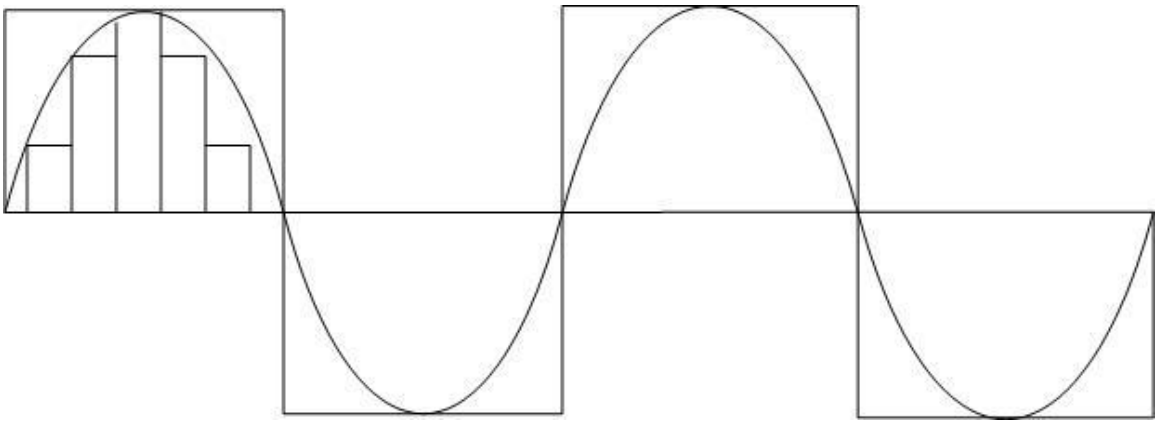

Figure (4.12) Difference between sinusoidal and square waves

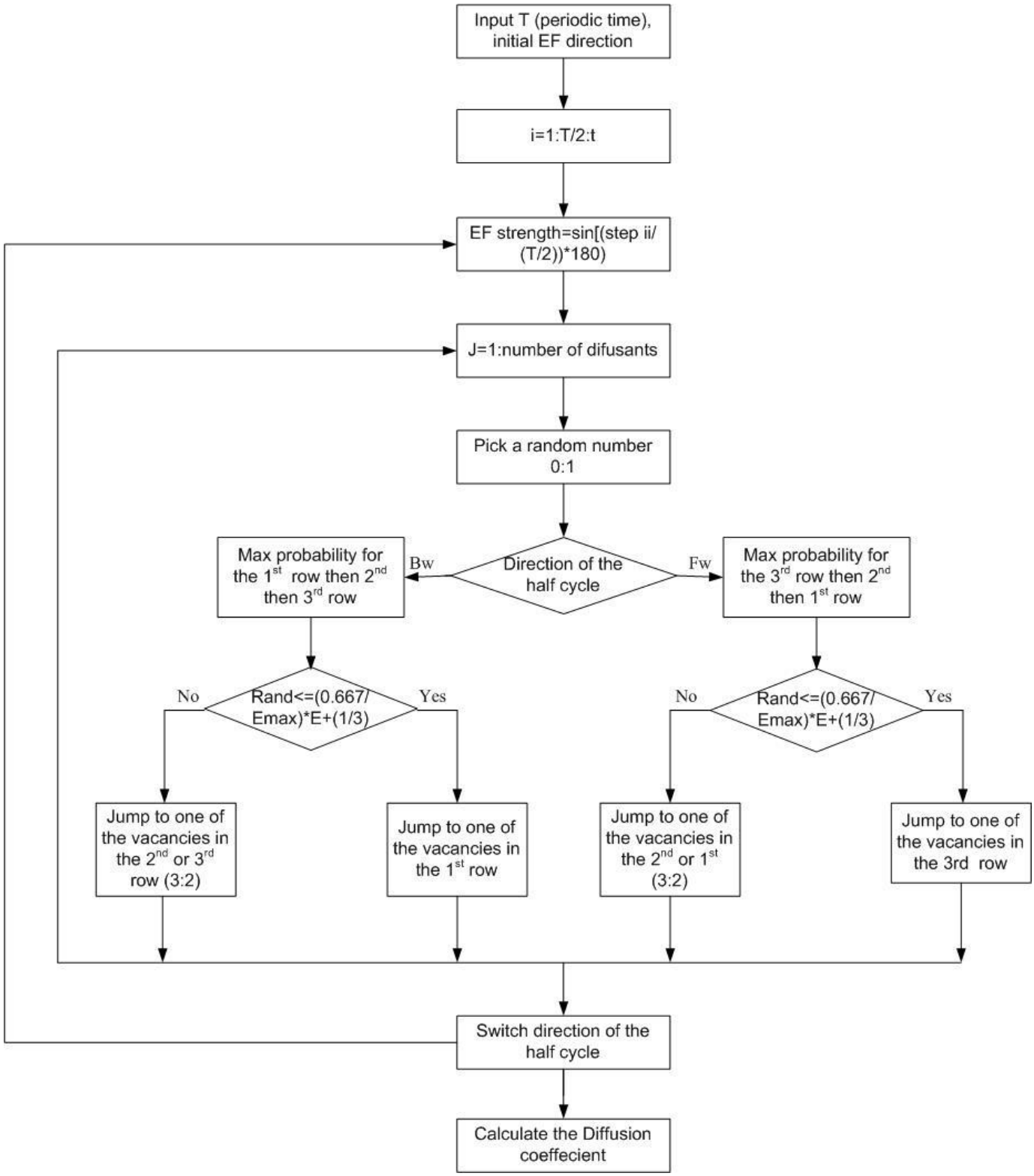

Figure (4.13) Flow chart of the effect of sinusoidal waves on the diffusion in semi-infinite system and constant surface concentration

CHAPTER 5: RESULTS

A personal computer (3 GB Ram, Intel core 2 Duo CPU 2 GHz) was used to run the simulation model. The simulation was programmed first in Matlab that works under windows. The program was then transformed to C language with the help of computer science team. The transforming helped in enhancing the speed of running the program and expanding the size of the matrix. The analysis was done then by Matlab which has a huge library in statistics and graphics.

5.1. The free random walk pattern in two- dimensions space:

Simulation of diffusion process as a random walk phenomenon suffers from two basic problems, namely the true randomness is almost impossible to achieve and the use of the random number generator can only produce a pseudorandom distribution, which depends on the seed among other factors. Also, the initial jump direction of a single particle imposes an overall bias of the diffusion pattern. Therefore, in the present work, a huge number of particles were considered to start from original point and all of them perform random walk of different seed numbers. In this case, the overall pattern after numerous jumps would take the expected uniform distribution along all possible directions.

5.1.1. Calculation of the radius of the random walk pattern:

The average radial distance r is a function of the number of jumps. It is computed according to the following equations:

All particles start from the center of the matrix. The final position of the particle is recorded after certain number of jumps; then the final radial distance of individual particle is calculated according to:

$$R_i = \sqrt{{x_i}^2 + {y_i}^2}$$

x: The final displacement in the x direction

y: The final displacement in the y direction

Hence, the average radial distance of N particles can be written as:

$$< \overline{R} >= \sum_{i=1}^{N} {R_i}/{N}$$

The mean squared radius can be written as:

$$< R^2 >= \sum_{i=1}^{N} R_i^2 /_N$$

The mean square value of the radius of the diffusion pattern is recorded over a number of time steps.

$< R^2 >$ Vs. time steps is plotted. The straight line is fitted and the diffusion coefficient can be calculated from the slope of the line according to:

$$D = < R^2 > /_{4t}$$

Results of: 100,000 particles start from the center of 10,000 x 10,000 matrix and perform free diffusion

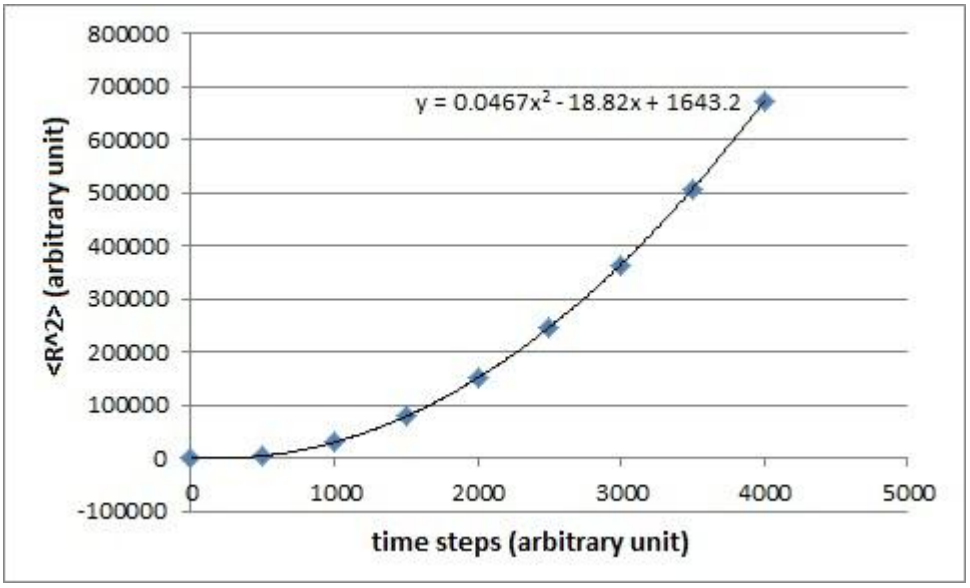

Figure (5.1) Variation of the mean square displacement with time steps for 100,000 particles

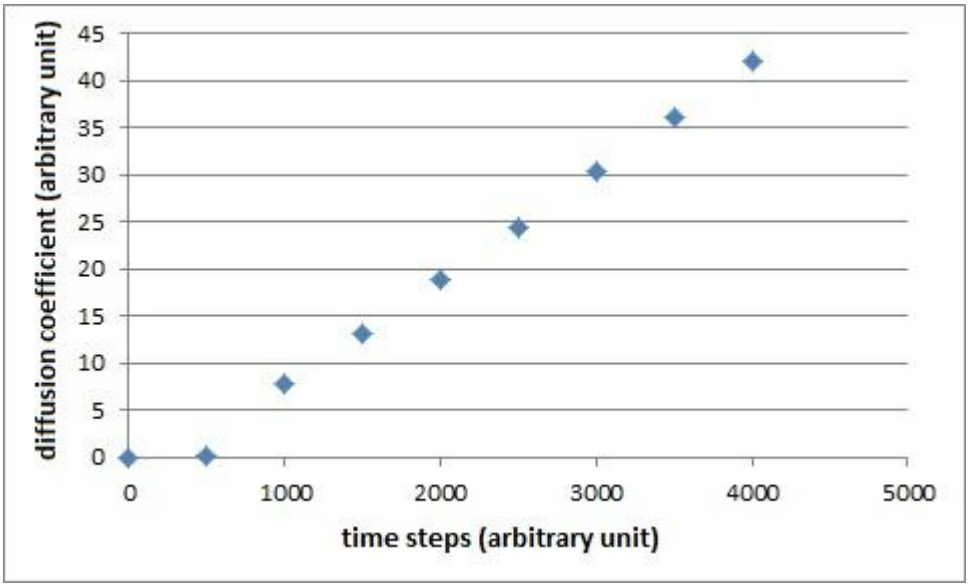

Figure (5.2) Variation of the diffusion coefficient with time steps for 100,000 particles

a)

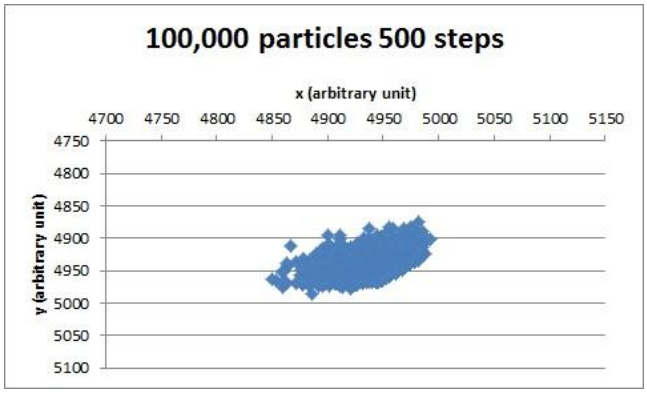

b)

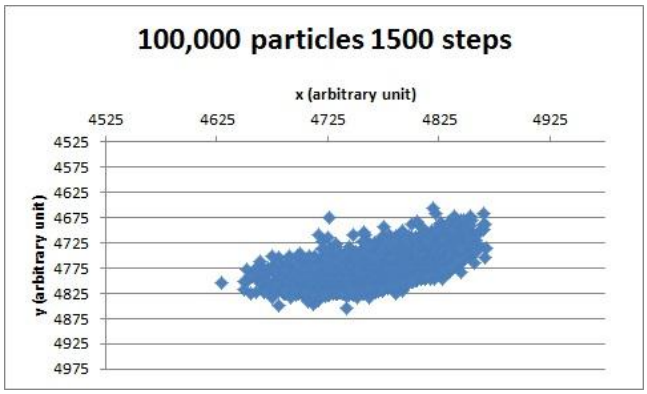

c)

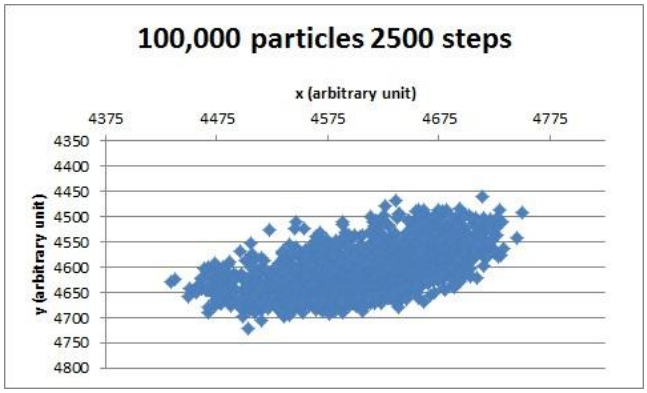

d)

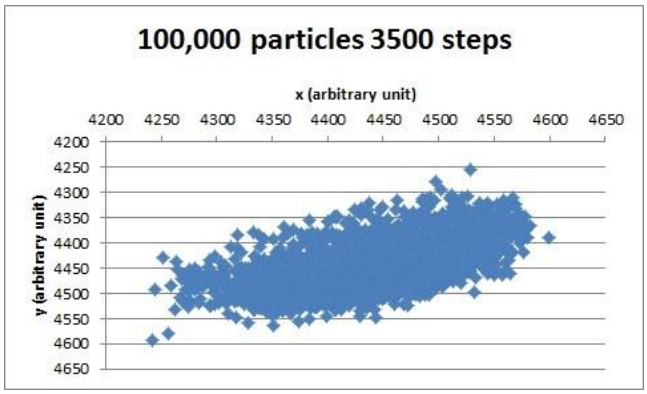

Figure (5.3) the pattern for 100,000 particles executing free random walk for a) 500 steps, b) 1500 steps, c) 2500 steps and d) 3500 steps

Results of: 500,000 particles start from the center of 30,000 x 30,000 matrix and perform free diffusion

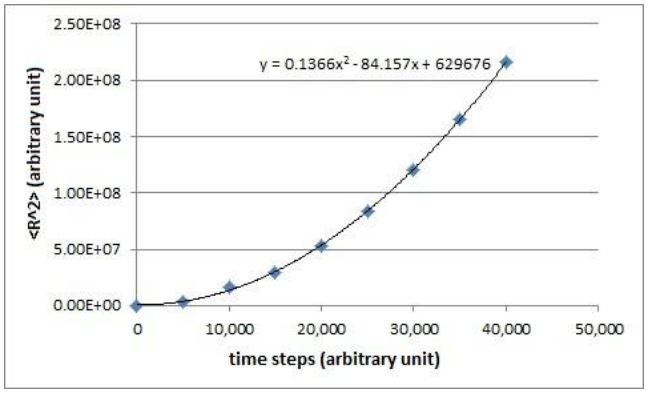

Figure (5.4) Variation of the mean square displacement with time steps for 500,000 particles

a)

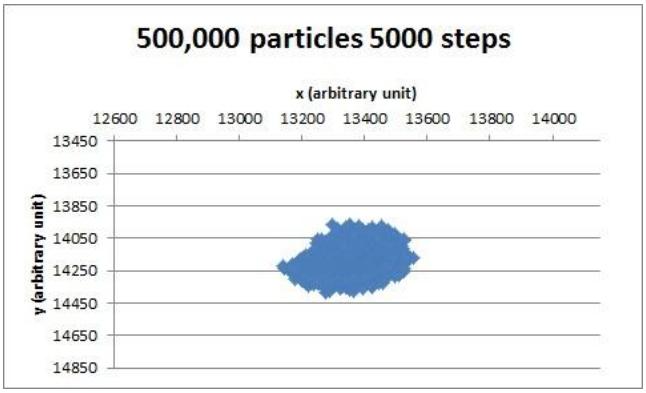

b)

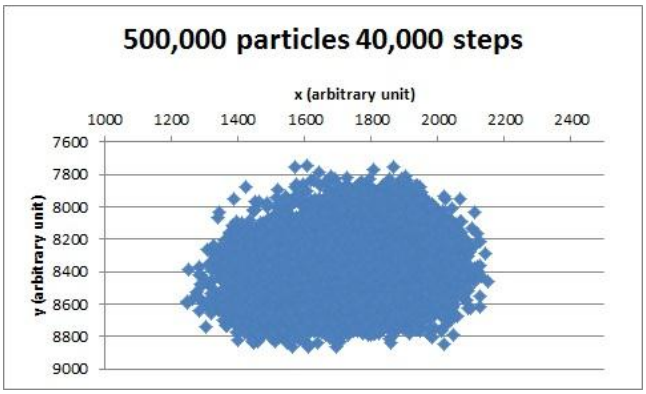

Figure (5.5) the pattern for 500,000 particles executing free random walk for a) 5000 steps, b) 40,000 steps

5.2. Simulation of infinite system and continuous flow of diffusants from the surface:

1. A matrix of 10,000x 10,000 is used to simulate a part of the biological tissue. Each element is either a host particle or vacancy. The diffusants lie on the surface of the matrix. The diffusants are in continuous flow; each particle leaves the surface into the matrix is replaced by another particle.
2. The jumps occur at random. Each time step a diffusant is selected at random to perform the jump.
3. Each diffusant chooses one of the nearest six neighbor vacancies at random.
4. The matrix is sectioned after the diffusion time into several sections such that the thickness of each one is very small compared to the matrix length. Each section is five rows.
5. The counts of diffusants in each section represent the concentration of diffusants.
6. By following the time steps, the top of the Gaussian distribution of the concentration vs. penetration distance is decreased. The diffusants penetrate deeper layers as time increases.
7. The logarithm of concentration against x^2 is plotted for different time steps and different vacancies concentration.
8. The straight line is fitted and D can be calculated from:
   $Slope = {}^{-1}/_{4Dt}$
9. The vacancies concentration is varied from 5% to 80% with constant time steps (1,000,000) figures (5.8 a:f)
10. The annealing time is varied from 1,000 to 1,500,000 time steps with constant vacancies concentration (50%) figures (5.11 a :f)

5.2.1. Variation of penetration distance and diffusion coefficient with vacancies concentration:

Results of: Matrix 10,000 x 10,000 time steps=1,000,000

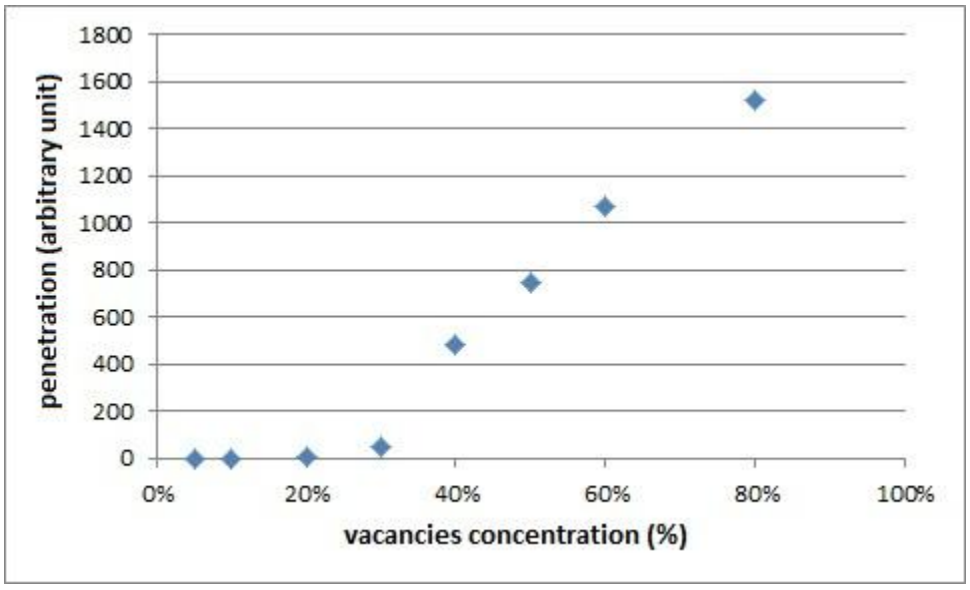

Figure (5.6) Variation of penetration distance with vacancies concentration

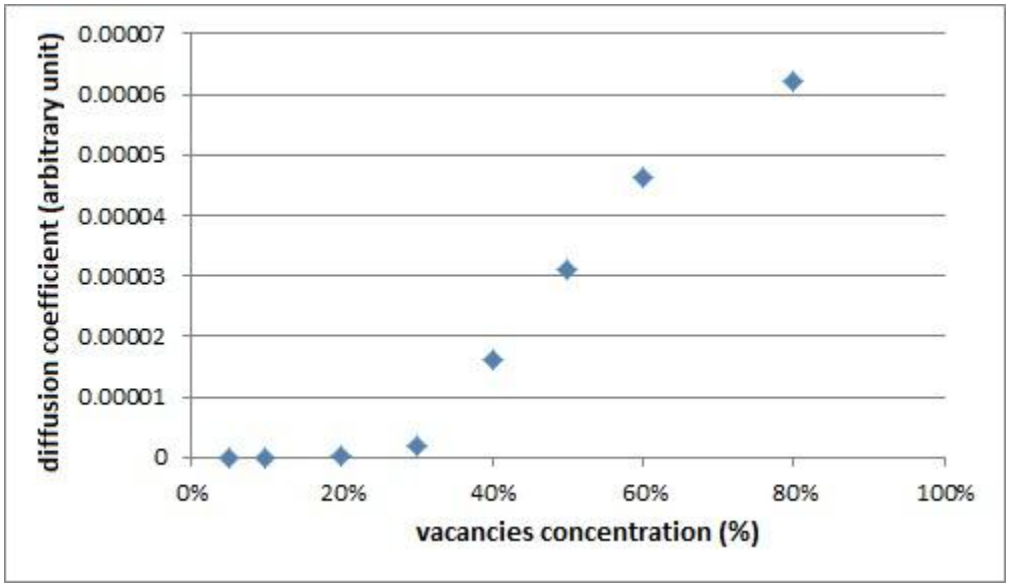

Figure (5.7) Variation of diffusion coefficient with the vacancies concentration

Figures (5.8 a:f) The relation of concentration vs. penetration distance and ln (concentration) vs. penetration^2 for different vacancies concentration:

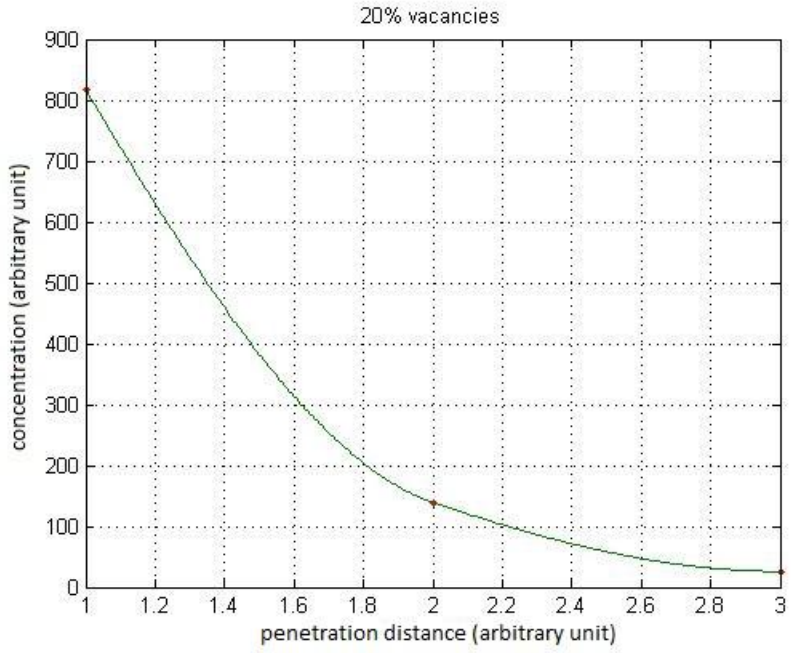

Figure (5.8 a) penetration profile for 20% vacancies concentration matrix

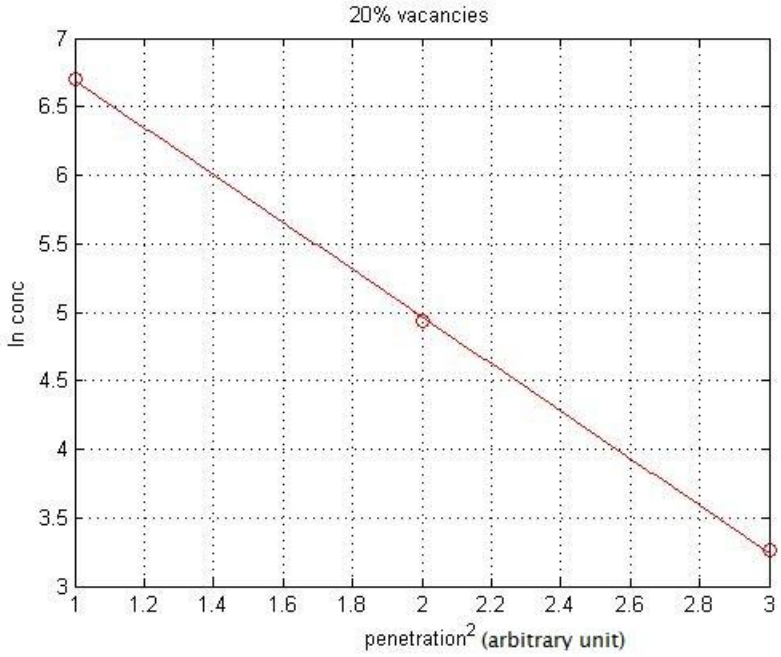

Figure (5.8 a') Variation of ln (concentration) with penetration distance^2 for 20% vacancies concentration matrix

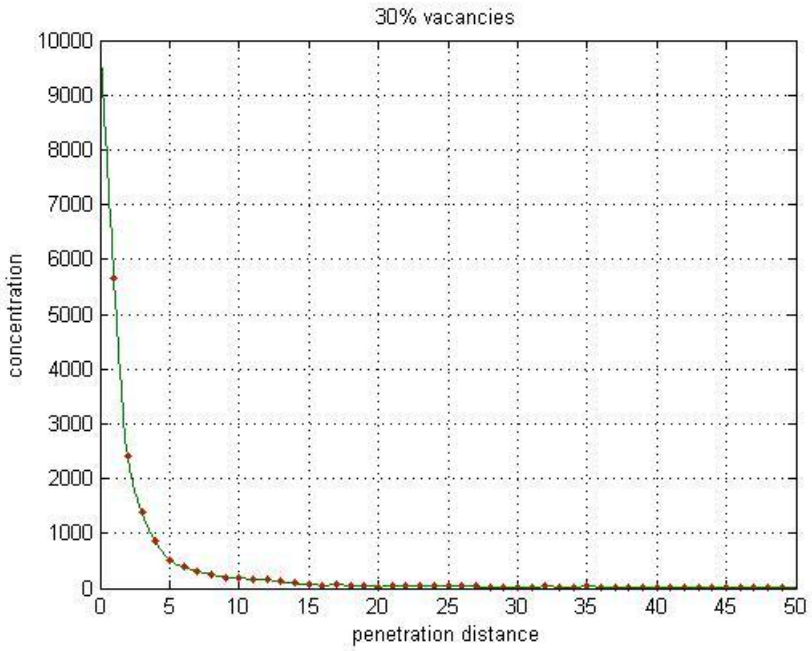

Figure Figure (5.8 b) penetration profile for 30% vacancies concentration matrix

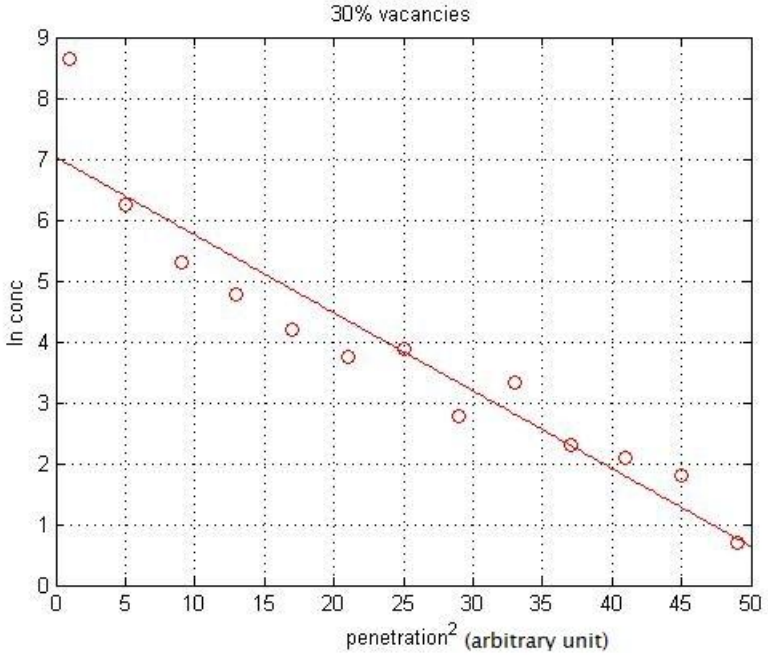

(5.8 b') Variation of ln (concentration) with penetration distance^2 for 30% vacancies concentration matrix

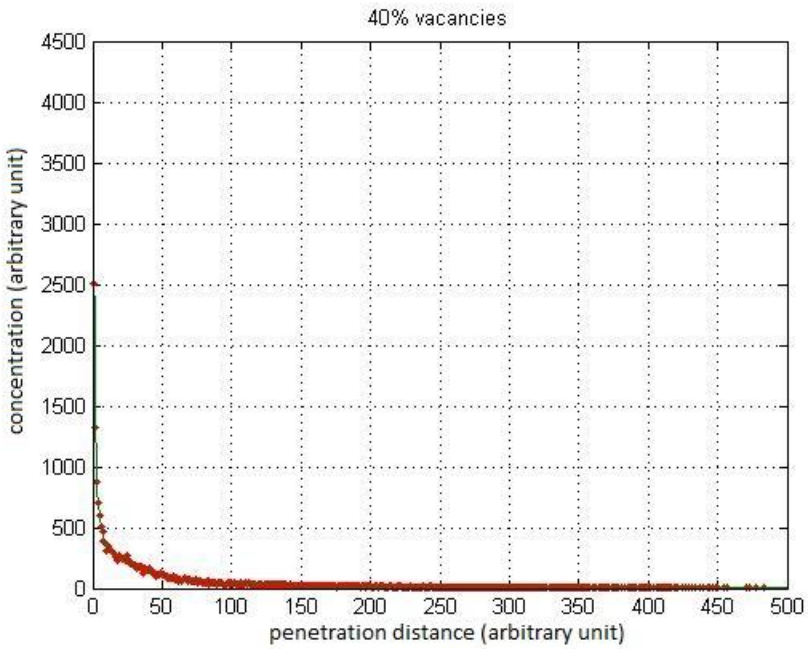

Figure (5.8 c) penetration profile for 40% vacancies concentration matrix

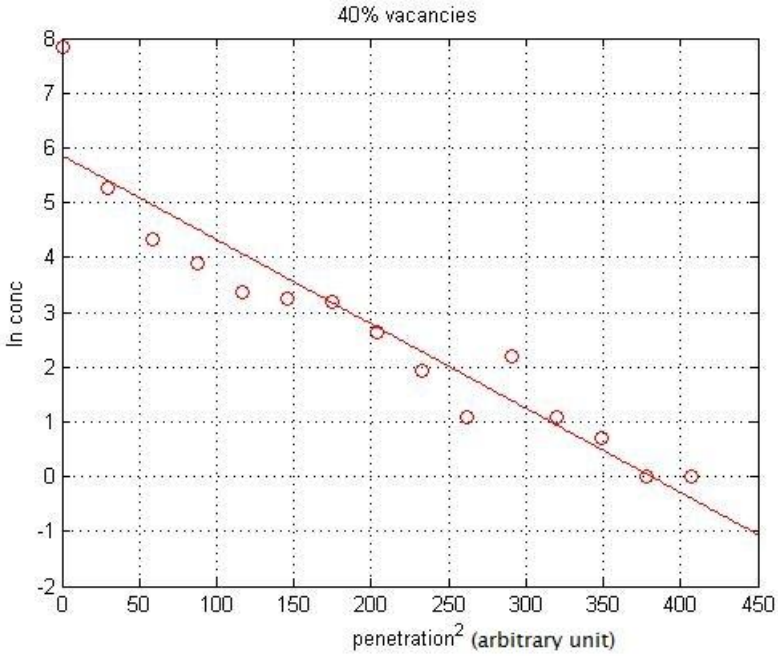

(5.8 c') Variation of ln (concentration) with penetration distance^2 for 40% vacancies concentration matrix

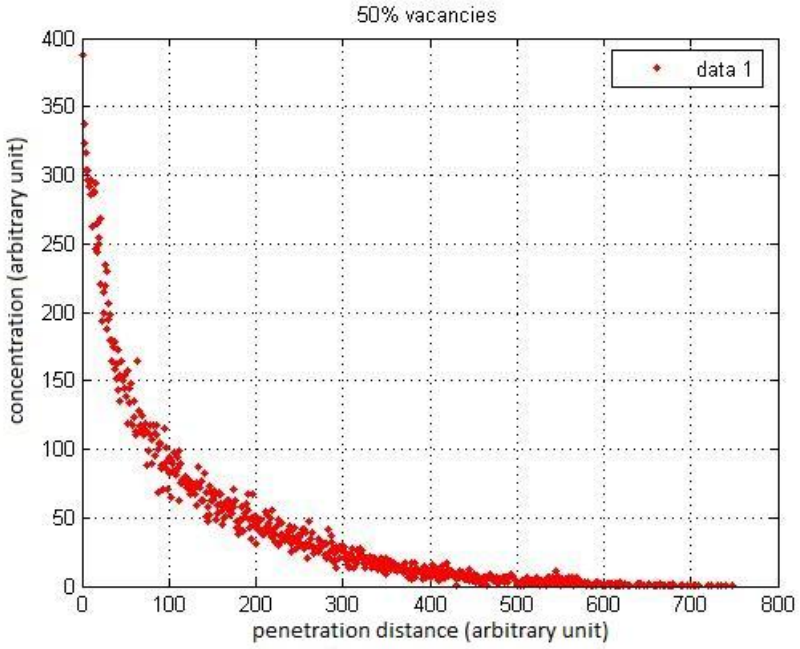

Figure (5.8 d) penetration profile for 50% vacancies concentration matrix

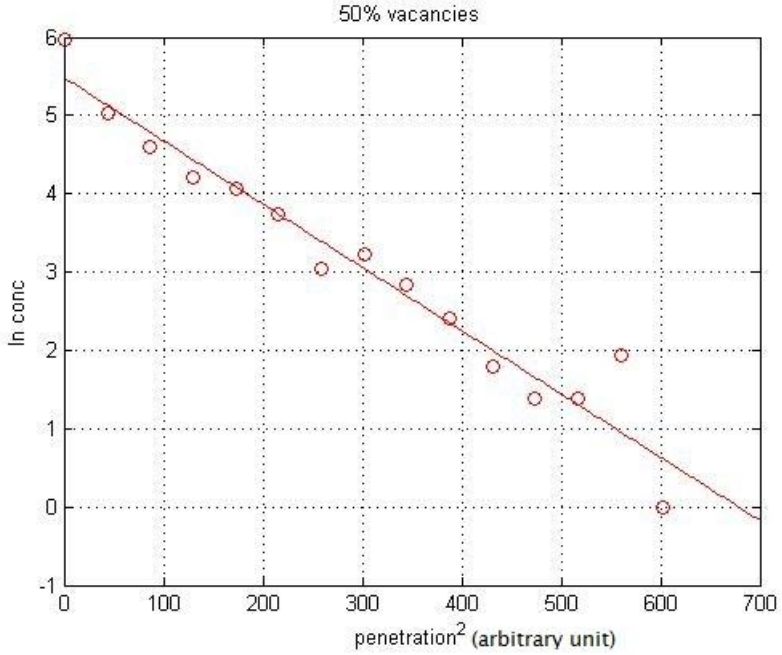

(5.8 d') Variation of ln (concentration) with penetration distance^2 for 50% vacancies concentration matrix

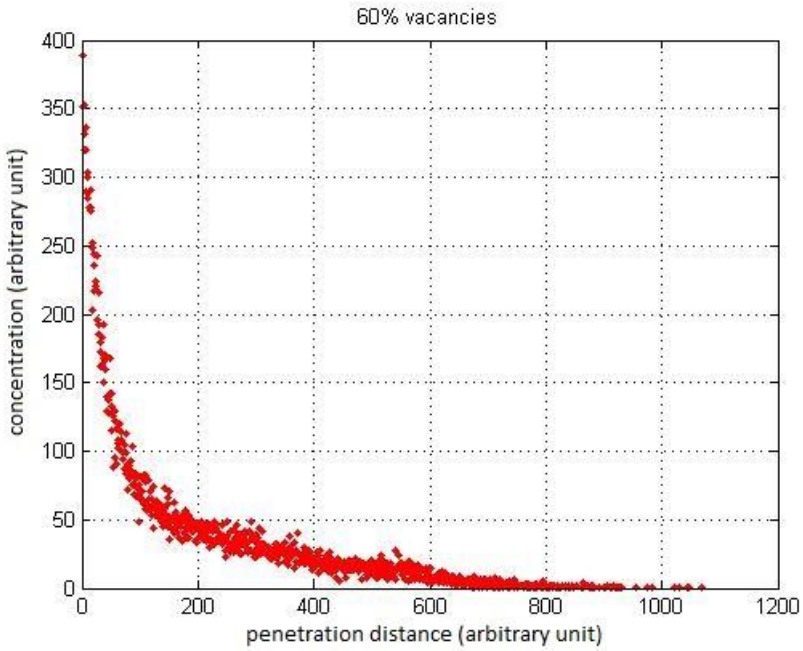

Figure (5.8 e) penetration profile for 60% vacancies concentration matrix

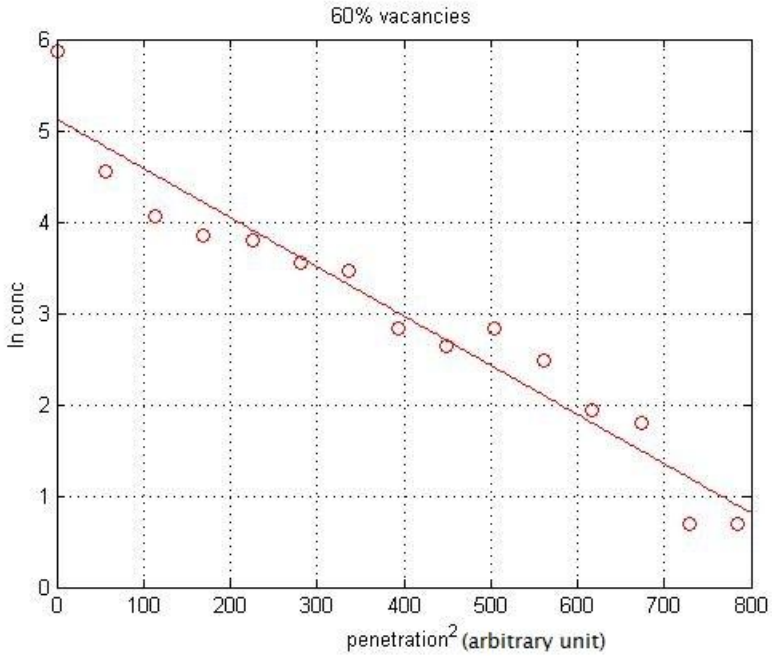

(5.8 e') Variation of ln (concentration) with penetration distance^2 for 60% vacancies concentration matrix

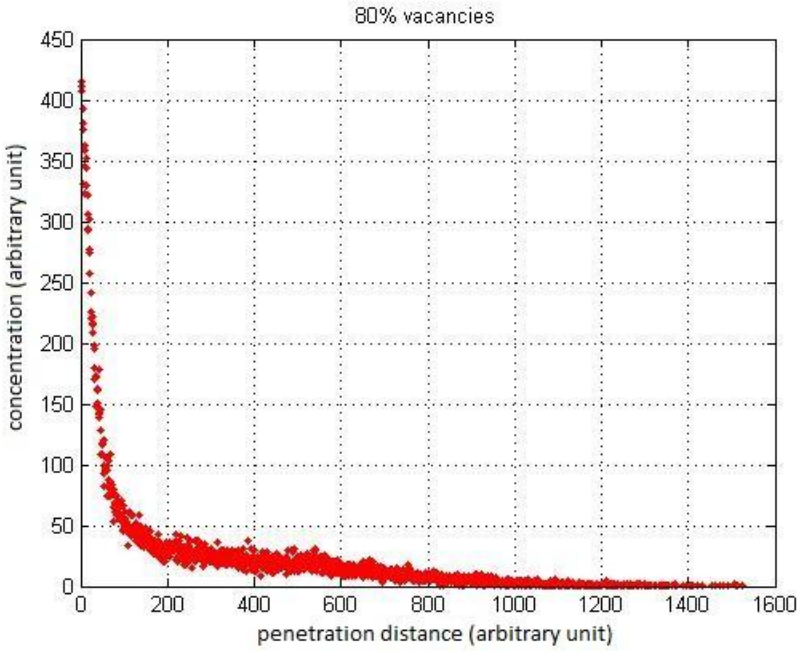

Figure (5.8 f) penetration profile for 80% vacancies concentration matrix

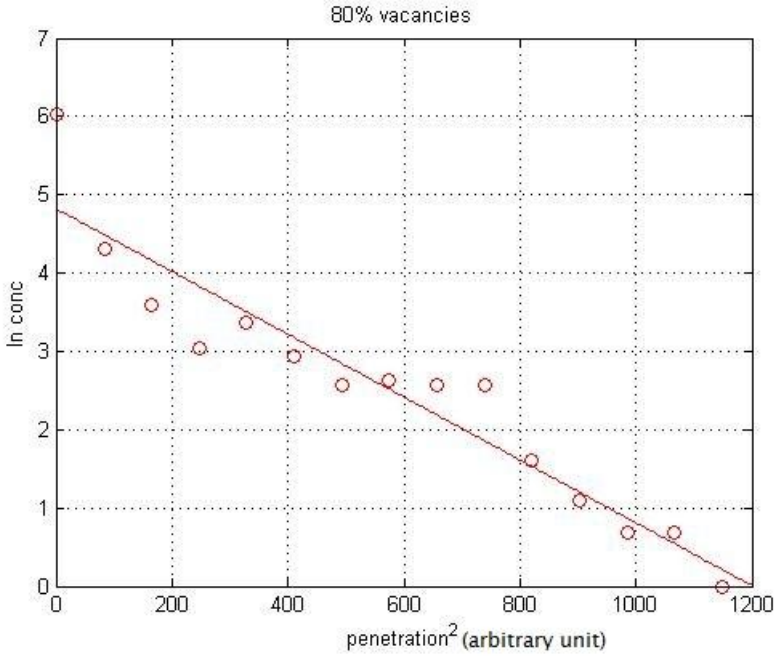

(5.8 f') Variation of ln (concentration) with penetration distance^2 for 80% vacancies concentration matrix

5.2.2. Variation of penetration distance and diffusion coefficient with annealing time:

Results of: Matrix 10,000 x 10,000 vacancies percentage 50%

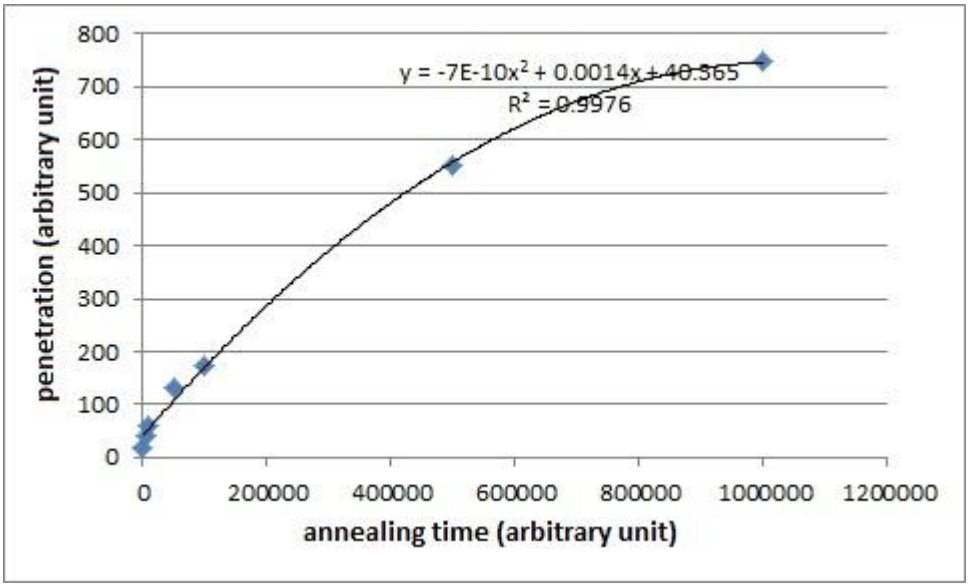

Figure (5.9) Variation of penetration distance with annealing time

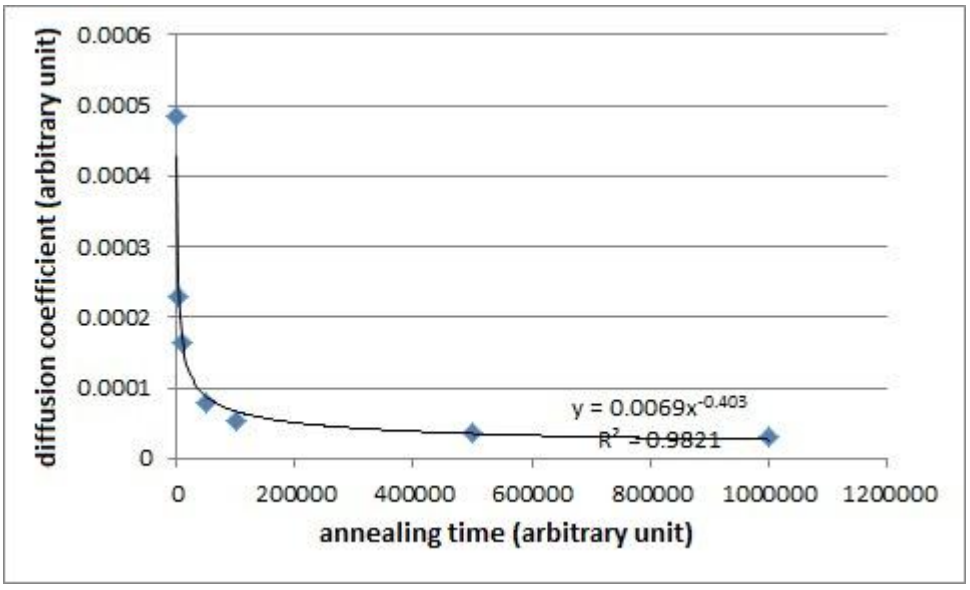

Figure (5.10) Variation of diffusion coefficient with annealing time

Figures (5.11 a:f) show the relation of concentration vs. penetration distance and ln (concentration) vs. penetration^2 for different annealing times:

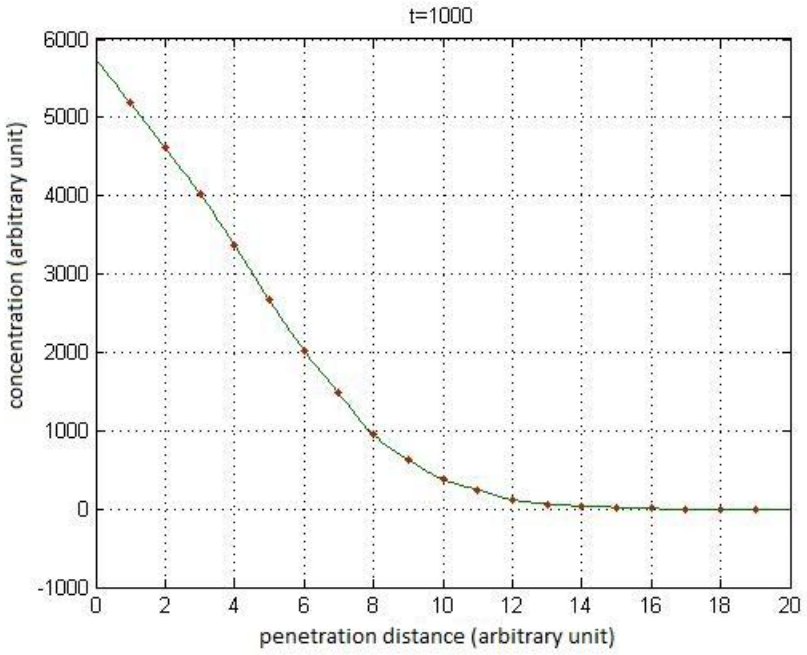

Figure (5.11 a) penetration profile for annealing time=1000

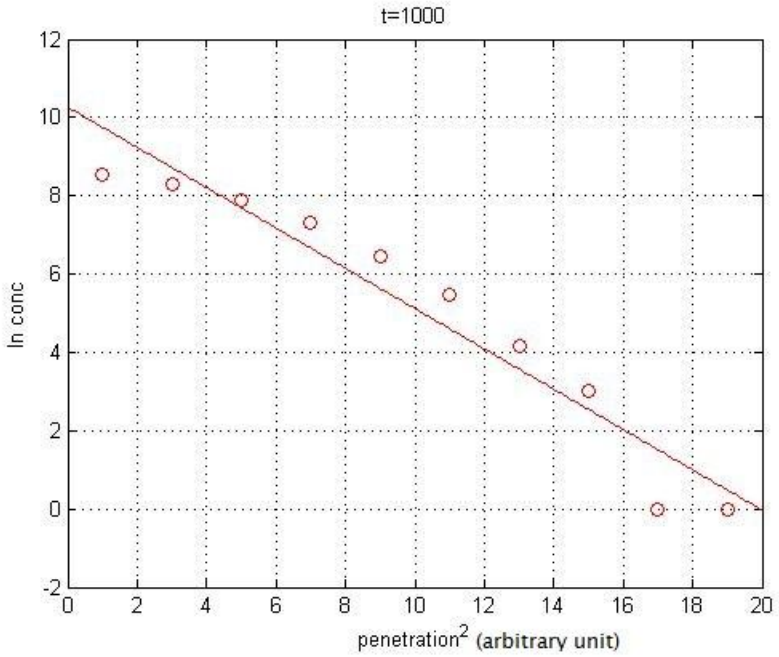

(5.11 a') Variation of ln (concentration) with penetration distance^2 for annealing time=1000

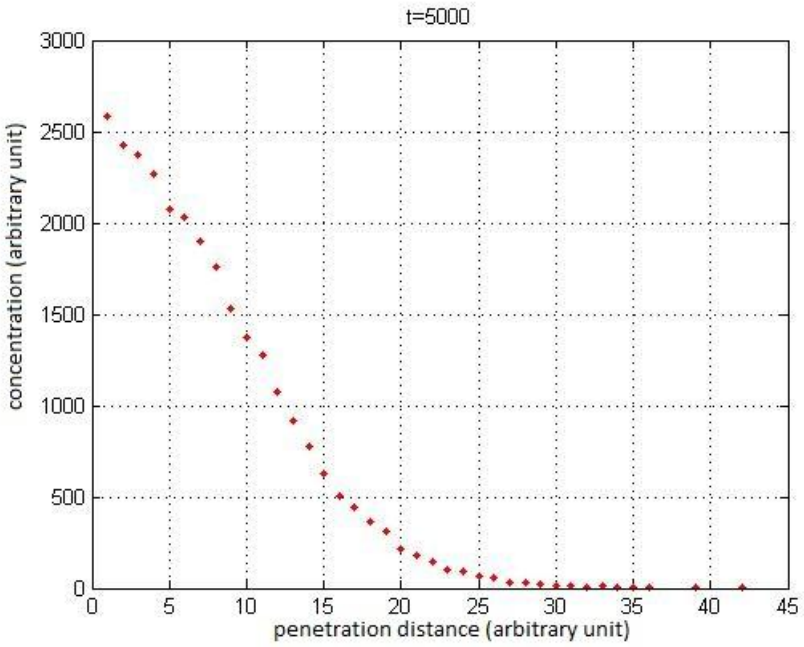

Figure (5.11 b) penetration profile for annealing time=5000

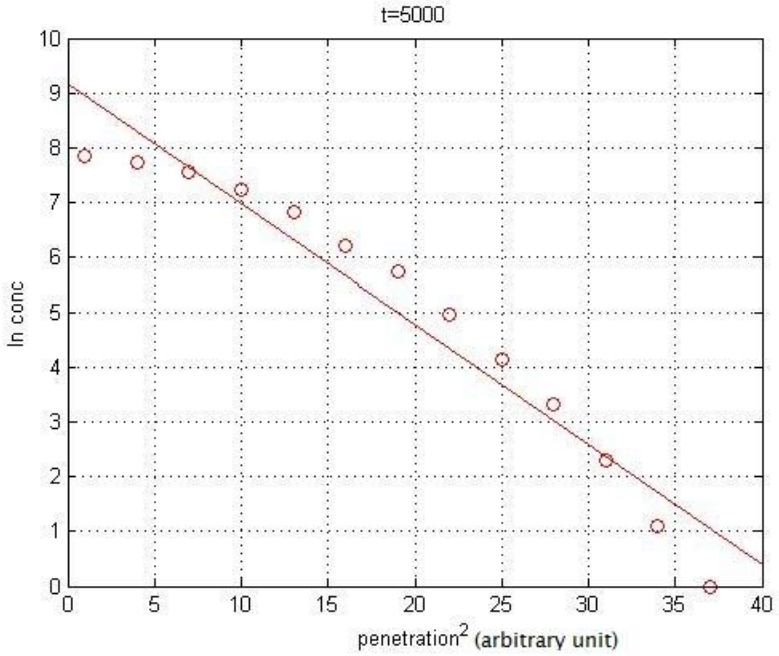

(5.11 b') Variation of ln (concentration) with penetration distance^2 for annealing time=5000

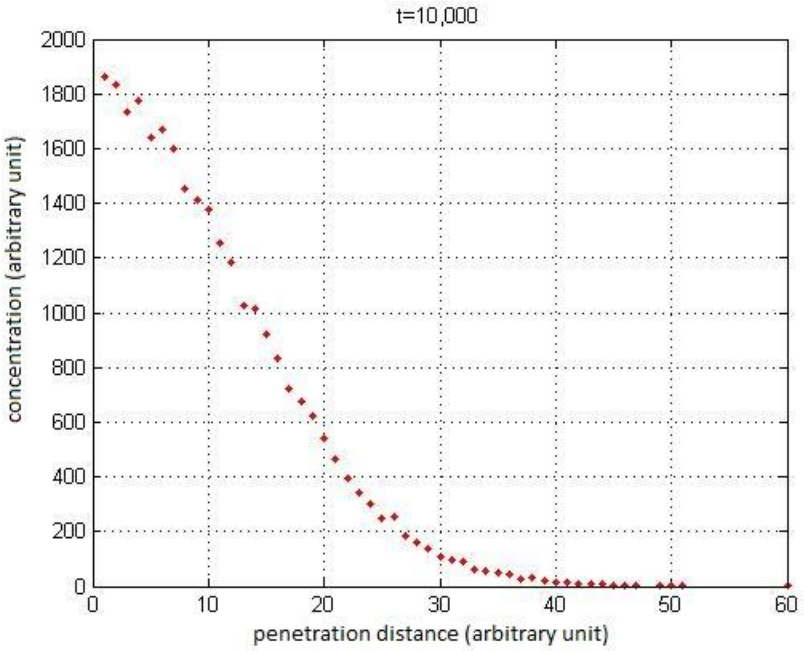

Figure (5.11 c) penetration profile for annealing time=10,000

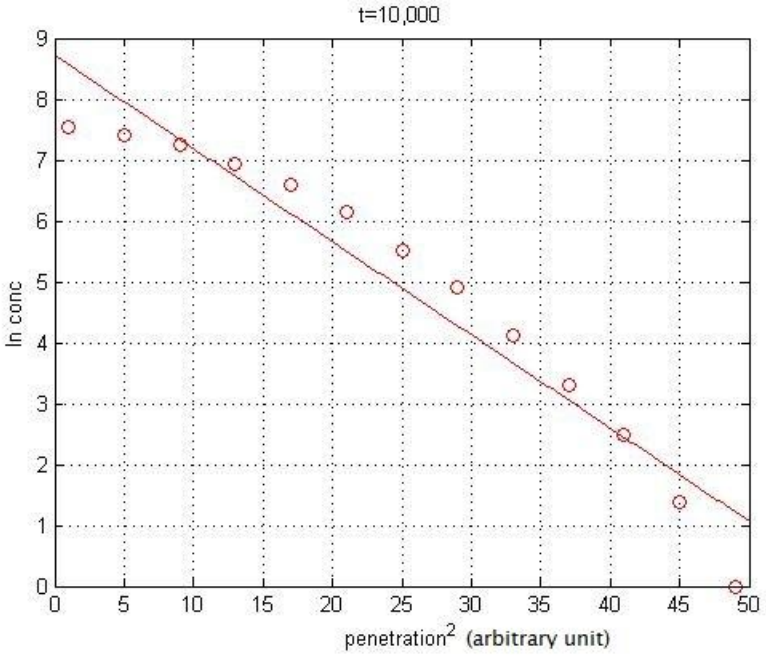

(5.11 c') Variation of ln (concentration) with penetration distance^2 for annealing time=10,000

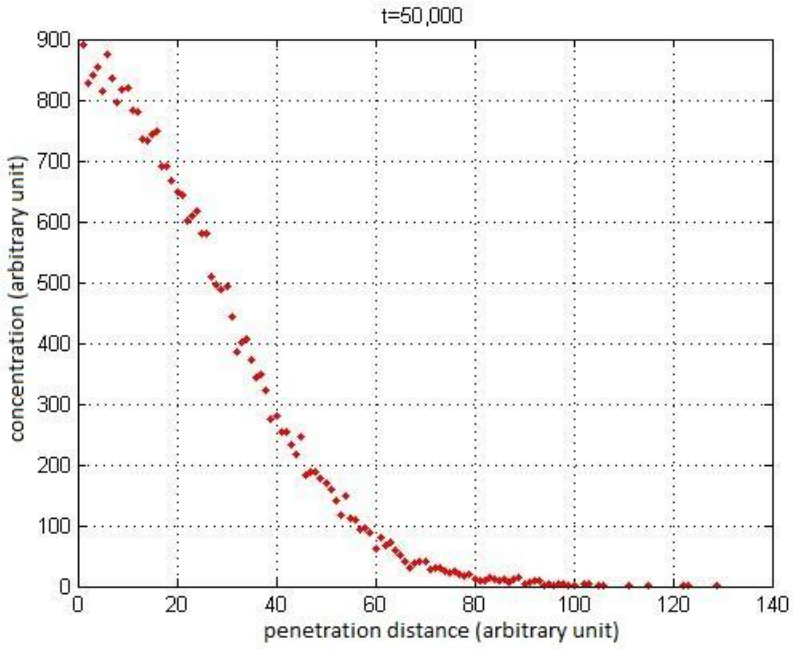

Figure (5.11 d) penetration profile for annealing time=50,000

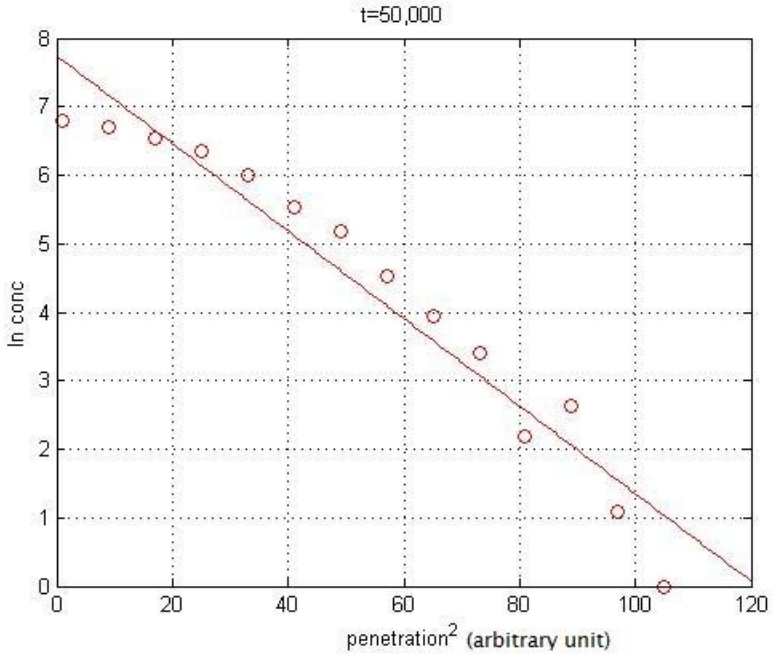

(5.11 d') Variation of ln (concentration) with penetration distance^2 for annealing time=50,000

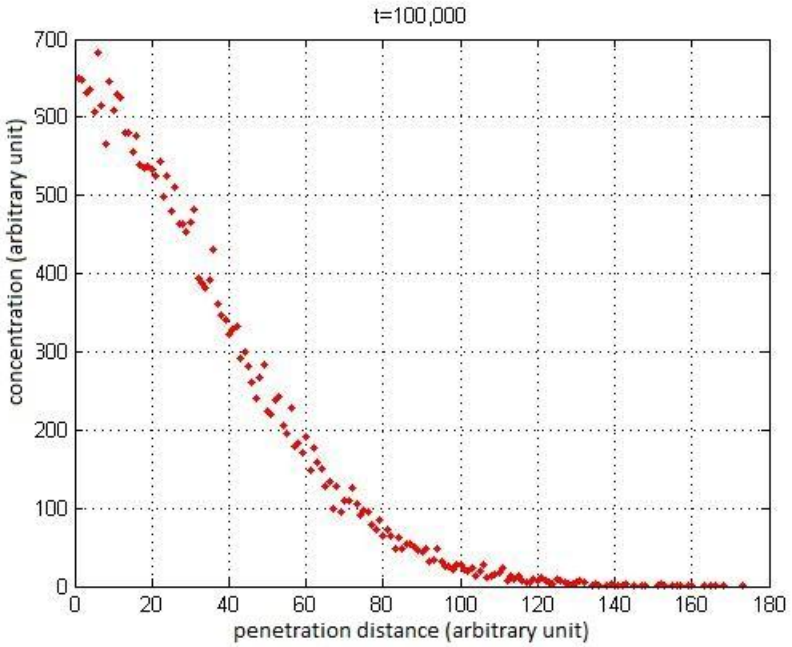

Figure (5.11 e) penetration profile for annealing time=100,000

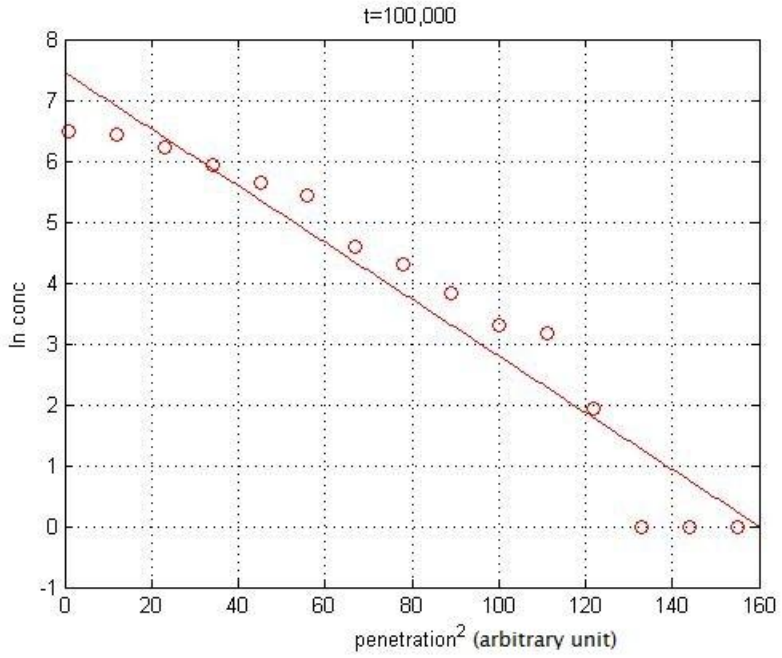

(5.11 e') Variation of ln (concentration) with penetration distance^2 for annealing time=100,000

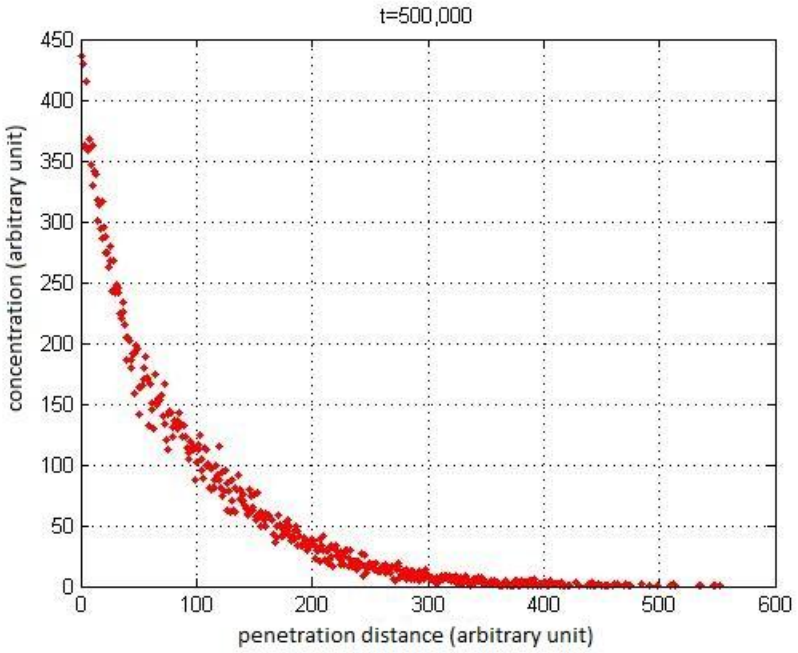

Figure (5.11 f) penetration profile for annealing time=500,000

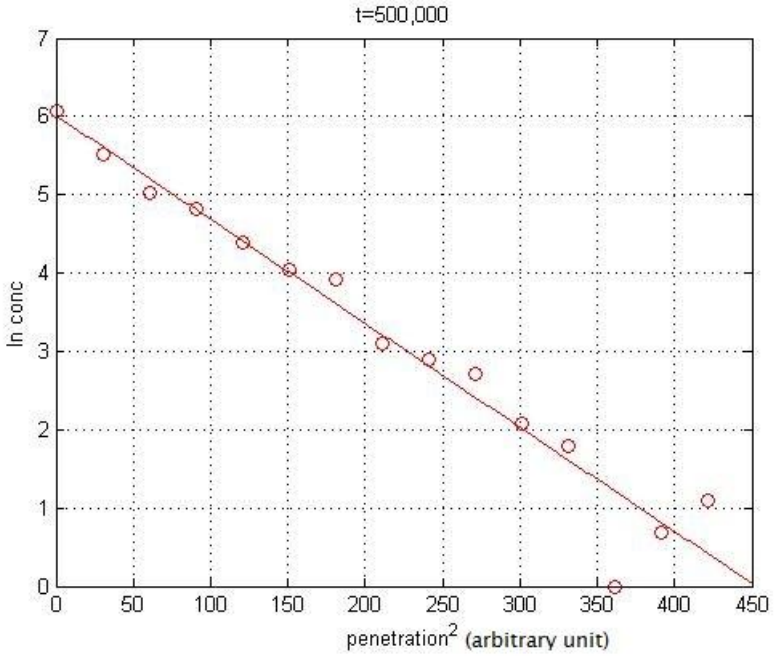

(5.11 f') Variation of ln (concentration) with penetration distance^2 for annealing time=500,000

5.3. Effect of electric field on the penetration of ions:

5.3.1. Effect of direct current (forward /backward directions):

Following the algorithm illustrated in figure (4.11), the effect of direct current in the forward and backward directions on diffusion of positive ions in biological host is examined for different current strengths. Also the effect of different time steps and vacancies concentration with the presence of direct current electric field is examined.

The electric field strength is varied from 0 to 1.

Results of: Matrix 1000 x 1000, vacancies= 90%, t=1000 time steps

Figures (5.12) show the penetration profiles for different current strengths in forward direction in a matrix of 90% vacancies:

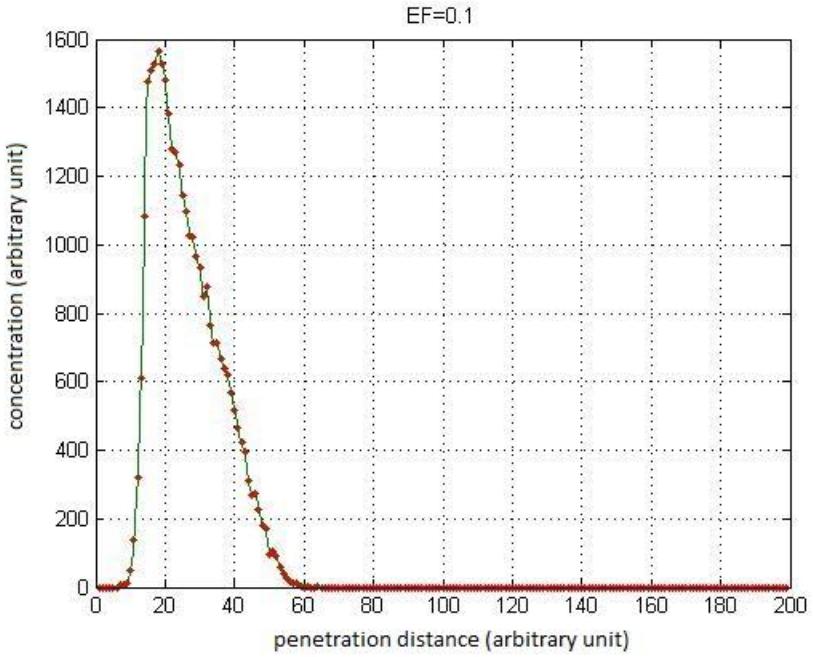

Figure (5.12 a) Penetration profile for EF=0.1 direct current in forward direction in a matrix of 90% vacancies

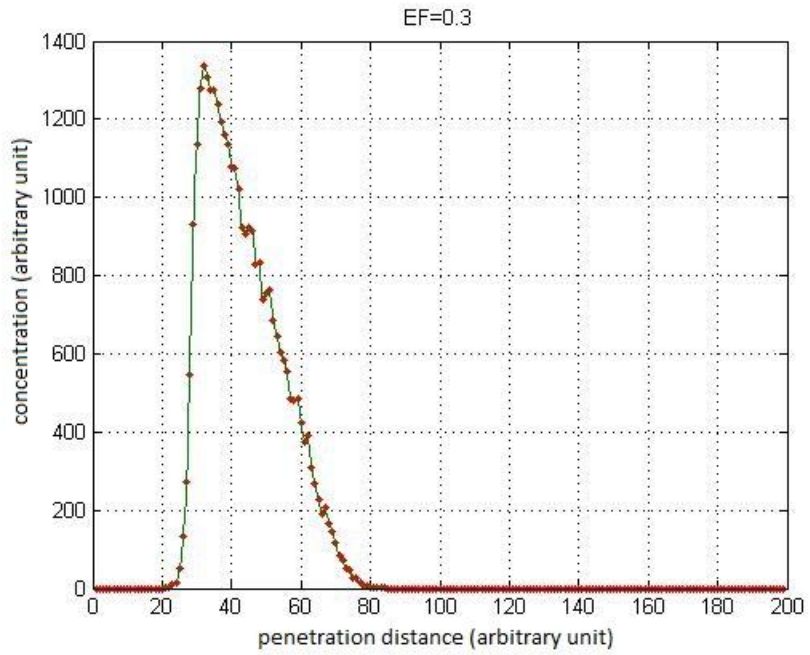

Figure (5.12 b) Penetration profile for EF=0.3 direct current in forward direction in a matrix of 90% vacancies

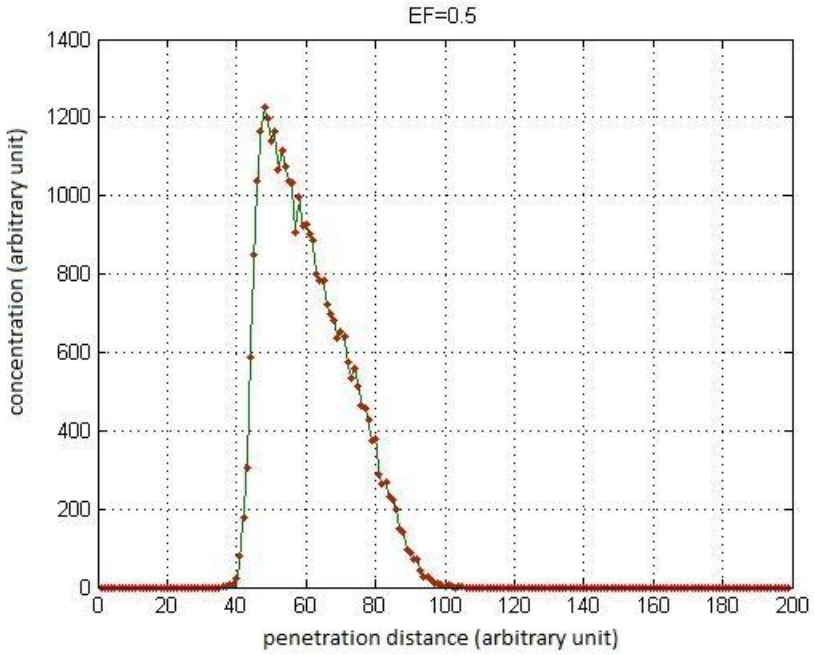

Figure (5.12 c) Penetration profile for EF=0.5 direct current in forward direction in a matrix of 90% vacancie

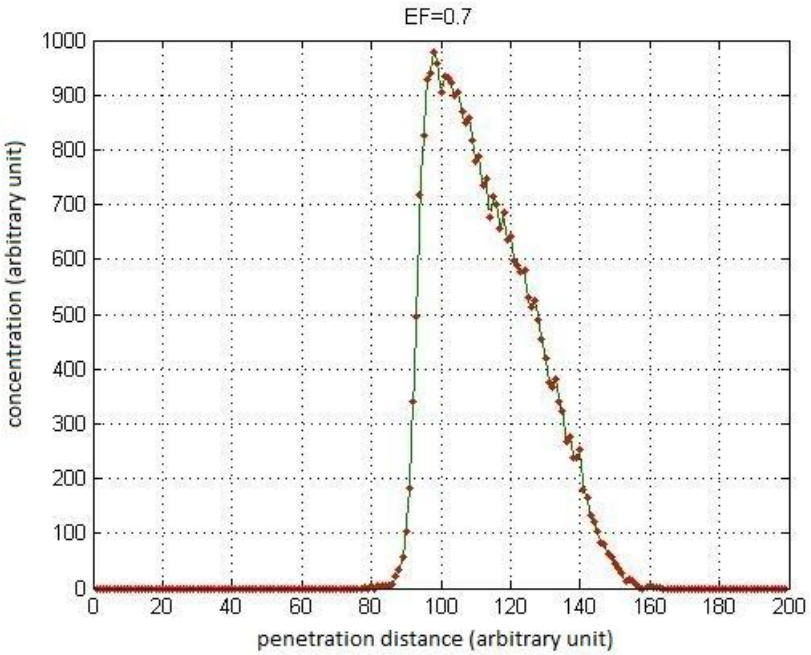

Figure (5.12 d) Penetration profile for EF=0.7 direct current in forward direction in a matrix of 90% vacancies

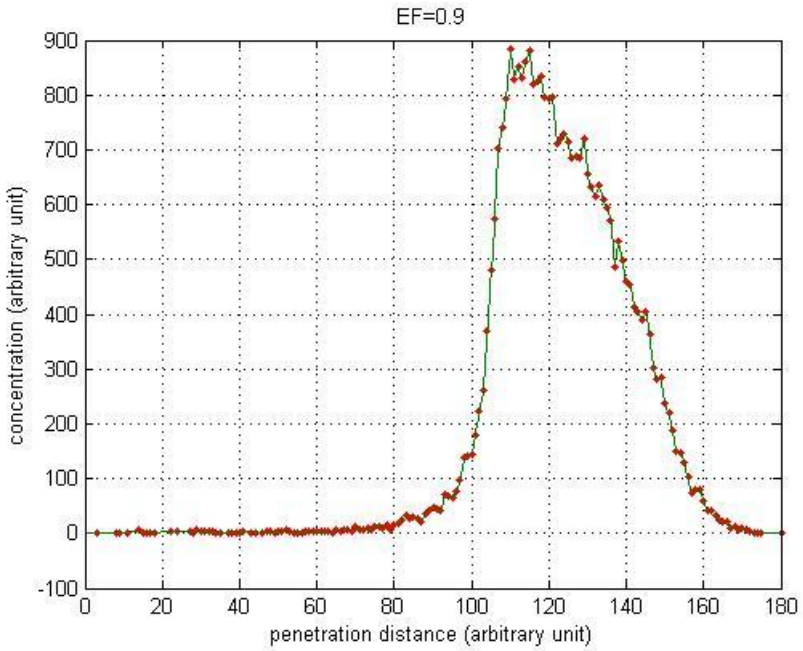

Figure (5.12 e) Penetration profile for EF=0.9 direct current in forward direction in a matrix of 90% vacancies

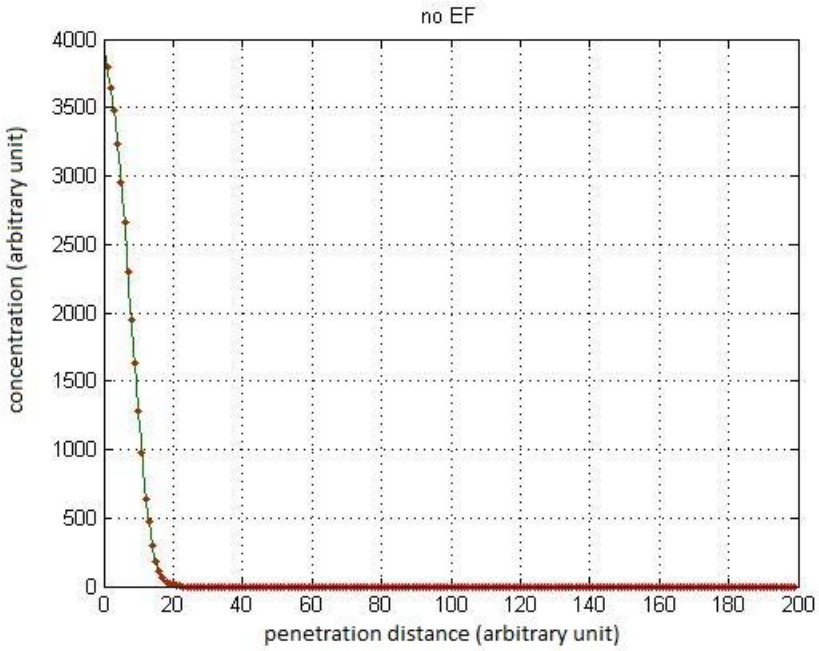

Figure (5.12 f) Penetration profile for EF=0 in a matrix of 90% vacancies

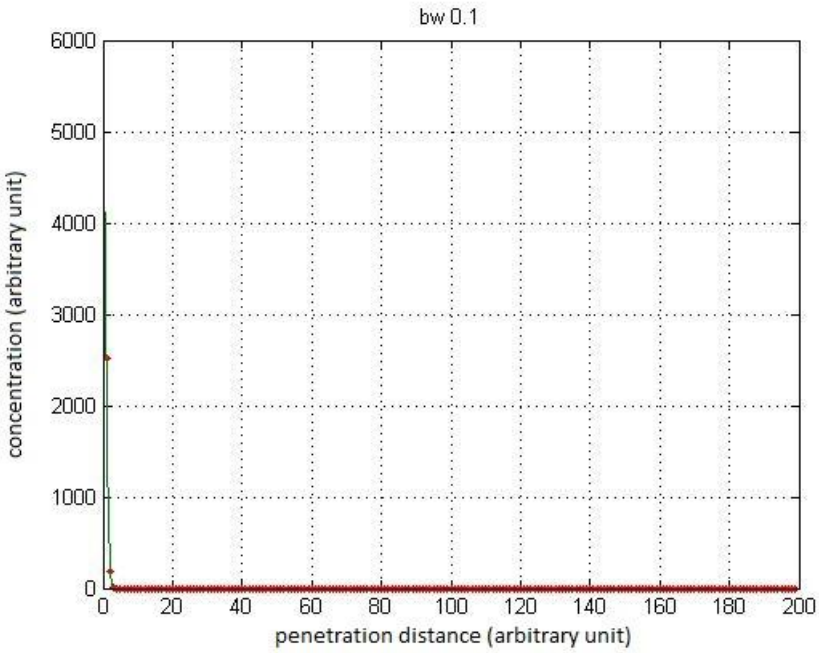

Figure (5.12 g) Penetration profile for EF= 0.1 direct current in backward direction in a matrix of 90% vacancies

Results of: Matrix 1000 x 1000, vacancies=50%, t=1000 time steps

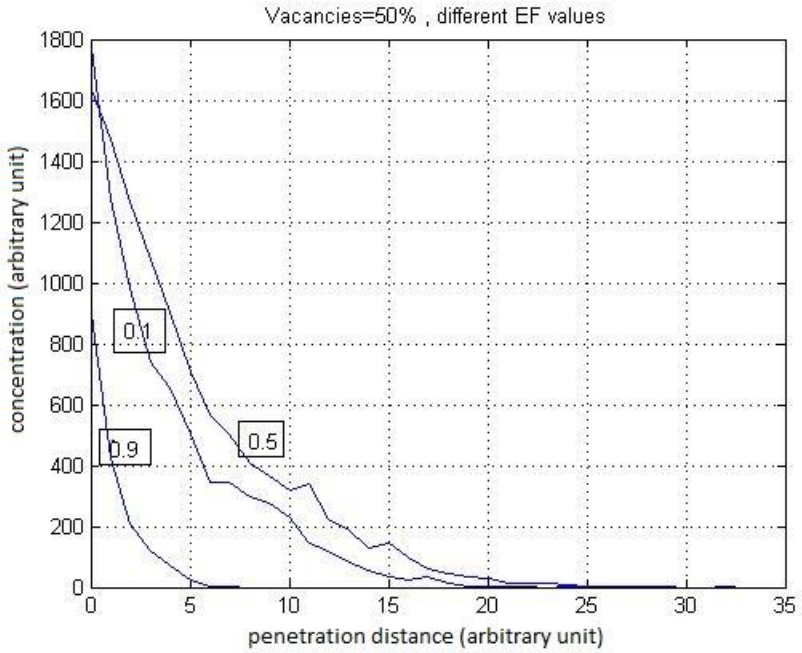

Figure (5.13) Penetration profiles for different direct current strengths in forward direction in a matrix of 50% vacancies

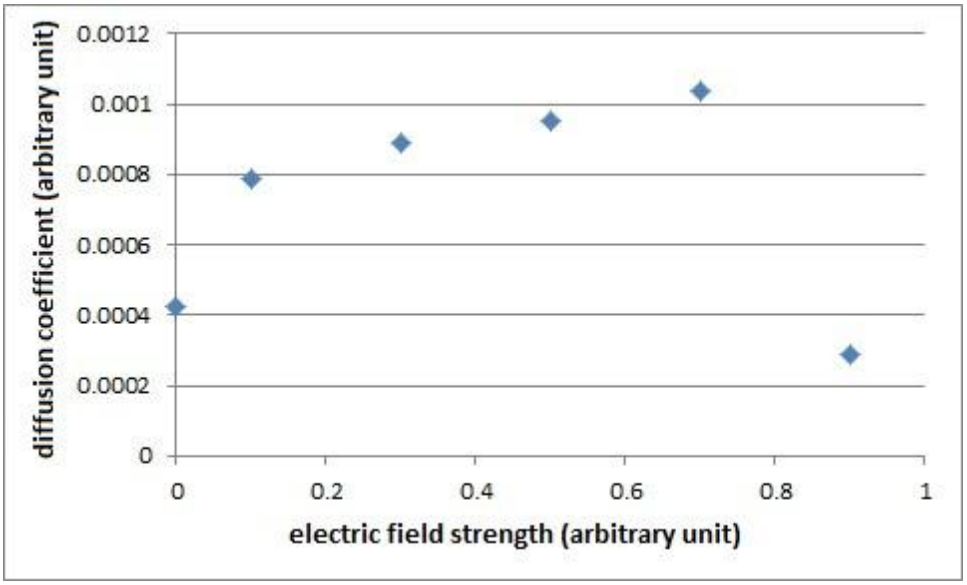

Figure (5.14) Variation of diffusion coefficient with the electric field strength for the direct current in forward direction in a matrix of 50% vacancies

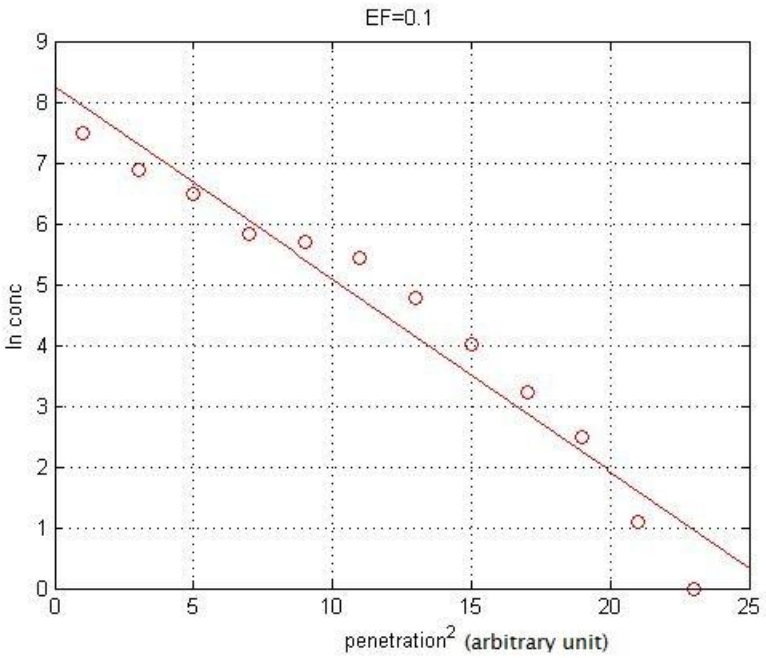

Figure (5.15 a) Variation of ln (concentration) with penetration distance^2 for EF=0.1 in forward direction in a matrix of 50% vacancies

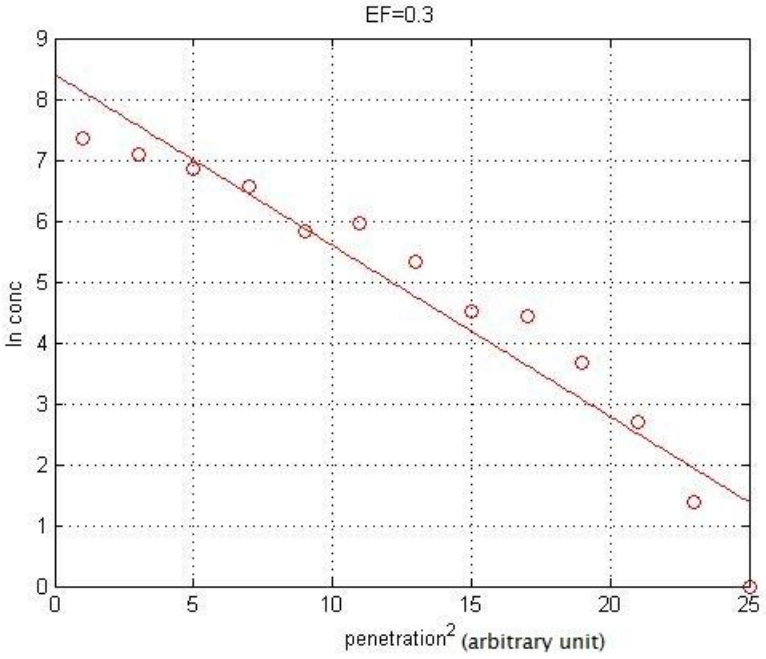

Figure (5.15 b) Variation of ln (concentration) with penetration distance^2 for EF=0.3 in forward direction in a matrix of 50% vacancies

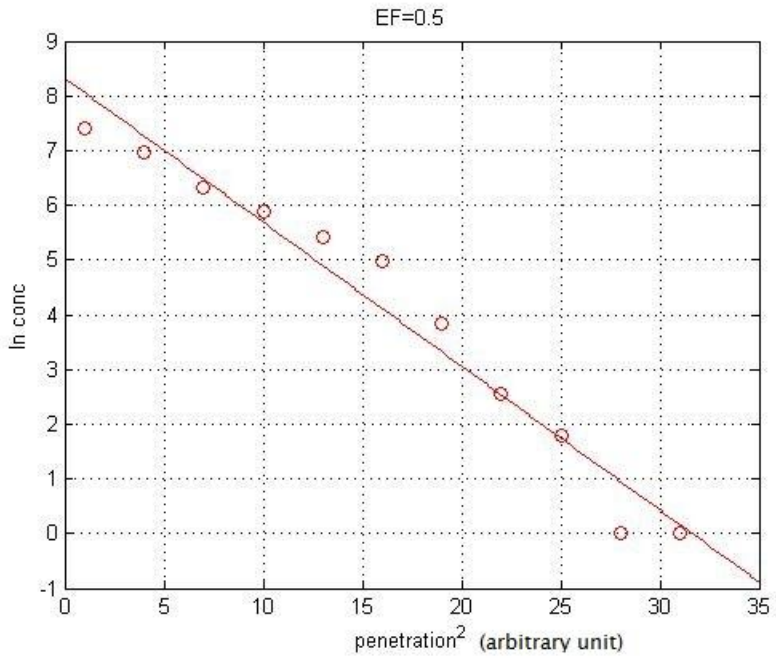

Figure (5.15 c) Variation of ln (concentration) with penetration distance^2 for EF=0.5 in forward direction in a matrix of 50% vacancies

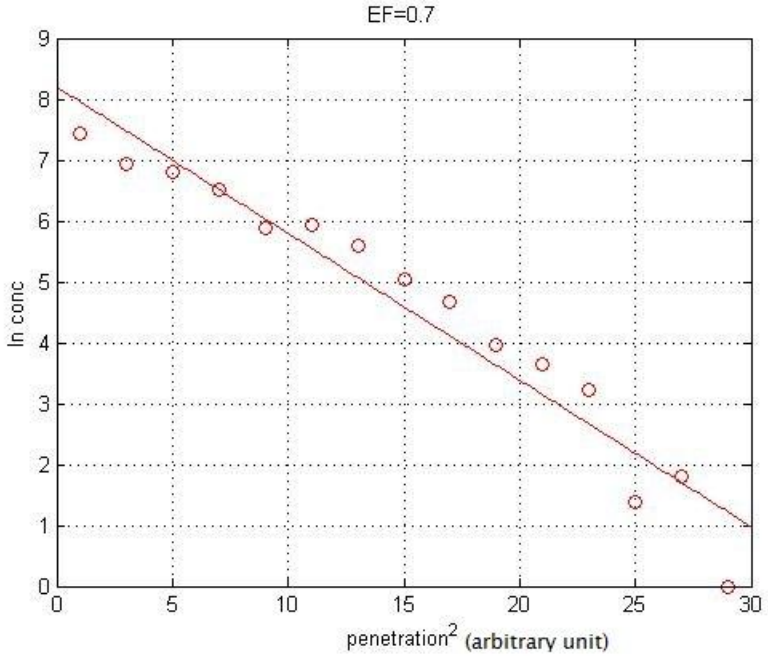

Figure (5.15 d) Variation of ln (concentration) with penetration distance^2 for EF=0.7 in forward direction in a matrix of 50% vacancies

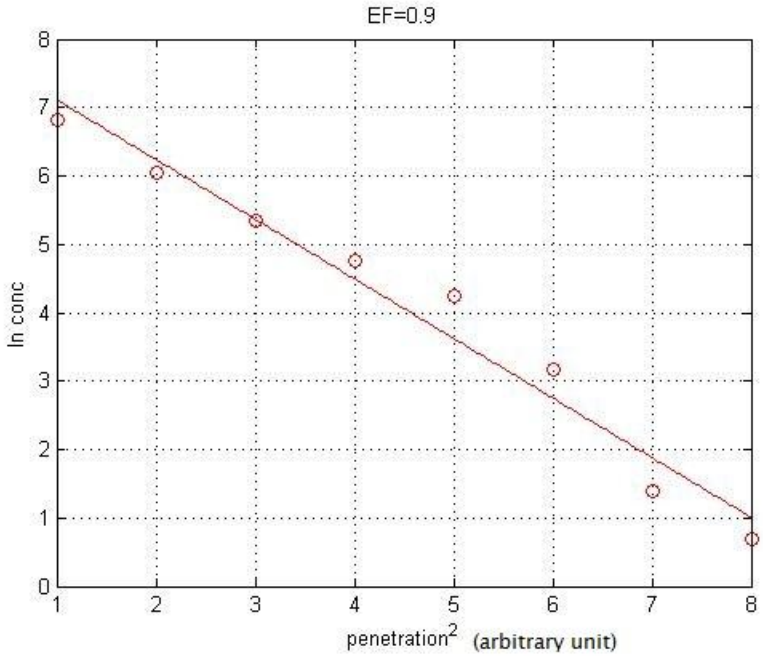

Figure (5.15 e) Variation of ln (concentration) with penetration distance^2 for EF=0.9 in forward direction in a matrix of 50% vacancies

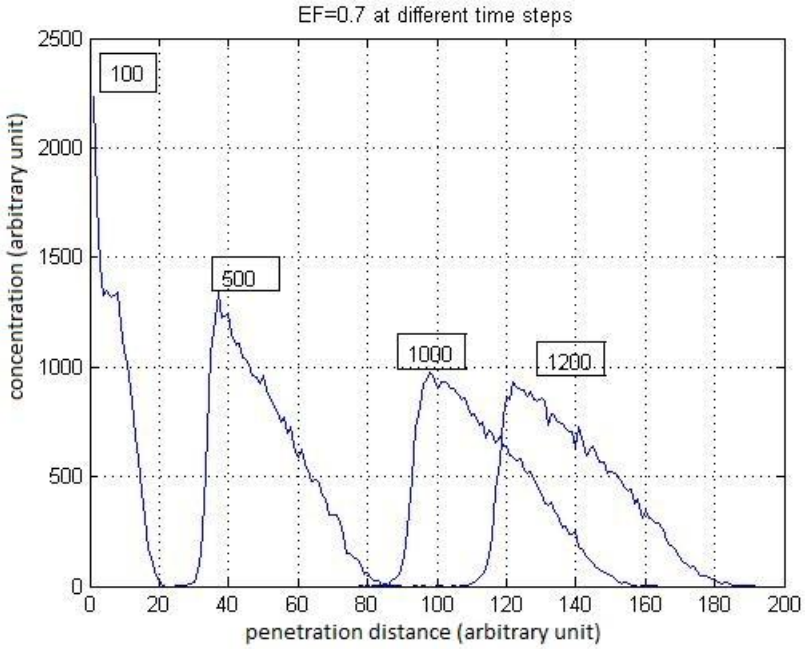

Figure (5.16) Penetration profiles for forward direct current (EF=0.7) at different time steps in a matrix with 90% vacancies concentration

5.3.2. Effect of alternating electric field on the penetration of ions:

Matrix 10,000 x 10,000 vacancies percentage 50% annealing time: 1,000,000

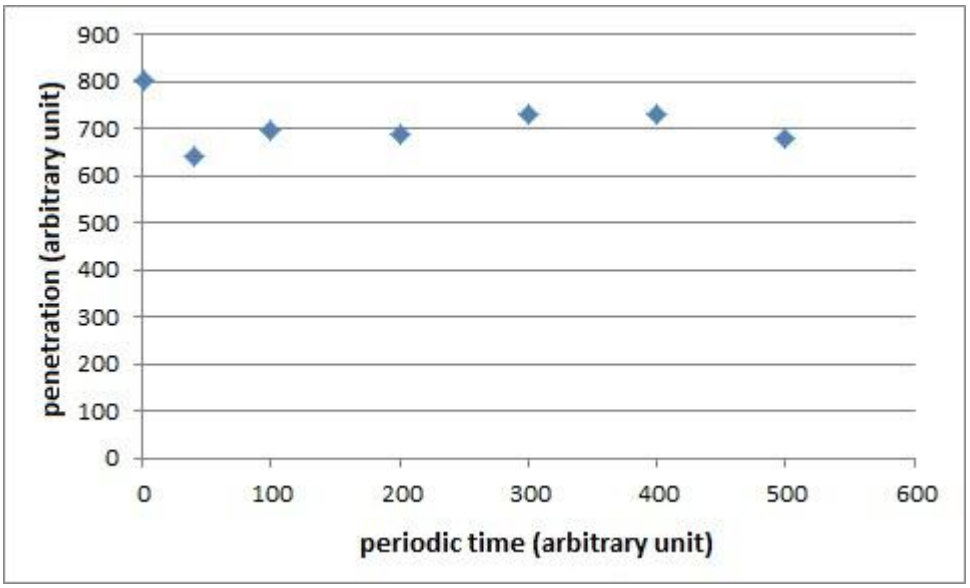

Figure (5.17) variation of penetration distance with periodic time of sinusoidal wave in a matrix of 50% vacancies

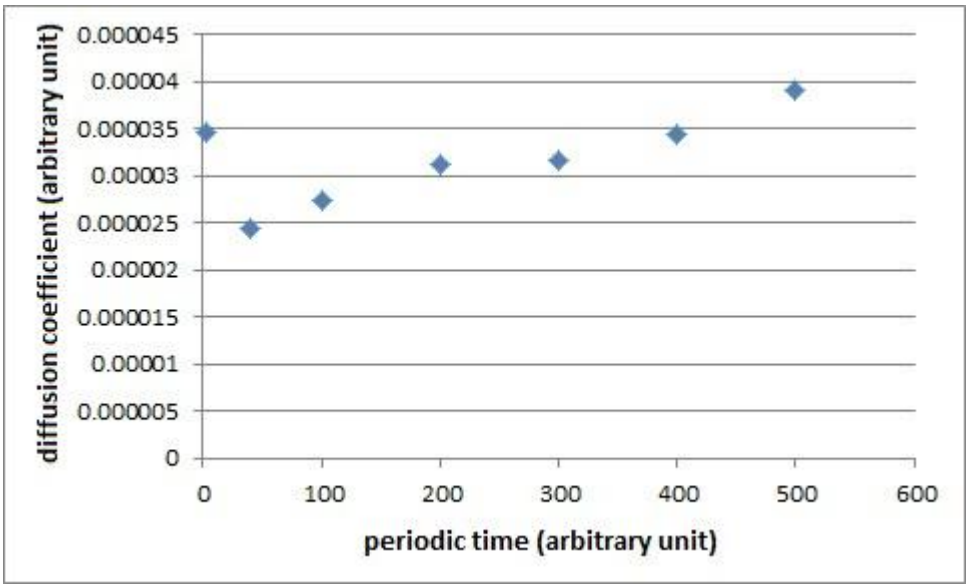

Figure (5.18) variation of diffusion coefficient with the periodic time of sinusoidal wave in a matrix of 50% vacancies

Figures (5.19 a:g) show the relation of concentration vs. penetration distance and ln (concentration) vs. penetration^2 for different periodic times in a matrix of 90% vacancies

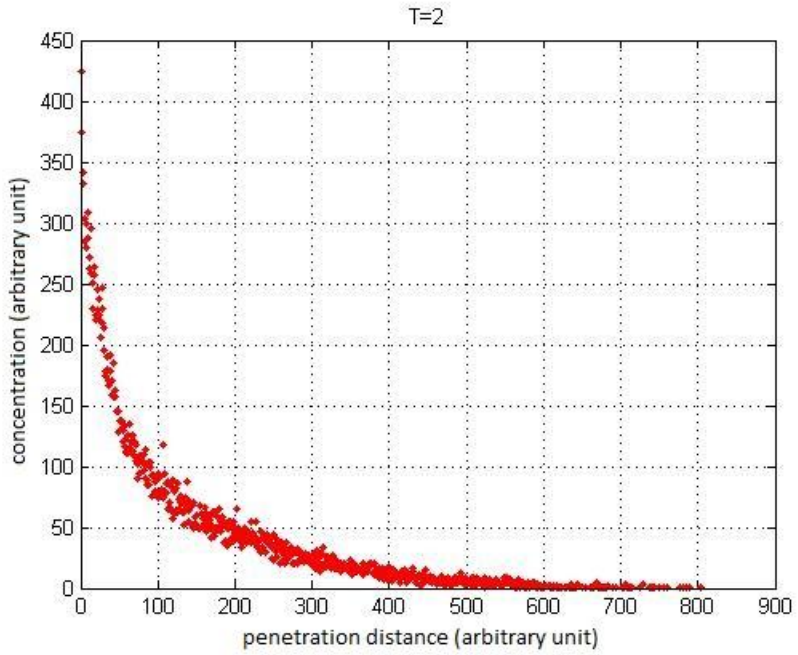

Figure (5.19 a) Penetration profile for sinusoidal wave with periodic time T=2 in a matrix of 90% vacancies

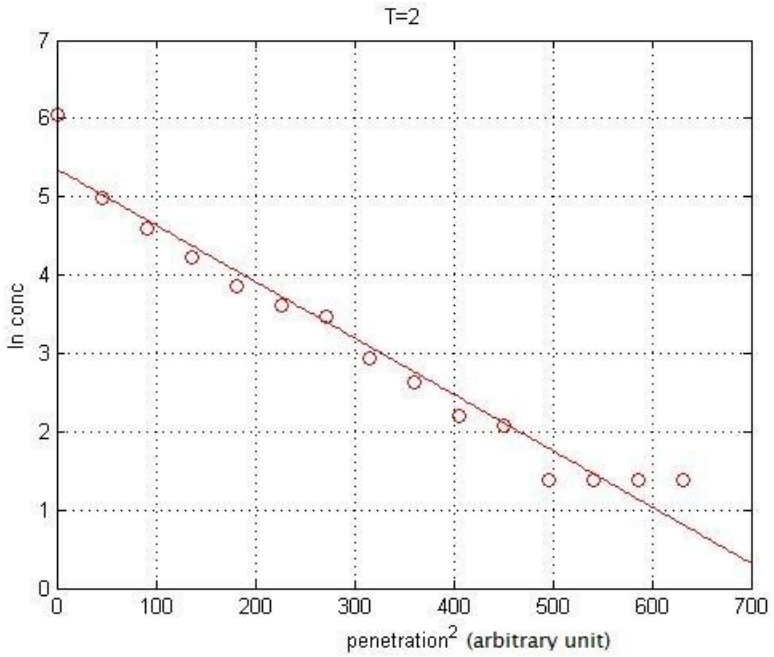

Figure (5.19 a') Variation of ln (concentration) with penetration distance^2 for sinusoidal wave with periodic time T=2 in a matrix of 90% vacancies

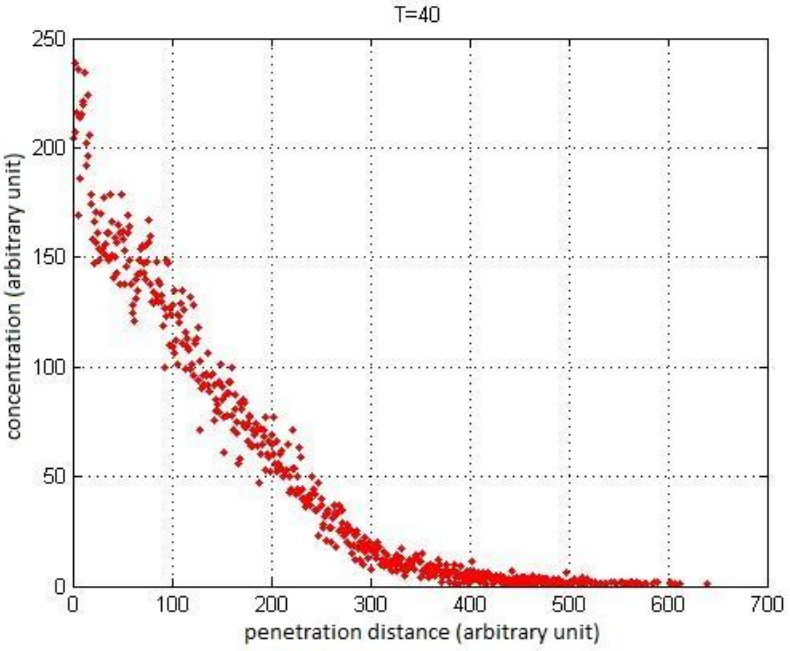

Figure (5.19 b) Penetration profile for sinusoidal wave with periodic time T=40 in a matrix of 90% vacancies

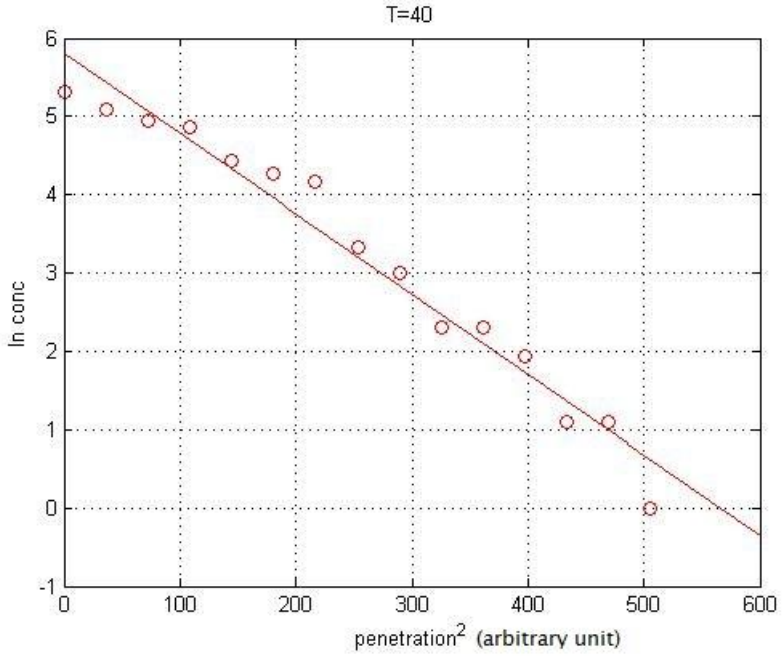

Figure (5.19 b') Variation of ln (concentration) with penetration distance^2 for sinusoidal wave with periodic time T=40 in a matrix of 90% vacancies

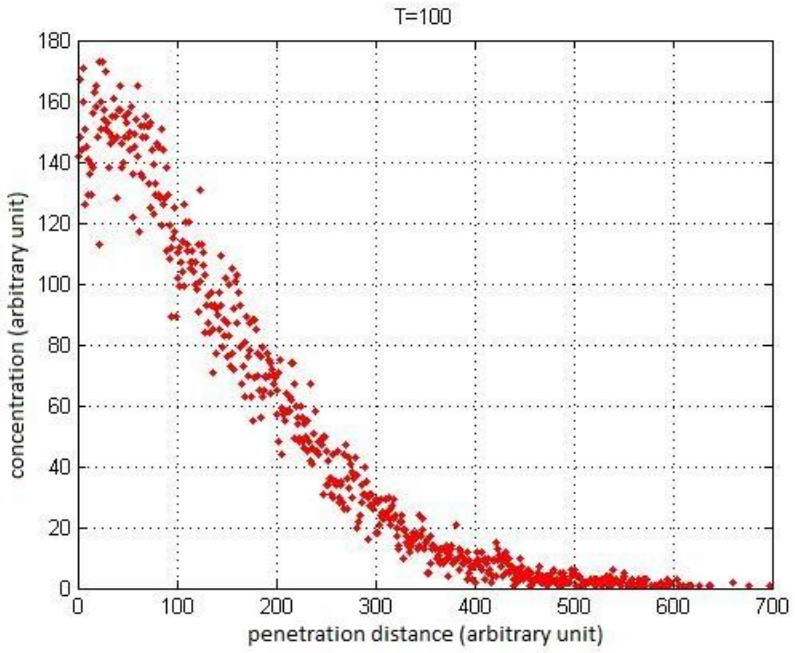

Figure (5.19 c) Penetration profile for sinusoidal wave with periodic time T=100 in a matrix of 90% vacancies

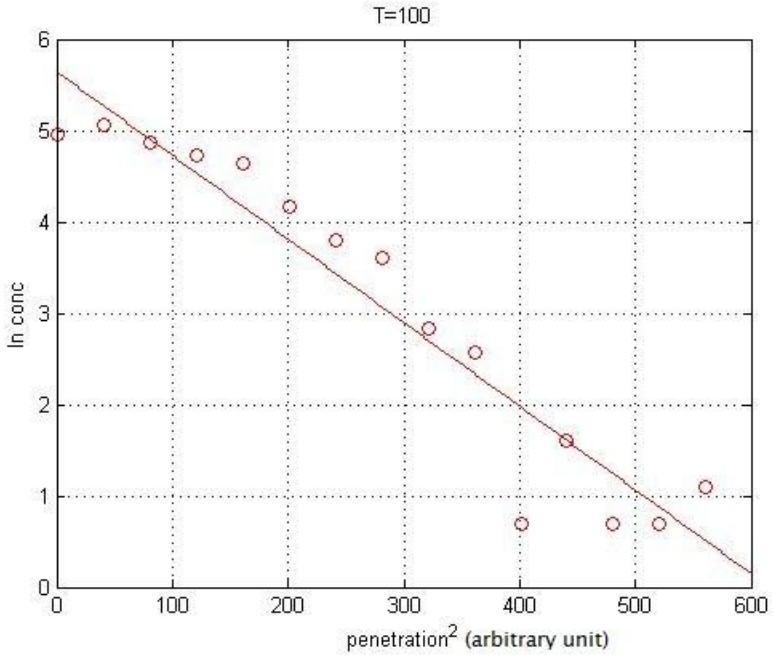

Figure (5.19 c') Variation of ln (concentration) with penetration distance^2 for sinusoidal wave with periodic time T=100 in a matrix of 90% vacancies

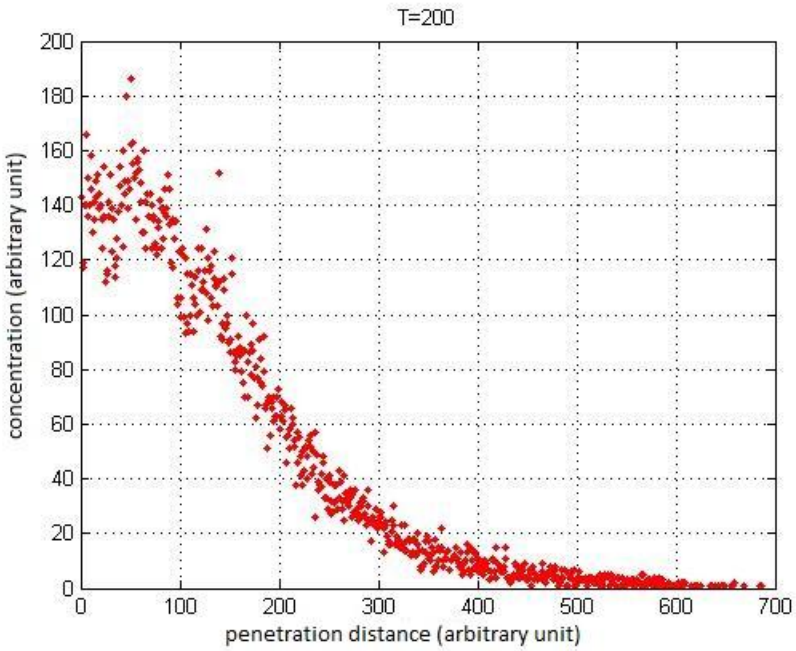

Figure (5.19 d) Penetration profile for sinusoidal wave with periodic time T=200 in a matrix of 90% vacancies

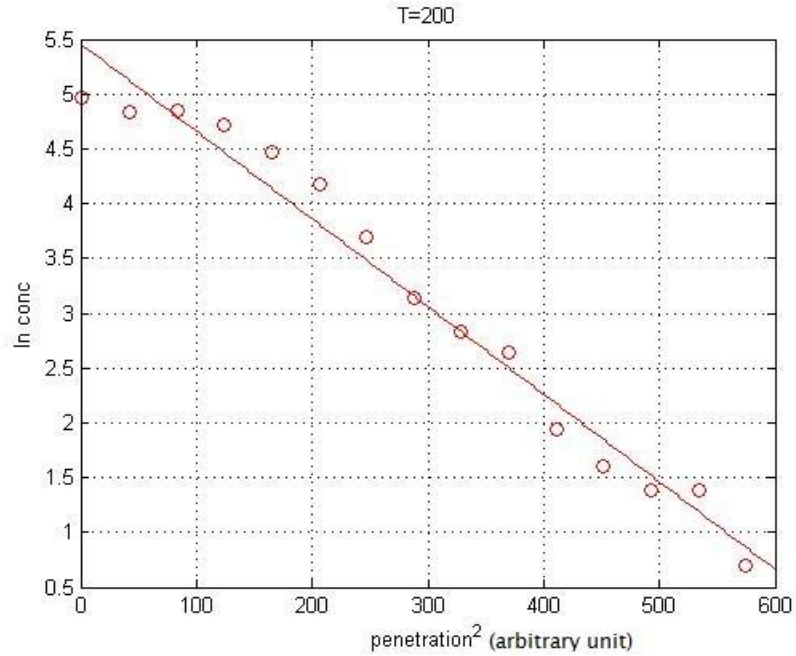

Figure (5.19 d') Variation of ln (concentration) with penetration distance^2 for sinusoidal wave with periodic time T=200 in a matrix of 90% vacancies

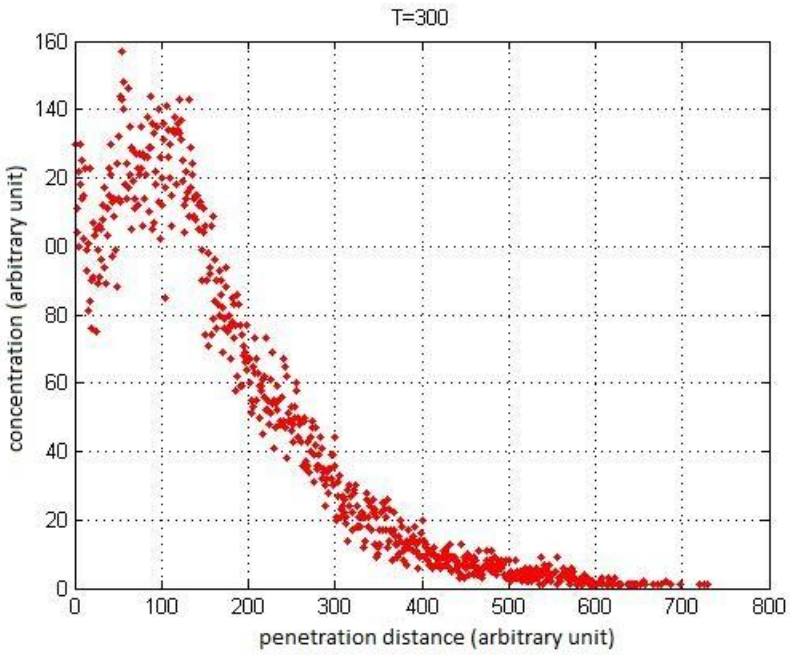

Figure (5.19 e) Penetration profile for sinusoidal wave with periodic time T=300 in a matrix of 90% vacancies

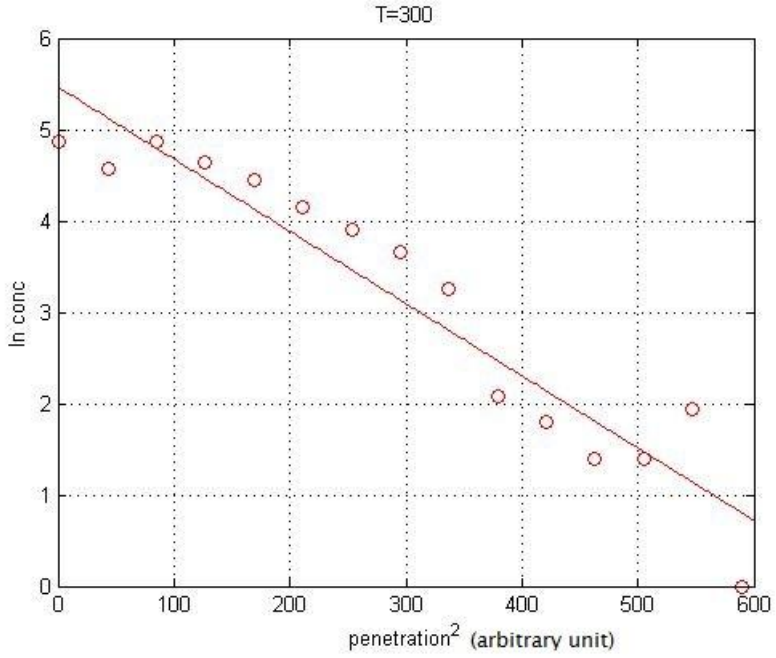

Figure (5.19 e') Variation of ln (concentration) with penetration distance^2 for sinusoidal wave with periodic time T=300 in a matrix of 90% vacancies

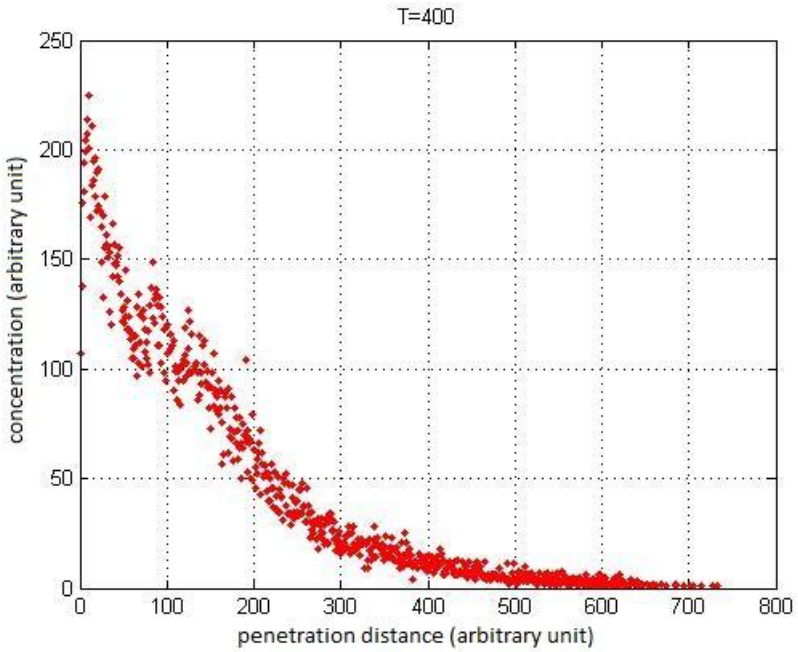

Figure (5.19 f) Penetration profile for sinusoidal wave with periodic time T=400 in a matrix of 90% vacancies

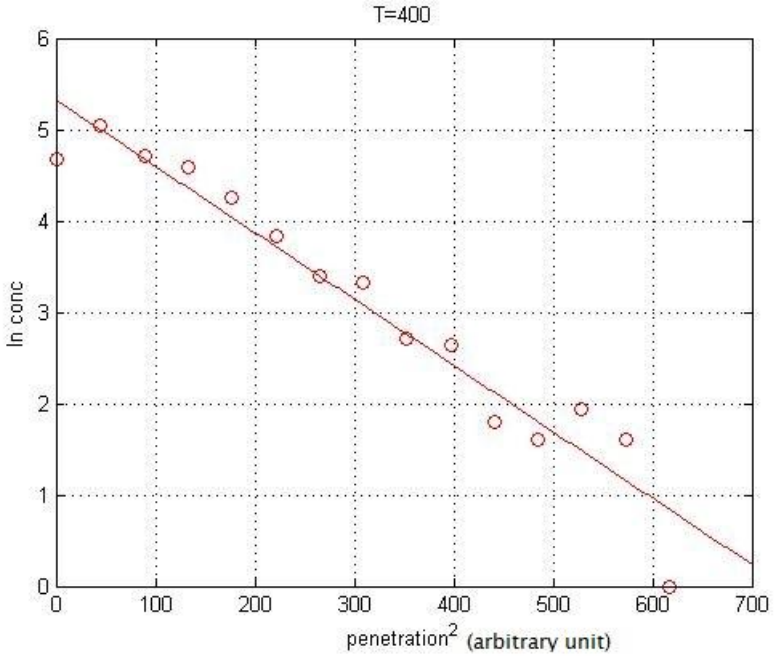

Figure (5.19 f') Variation of ln (concentration) with penetration distance^2 for sinusoidal wave with periodic time T=400 in a matrix of 90% vacanci

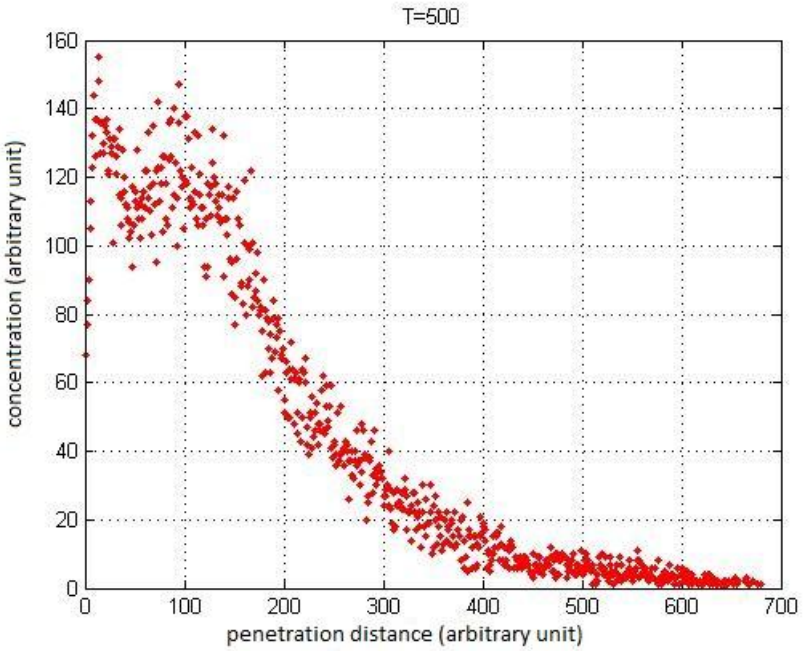

Figure (5.19 g) Penetration profile for sinusoidal wave with periodic time T=500 in a matrix of 90% vacancies

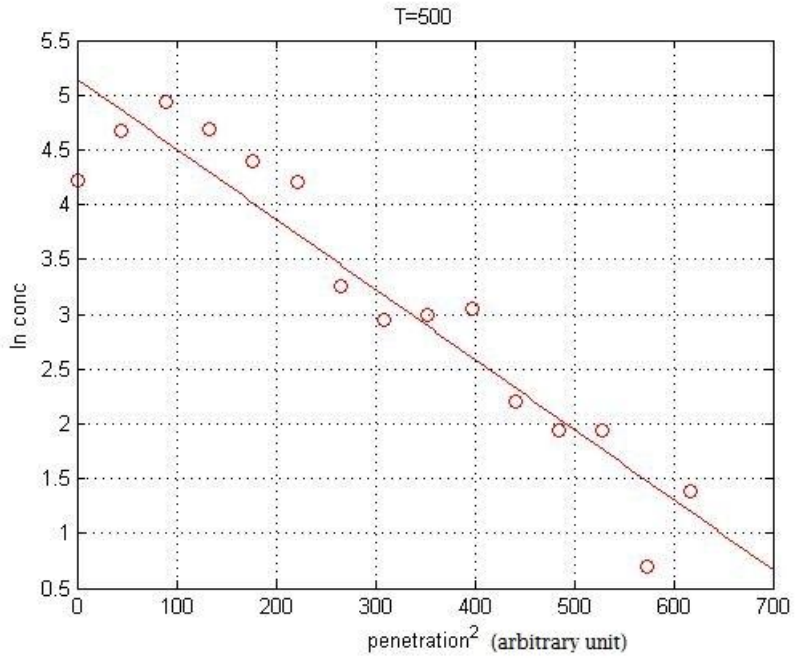

Figure (5.19 g') Variation of ln (concentration) with penetration distance^2 for sinusoidal wave with periodic time T=500 in a matrix of 90% vacancies

5.3.3. Effect of sinusoidal vs. square waves on penetration in biological tissues at different vacancies concentration:

Matrix size 1000 x 1000, vacancies 90%, t=1000 time steps

a)

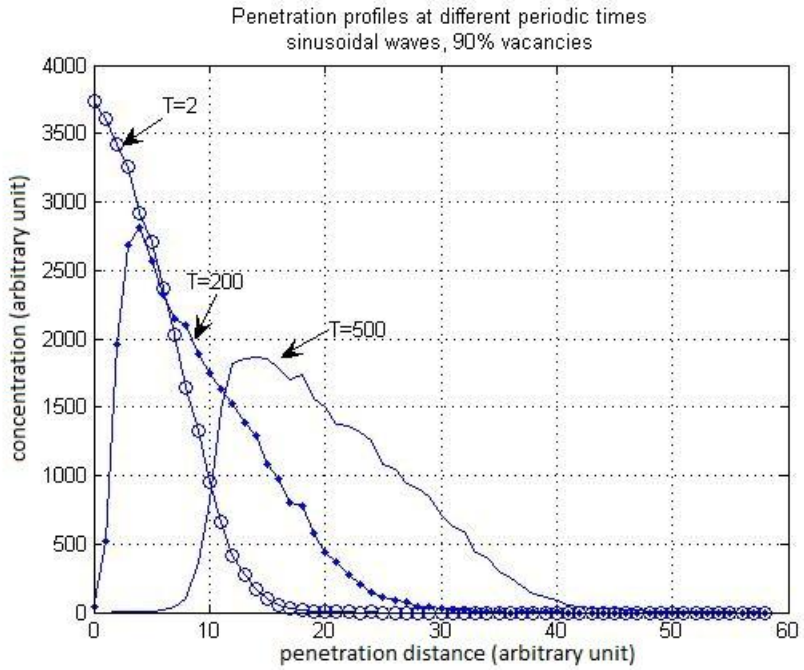

b)

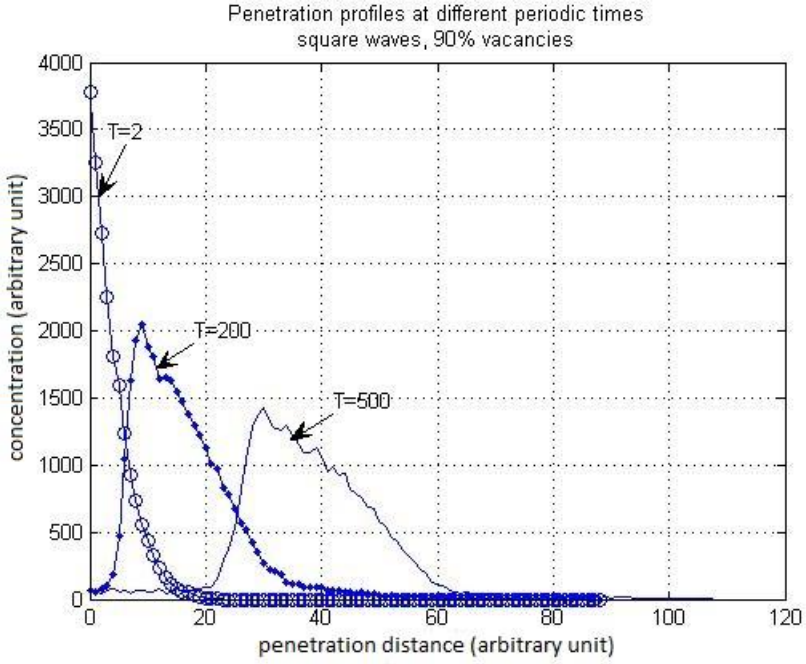

Figure (5.20) Penetration profiles at different periodic times in a matrix of 90% vacancies for a) sinusoidal waves, b) square waves

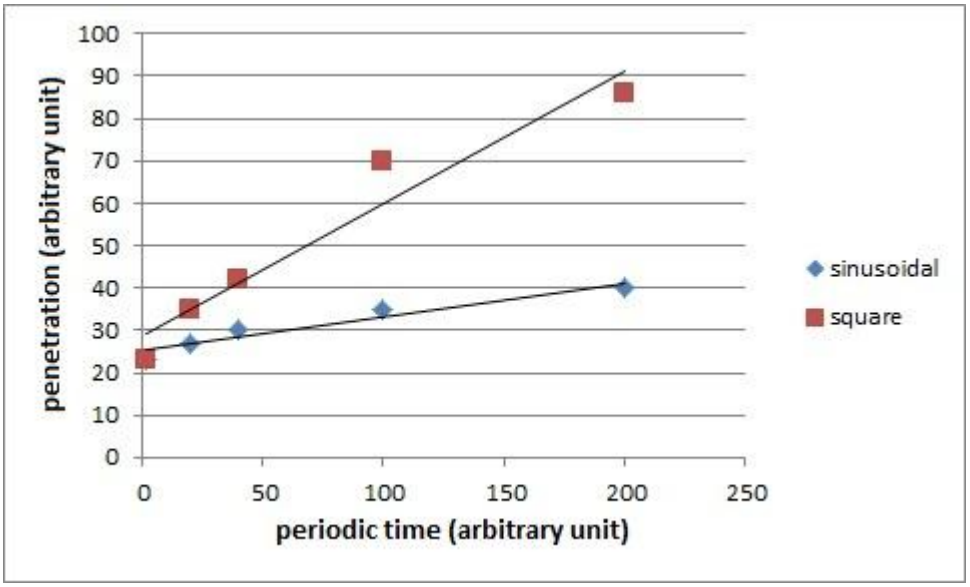

Figure (5.21) variation of the penetration distance with the periodic time in the sinusoidal and square waves

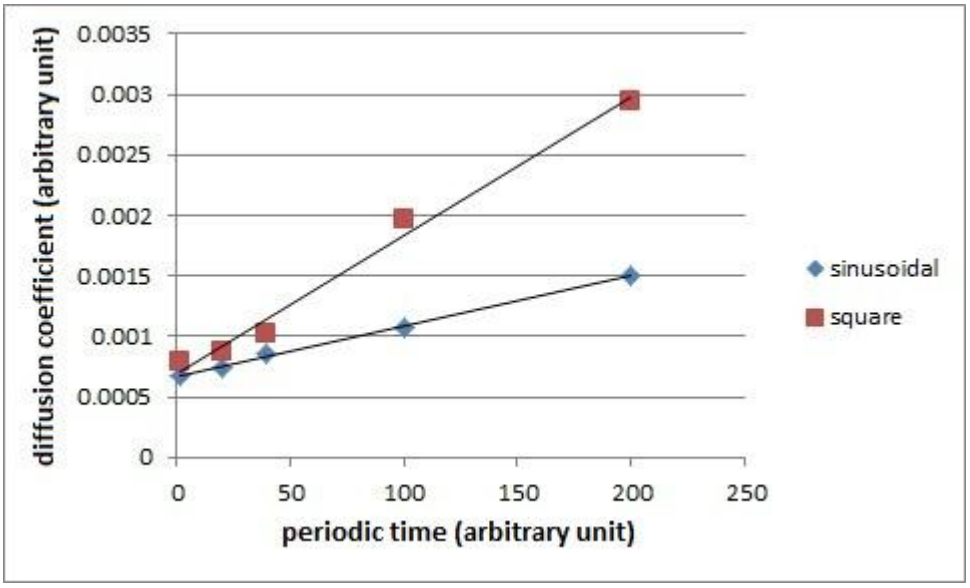

Figure (5.22) variation of the diffusion coefficient with the periodic time in the sinusoidal and square waves

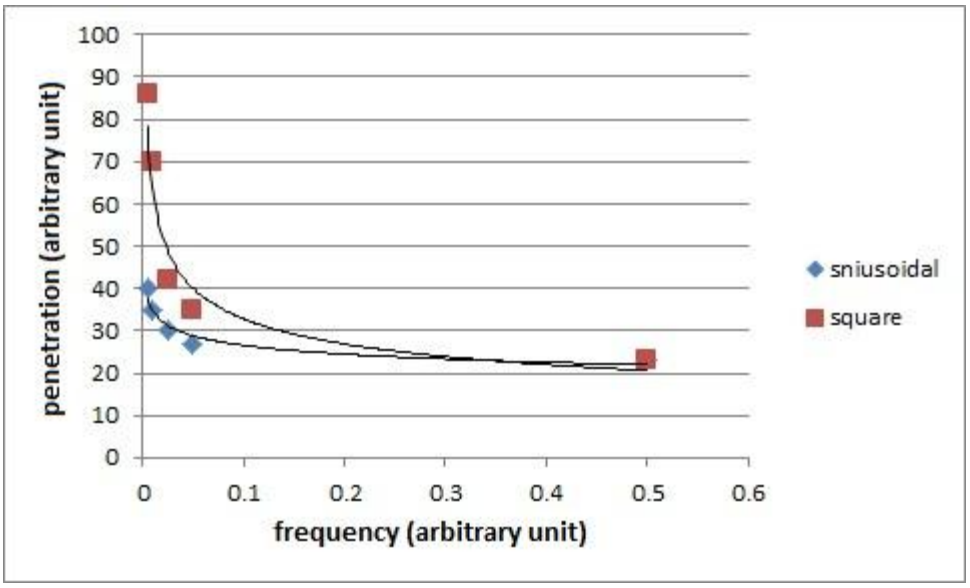

Figure (5.23) variation of the penetration distance with the frequency in the sinusoidal and square waves

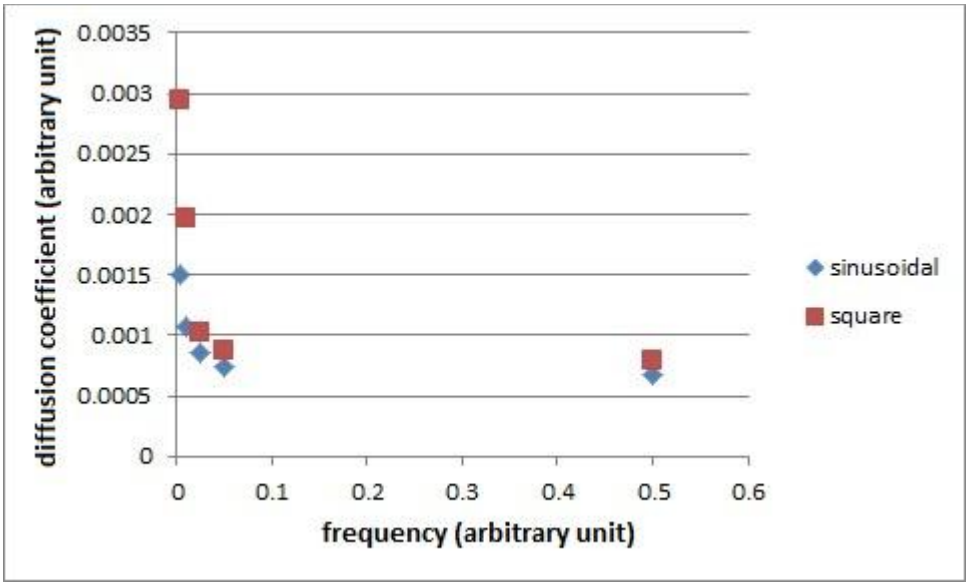

Figure (5.24) variation of the diffusion coefficient with the frequency in the sinusoidal and square waves

CHAPTER 6: DISCUSSION AND CONCLUSION

6.1. Modeling of the biological tissue:

Cellular geometry was analyzed by Dormer [47] who considered the cells as a system of polygons and came to a conclusion that a central cell may be surrounded with a maximum of six neighbors. In the present model a two dimensional honey comb cellular pattern is simulated such that it allows six maximum possible communications.

6.2. Free diffusion in two dimensional empty lattice

Free diffusion occurs in infinite space, which means that there are no boundaries which the diffusants may reach in a given time. For a collection of particles starting from the origin, such that each of them executes the random walk, the expected pattern is circular pattern. In the present model, the matrix is in hexagonal shape and the particles have only six neighbors to choose from. The resulting pattern for 100,000 particles executing random walk in an empty lattice as shown in figures (5.3) is more elliptical than circular. As the number of particles increase to 500,000 as in figure (5.5) the shape is getting more circular. Figures (5.3) and (5.5) show that the random walk pattern increases with time. The mean square values of the radius of the pattern were plotted against time as illustrated in figures (5.1) and (5.4).

The results of 100,000 and 500,000 particles show different configurations of the six nearest neighbors. The 100,000 particles case follows the configuration shown in figure (4.4 c)

From the analysis of the data in the case of 100,000 particles, the relation of the mean square displacement and time steps can be fitted to the equation:

$$0.0467\,x^2 - 18.82\,x + 1643.2$$

The 500,000 particles follows the configuration shown in figure (4.4 b).

The relation of the mean square displacement and time steps can be fitted to the equation:

$$0.1366\,x^2 - 84.157\,x + 629676$$

6.3. Simulation of infinite system and constant surface concentration:

Figures (4.8 a:f) show the concentration vs. penetration distance of diffusing ions that diffuse through an infinite biological tissue for different vacancies concentration. The penetration profile follows the exact Gaussian distribution that obeys the equation:

$$c(x,t) = constant \times e^{\frac{-x^2}{4Dt}}$$

Figures (4.8 a:f) show the logarithmic plot of the diffusing ions concentration against square of penetration distance. By application of least square analysis on the data, one can obtain the value of diffusion coefficient D. Appendix (B) shows the table of D values for different vacancies concentration. The value of D at 40% vacancies concentration is 1.63 x 10^{-5} cm^2/sec which is close to diffusion coefficient of potassium ions in the axoplasm given by Hodkin and Keynes [48].

In figures (4.6) and (4.7) it is noticed that from 0 to 30% vacancies, the penetration of diffusing ions and thereby the diffusion coefficient doesn't increase much. As the vacancies concentration increases more than 30%, the penetration of diffusing ions and thereby the diffusion coefficient increase linearly with the vacancies concentration.

Vacancies	penetration layer	D
5%	0	0
10%	1	0
20%	3	1.45E-07
30%	49	1.96E-06
40%	483	1.63E-05
50%	747	3.09E-05
60%	1068	4.64E-05
80%	1524	6.23E-05

The penetration profiles for different annealing times are shown in figures (5.11 a:f). The penetration of the diffusing ions increases as the time increases. The average diffusion coefficient can be driven from the table in appendix (B) to be 1.5 x 10^{-4} cm^2/sec.

Figure (5.9) shows that the penetration distance and the annealing time could be expressed as a second degree equation:

$$y = -7 \times 10^{-10}x^2 + 0.0014x + 40.365$$

Figure (5.10) show the relation between the diffusion coefficient and the annealing time to be a power equation:

$$y = 0.0069x^{-0.403}$$

6.4. Simulation of direct current effect:

A continuous layer of positive ions is positioned above the biological host. Two structural compositions of the biological tissues were tested under the effect of direct current, the 90% and 50% vacancies concentration.

Figures (5.12 a:e) show the forward direct current effect on 90% vacancies tissue. We can see that the diffusing ions appear to travel as a combined layer from the surface. The penetration of this combined layer increases as the electric field strength increases for the forward direction current. Figures (5.12 e) and (5.12 f) compare the effect with no electric field and the effect of backward direction current on penetration of ions in the biological tissue.

The backward direction seems to hinder the movement of positive ions; they remain in the 3rd layer. In the case of EF=0, the ions reached the 20th layer, which is less than the effect of the minimum EF strength applied (0.1) that reached the 60th layer.

The diffusion coefficient couldn't be calculated from these patterns using our model as the taking the logarithm of the penetration profile isn't applicable for the bell shaped profile.

Another application for the same model with lower vacancies concentration was made. The 50% vacancies concentration host allows the positive ions to diffuse more gradually than the 90% vacancies host.

Figure (5.13) show the penetration profile for forward current strengths (0.1, 0.5, and 0.9). The variation of the diffusion coefficient with the direct current strengths is shown in figure (5.14).

Figures (5.15 a:e) show the logarithmic plot of the diffusing ions concentration against square of penetration distance from which the diffusion coefficient is calculated.

Appendix (C) gives the table of the diffusion coefficient values in the case of direct current. When EF=0.1, D=0.000788445 cm^2/sec. When EF=0.7, D= 0.001038508 cm^2/sec. This is a high value compared with EF=0, D=0.000425409 cm^2/sec

EF	penetration	D
0.1	25	0.000788445
0.3	28	0.000889268
0.5	33	0.000950354
0.7	31	0.001038508
0.9	8	0.000286812

6.4.1. Comparison of penetration profiles for direct current at 50% and 90% vacancies concentration:

In the 50% vacancies configuration, as the EF increases the penetration increase up to a point after which it decreases again. This effect is apparent because as the field increase, the positive ions are more biased to movement in the direction of the current. In comparing 50% vacancies with 90% vacancies matrix, there is no much space for movement of the ions, and some of them appear to be hindered in the structure of the matrix. On the other hand, in 90% vacancies structure, the positive ions have more space to move in and as the strength increases, the penetration increases.

Figure (5.16) show the penetration profiles for a fixed forward direct current strength (EF=0.7) with different time steps in a tissue with 90% vacancies concentration. The figure shows that as the time increase, the width of the penetrating layer increase and also the penetration distance increase with time.

6.5. Simulation of alternating current effect

The model represents the effect of alternating current on the movement of positive ions placed above the biological tissue. Two structural compositions, the 90% and 50% vacancies concentration, of the biological tissues were tested under the effect of sinusoidal waves.

The minimum periodic time in the present model is 2, which represents a time step in upward direction and another downward. This periodic time corresponds to a frequency of 0.5. This frequency can be scaled to apply the present model to different frequencies.

In the case of 50% vacancies structure, a matrix of size 10,000x10,000 and annealing time of 1,000,000 were used to do the simulation. Appendix (D) illustrates the table of values of D under that conditions. Figures (5.17), (5.18) and (5.19) demonstrate that the penetration distance and the diffusion coefficient slightly change with increasing the periodic time of the wave. The average diffusion coefficient over the different periodic times is $3.18x10^{-5}cm^2/sec$. This value is close to the no filed effect which is $3.09x10^{-5}cm^2/sec$.

Why low frequencies have more effect on diffusion?

Figure (5.24 a) shows the case of 90% vacancies. From the appendix (D), figures (5.23) and (5.24), one can notice that the penetration decreases as the frequency increases. This is explained in section 2.8.1. (Penetration in biological tissues). At high frequencies, the penetration and diffusion coefficient values are close to EF=0 effect. As the frequency decrease, the penetration and diffusion coefficient values increase and are more like the direct current values.

An explanation of such phenomenon is given by Goldsworthy [49]. He stated that extremely low frequencies (ELF) such as those from power-lines and domestic appliances

are more potent than higher frequencies. There is usually little or no biological response to the much higher frequencies of radio waves, unless they are pulsed or amplitude modulated at a biologically active lower frequency (i.e. when the radio signal strength rises and falls in time with the lower frequency). Regular GSM mobile phones and PDAs emit both pulsed radio waves (from the antenna) and ELF (from the battery circuits).

Bawin et al. [50] found that exposing brain tissue to weak VHF radio signals modulated at 16Hz (16 cycles per second) released calcium ions (electrically charged calcium atoms) bound to the surfaces of its cells. Blackman et al. [51] followed this up with a whole series of experiments testing different field-strengths and frequencies and came to the surprising conclusion that weak fields were often more effective than strong ones.

Calcium ions bound to the surfaces of cell membranes are important in maintaining their stability. They help hold together the phospholipid molecules that are an essential part of their make-up [52]. Without these ions, cell membranes are weakened and are more likely to tear under the stresses and strains imposed by the moving cell contents. Although the resulting holes are normally self-healing they still increase leakage while they are open and this can explain the bulk of the known biological effects of weak electromagnetic fields.

6.5.1. Comparison of penetration profiles for sinusoidal and square waves in a tissue of 90% vacancies concentration:

T (periodic time)	penetration layer	D
2	23	0.000672115
20	27	0.000749805
40	30	0.00085118
100	35	0.001077865
200	40	0.001501051
2 (square)	23	0.000784338
20 (square)	35	0.000869959
40 (square)	42	0.00102758
100 (square)	70	0.001971453
200 (square)	86	0.002941799
no EF	22	0.000763359

In this application of the model, the effect of square wave was compared to the sinusoidal wave. In figures (5.20 a and b), the penetration in the case of square wave is more than the sinusoidal one. This effect is illustrated in figures (5.21 :5.24).

6.5.2. Why square waves have more effect than sine waves?

Goldsworthy [49] described the effect of ELF on ions diffusion. He explained why pulsed and square waves do more damage than sine waves.

The electromagnetic fields generate electrical 'eddy currents' flowing in and around the cells or tissues. Both the electrical and magnetic components of the fields can induce them and they tend to follow low impedance pathways. The blood system, filled with highly conductive salts, forms an excellent low resistance pathway for DC and low frequency AC.

Only if the frequency is low will the calcium ions have time to be pulled clear of the membrane and replaced by potassium ions before the field reverses and drives them back. Pulses and square waves work best because they give very rapid changes in voltage that catapult the calcium ions well away from the membrane and then allow more time for potassium to fill the vacated sites. Sine waves are smoother, spend less time at maximum voltage, and so allow less time for ion exchange.

Continuous waves are not sharply pulsed, therefore we might expect them to need stronger fields and/or longer exposure times if they are to give effects.

6.5.3. The square wave penetration in 50% vacancies tissue

The square wave when applied in a 50% vacancies matrix show different effect than the 90% vacancies tissue. The diffusion coefficient is this case is less than the sinusoidal one. Appendix (D), the value of $D=4.58085 \times 10^{-6}$.

The explanation for such a phenomenon comes from that in the square wave the current is maximum in upward and downward cycles. Given the maximum effect, all the ions will tend to go in the forward/backward direction. If the host doesn't have much space for movement, the diffusing ions will be hindered. On the other hand, 90% vacancies concentration in which the diffusants have more space to move in and the square wave appears to have more penetration and diffusion coefficient values than the sinusoidal ones.

6.6. Effect of structure on diffusion

Comparing the 50% and 90% vacancies concentration tissues from the above results show that the diffusing ions behave differently if they got more space for movement. As the structure is more occupied, the diffusion coefficient decreases.

A possible explanation of the effect of structure on hindering diffusion is given by Sykova´ and Nicholson [18]. In earlier work, Levin et al. [53] showed that small molecules such as inulin and sucrose could diffuse through the extracellular space (ECS) with an effective diffusion coefficient (D^*) that was some two to three times less than the free diffusion coefficient (D).

Sykova´ and Nicholson [18] studied the effective diffusion coefficient in brain extracellular space. They state the factors affecting the diffusion of a molecule in the extracellular space (ECS). These are as follows:

a) Geometry of ECS which imposes an additional delay on a diffusing molecule compared with a free medium;

b) Dead-space microdomain where molecules lose time exploring a dead-end

c) Obstruction in the form of extracellular matrix molecules

d) Binding sites for the diffusing molecule either on cell membranes or extracellular matrix

e) Fixed negative charges, also on the extracellular matrix, that may affect the diffusion of charged molecules.

6.7. Possible applications of the present model:

a) Investigation of the hazards of mobile phones

During the last century the levels of ELFs and MWs have been hugely increased in our environment. Devices such as mobile phones, computers, power lines and domestic wiring can be hazardous to humans. The energy of the fields is too low to give significant heating; yet, the evidence that electromagnetic fields can have “non-thermal” biological effects is now overwhelming. The non-thermal biological effects of electromagnetic fields have puzzled scientists for decades and, until now, there has been no clear explanation. The present model could be used to test the effect of certain frequencies on the diffusion in biological tissues.

b) Studying drug delivery in the central nervous system:

When substances diffuse in the brain, they predominantly move through the narrow extracellular space (ECS) that separates one cell membrane from another. Measurements of the diffusion properties of the ECS are important from two perspectives: first as a means of determining specific diffusion coefficients and second as a means of exploring the structure of the ECS. [18]

To predict the distribution of a substance, it is essential to know the effective diffusion coefficient in brain tissue as well as the relative importance of diffusion versus clearance processes that may remove that substance from the ECS. The substance may be a neurotransmitter spilling over from a synapse to affect adjacent sites or a neuromodulator that utilizes the ECS as a conduit for signaling to other cells; this type of communication is variously called volume transmission, nonsynaptic or extrasynaptic

transmission. Knowledge of effective diffusion coefficients and diffusion properties are equally crucial for defining drug delivery within the CNS.

c) Electroconvulsive therapy

Electroconvulsive therapy (ECT) was introduced as a treatment for psychiatric disorders by the Italian neurologist Ugo Cerletti in 1938. Cerletti developed a method of electrically inducing seizures in laboratory animals as a means of studying epilepsy. Aware of the observation that individuals with epilepsy and depression experienced an improvement in mood following a seizure, he postulated that inducing a seizure in a depressed individual might improve his or her condition. In 1938, he reported the first case of a psychiatric patient treated with ECT with dramatic, positive results

The present model can help in clinical testing of the effects of the pulse-wave and sine-wave ECT apparatus. The pulse wave can be dosed by adjusting the pulse width, the amplitude of the wave, the frequency, and the duration.

D) Food industry

Mass transfer processes are important unit operations in food industry requiring the disintegration of biological material. Especially the processing of plant cells is of great commercial interest because of the high amount of health related ingredients, pigments and cell liquid in the vacuoles but also due to the diversified potential to be further manufactured.

The newly emerged application of Pulsed Electric Fields (PEF) constitutes an alternative to conventional processing of plant cell material, with the main aim of mass transport enhancement through permeabilization of the cell membrane [12].

Also López et al. [54] investigated in PEF assisted extraction of sucrose from sugar beets and found out that temperature of thermal treatment could be reduced from 70° C to 40° C after PEF pre-treatment.

The critical external field strength is highly dependent on cell size as well as on cell orientation in the field [55].

Ohmic heating has been used commercially as a way of rapidly providing volumetric heating for sterilization or pasteurization of foods. Kemp and Fryer [56] studied the enhancement of diffusion through foods using alternating electric fields. They found that electric fields enhance diffusion by 70%.

The present model can investigate the effects of electric field on different tissues which can help in food industry.

6.8. Future work

- Build a 3D model of the biological tissue, and study diffusion on it.
- Represent more than one ion diffusion, and investigate the competition between them.
- Use a computer cluster network to divide the matrix and perform simultaneous diffusion of ionic species.
- Specify the host structure according to application.
- Use the model in one of the proposed applications.

REFERENCES:

1. Guttorp, P.,"Stochastic modeling of scientific data**",** Chapman and Hall, first edition, (1995).
2. Buda, F., Chiarotti and Car, R., "Hydrogen in crystalline and amorphous silicon", pp 98-103,Italy, physica B, 119, (1991).
3. Weeks, E. R and Swinny, H.L., "Anomalous diffusion in assymetric random walks", physica D 97, pp 291-310, USA, (1996).
4. Moshfegh, A. Z., "Computer simulation of diffusion in solids: Cu/Si and C/Fe systems", Materials and manufacturing, 12,1, 95-105, (1997).
5. Sholl, C.a., Cameron, L.M., "random walk theory of dilute impurity effects on diffusion in crystals", Ber. Bunsenges. Phys. Chem., 9, Australia, (1997).
6. Li, H., Szpunar, J.A.,"Computer simulation of diffusion process in polycrystalline material", proceedings of the third Int. Conf. of grain growth, Canada, TMS publications, 343-348, (1998).
7. Kuklja, M.M., Kotomin, E.A. and Popov, A.I., "Semi-empirical simulations of f-center diffusion in KCl crystals", 103-106, J.Phys. Chem Solids, 58, 1, (1996).
8. Yajun Liu, Xianming Shi, "Ionic transport in cementitious materials under an externally applied electric field: Finite element modeling", Construction and Building Materials 27, 450–460, (2012).
9. Alessandro Bagno, Fabio D'Amico, Giacomo Saielli "Computer simulation of diffusion coefficients of the room-temperature ionic liquid [bmim][BF4]: Problems with classical simulation techniques" Journal of Molecular Liquids 131–132 ,17–23, (2007).
10. Jansson, F., Nenashev, A.V., Baranovskii, S.D., Gebhard, F., Österbacka, R., "Effect of electric field on diffusion in disordered materials", Annalen der Physik, 18, 856 – 862, (2010).
11. Chitra Kusnadi, Sudhir K. Sastry, "Effect of moderate electric fields on salt diffusion into vegetable tissue", Journal of Food Engineering,110, 3, 329-336, (2012).
12. A. Janositz, A.-K. Noack, D. Knorr, "Pulsed electric fields and their impact on the diffusion characteristics of potato slices", LWT - Food Science and Technology, 44, 9, 1939-1945, (2011).
13. Krogh A. "The rate of diffusion of gases through animal tissues, with some remarks on the coefficient of invasion". The Journal of physiology, 52, 391-408, (1919).
14. Exner. Annalen der Physik, 155. (1875).
15. Tachiya, M., "Effect of an external electric field on the rate of diffusion-controlled reactions", Journal of Chemical Physics, 87, 8, (1987).
16. Leif G. Salford, Henrietta Nittby, Arne Brun, Gustav Grafström, Lars Malmgren, Marianne Sommarin, Jacob Eberhardt, Bengt Widegren and Bertil R. R. Persson, "The Mammalian Brain in the Electromagnetic Fields Designed by Man with Special Reference to

Blood-Brain Barrier Function, Neuronal Damage and Possible Physical Mechanisms", Prog. Theor. Phys. Supplement, 173, 283-309, (2008).
17. G.R Smith, M.S.P Sansom, "Effective diffusion coefficients of K+ and Cl− ions in ion channel models", Biophysical Chemistry, 79, 2, 129-151, (1999).
18. Eva Sykova´ and Charles Nicholson , "Diffusion in Brain Extracellular Space" Physiol Rev 88, 1277–1340, (2008).
19. Dekker, J.A., "Solid state physics", first edition, London, Macmillan & Co LTD, (1958).
20. Serway, A.R., "Physics for scientists and engineers", fourth edition, Saunders college publishing, (1996).
21. El-Messiry M.A., "Radio-tracer study of the isotope effect for sodium diffusion in liquids", Master thesis, Scotland, (1976).
22. Frenkel, J., "Kinetic theory of solids", Oxford, (1946).
23. Eyring, H., J.chem.phys., 3, 107, (1935).
24. Swalin R.A., Acta Met., 7, 736, (1959).
25. Nachtrieb, N., Ad. Phys., 16, 309, (1967).
26. Reynic, R.J., Trans. Met. Soc. AIME, 245, (1969).
27. Larson, S. and Lodding, A., "Diffusion process", first edition, Sherwood, (1977).
28. Brenner BM, Hostetter TH, Humes HD, "Molecular basis of proteinuria of glomerular origin". N Engl J Med 298, 826–833, (1978).
29. Brenner BM, Hostetter TH, Humes HD: "Glomerular permselectivity: Barrier function based on discrimination of molecular size and charge". Am J Physiol 234, F455–F460, (1978).
30. Rennke HG, Venkatachalam MA: "Glomerular permeability of macromolecules. Effect of molecular configuration on the fractional clearance of uncharged dextran and neutral horseradish peroxidase in the rat". J Clin Invest 63, 713–717, (1979).
31. Kriz W, Lemley KV, "The role of the podocyte in glomerulosclerosis", Curr Opin Nephrol Hypertens 8, 489–497, (1999).
32. Kreidberg JA, "Podocyte differentiation and glomerulogenesis", J Am Soc Nephrol 14, 806–814, (2003).
33. Pavenstadt H, Kriz W, Kretzler M, "Cell biology of the glomerular podocyte", Physiol Rev 83, 253–307, (2003).
34. Sheenan, "Physiology for Health Care and Nursing", Elsevier Health Sciences., 130. ,Kindlen (2003).
35. Shewmon, P., "Diffusion in solids", Second edition, A publication of the minerals, Metals & materials society, (1989).
36. Richard, J.B. and Dienes G.J., "An introduction to solid state diffusion", Academic press, USA, (1988).
37. Slifkin, L., "Tracer diffusion", Metallurgical Transactions A, 20A, 2577-2582, (l989).
38. S. Baranovski (ed.), "Charge Transport in Disordered Solids with Applications in Electronics", technology & engineering, (2006).

39. Bagotzky, V.S., "Fundamentals of Electrochemistry", Plenum Publishers, New York, (1993).
40. Bockris, J.O., Reddy, A.K.N., "Modern Electrochemistry1: Ionics", Plenum Press, (1998).
41. Vorst, A. vander , Arye Rosen, Youji Kotsuka "RF/microwave interaction with biological tissues" ,(2006).
42. E. Jordan, K. Balmain, "Electromagnetic Waves and Radiating Systems", (1968).
43. A. Gérin, B. Stockbroeckx, A. Vander Vorst, "Champs Micro-ondes et Santé, Louvain-la-Neuve", EMIC-UCL, (1999).
44. Law, A.M. and Kelton, W.D., "Simulation modeling and analysis", first edition, McGraw-Hill Book company, (1982).
45. Sargent, Robert G., "A tutorial on validation and verification of simulation models", Proc.Winter simulation conf. SCS, San Diego, 33-39, (l988).
46. Jack, "Statistical technique in simulation", part 1, Marcel Dekker Inc., New York, (l973).
47. K.J.Dormer, "Fundamental Tissue Geometry for Biologists", Cambridge University Press, New York, (1980).
48. A. L. Hodgkin and R. D. Keynes , "the mobility and diffusion coefficient of potassium in giant axons from sepia", j. physiol, II9, 5I3-528, (1953).
49. Goldsworthy A. "Effects of electrical and electromagnetic fields on plants and related topics". In: Volkov AG (ed.) Plant Electrophysiology – Theory & Methods Springer-Verlag Berlin Heidelberg, 247-267, (2006).
50. Bawin SM, Kaczmarek KL, Adey WR "Effects of modulated VHF fields on the central", (1975).
51. Blackman CF, Benane SG, Kinney LS, House DE, Joines WT 'Effects of ELF fields on Calcium-Ion Efflux from Brain Tissue in Vitro", radiation research, 92, 510-520 (1982).
52. Ha B-Y, 'Stabilization and destabilization of cell membranes by multivalent ions', (2001).
53. Levin VA, Fenstermacher JD, Patlak CS., "Sucrose and inulin space measurements of cerebral cortex in four mammalian species", Am J Physiol 219, 1528–1533, (1970).
54. N. López, E. Puértolas, S. Condón, J. Raso, I. Álvarez, "Enhancement of the solid-liquid extraction of sucrose from sugar beet (Beta vulgaris) by pulsed electric fields", LWT - Food Science and Technology, 42, 10, 1674–1680, (2009).
55. V. Heinz, I. Alvarez, A. Angersbach, D. Knorr, "Preservation of liquid foods by high intensity pulsed electric fields-basic concepts for process design Trends in Food Science and Technology", 12, 103–111, (2002).
56. M.R. Kemp, P.J. Fryer, "Enhancement of diffusion through foods using alternating electric fields", Innovative Food Science & Emerging Technologies, 8, 143-153, (2007).

APPENDIX A

RESULTS OF FREE RANDOM WALK PATTERN:

Table (A-1) Results of : 100,000 particles start from the center of 10,000 x 10,000 matrix

time steps	<R^2>=sum/n	D=<R^2>/(4t)
0	0	0
500	5.00E+03	0.250
1000	3.10E+04	7.75
1500	7.89E+04	13.1
2000	1.51E+05	18.8308
2500	2.45E+05	24.5
3000	3.64E+05	30.3173
3500	5.07E+05	36.2
4000	6.74E+05	42.1313

Table (A-2) Results of: 500,000 particles start from the center of 30,000 x 30,000 matrix:

time steps	<R^2>
0	0
5,000	3050400
10,000	16182200
15,000	29498000
20,000	53042000
25,000	83434000
30,000	120796000
35,000	165100000
40,000	2.16E+08

APPENDIX B

RESULTS OF VARIATION OF PENETRATION DISTANCE AND DIFFUSION COEFFICIENT WITH VACANCIES CONCENTRATION:

Table (B-1) Results of: Matrix 10,000 x 10,000 time steps=1,000,000

Vacancies	penetration layer	D
5%	0	0
10%	1	0
20%	3	1.45E-07
30%	49	1.96E-06
40%	483	1.63E-05
50%	747	3.09E-05
60%	1068	4.64E-05
80%	1524	6.23E-05

RESULTS OF VARIATION OF PENETRATION DISTANCE AND DIFFUSION COEFFICIENT WITH ANNEALING TIME:

Table (B-2) Results of: Matrix 10,000 x 10,000 vacancies percentage 50%

annealing time	penetration layer	D
1000	19	0.000485503
5,000	42	0.000228279
10,000	60	0.000163335
50,000	130	7.82387E-05
100,000	173	5.367E-05
500,000	552	3.76421E-05
1000000	747	3.0923E-05

APPENDIX C

RESULTS OF THE EFFECT OF DIRECT CURRENT

Table (C-1) Results of: Matrix 1000 x 1000, vacancies=50%, t=1000 time steps

EF	penetration	D
0.1	25	0.000788445
0.3	28	0.000889268
0.5	33	0.000950354
0.7	31	0.001038508
0.9	8	0.000286812

APPENDIX D

RESULTS OF THE EFFECT OF ALTERNATING ELECTRIC FIELD ON THE PENETRATION OF IONS:

Table (D-1) Results of: Matrix 10,000 x 10,000 vacancies percentage 50% , annealing time: 1,000,000

periodic time (T)	number of cycles	frequency	penetration layer	D
2	500,000	0.5	803	3.47377E-05
40	25,000	0.025	640	2.43451E-05
100	10,000	0.01	697	2.73167E-05
200	5,000	0.005	687	3.12664E-05
300	3333.333333	0.003333	729	3.1608E-05
400	2,500	0.0025	733	3.43903E-05
500	2000	0.002	680	3.90637E-05
200 (square)	2000	0.002	166	4.58085E-06
No EF	-	-	-	3.09E-05

RESULTS OF THE EFFECT OF SINUSOIDAL VS. SQUARE WAVES ON PENETRATION IN BIOLOGICAL TISSUES WITH DIFFERENT VACANCIES CONCENTRATION:

Table (D-2) Results of: Matrix size 1000 x 1000, vacancies 90%, t=1000 time steps

T (periodic time)	number of cycles	Frequency	penetration layer	D
2	500	0.5	23	0.000672115
20	50	0.05	27	0.000749805
40	25	0.025	30	0.00085118
100	10	0.01	35	0.001077865
200	5	0.005	40	0.001501051
2 (square)	500	0.5	23	0.000784338
20 (square)	50	0.05	35	0.000869959
40 (square)	25	0.025	42	0.00102758
100 (square)	10	0.01	70	0.001971453
200 (square)	5	0.005	86	0.002941799
no EF	-	-	22	0.000763359